National Library of Canada
Bibliothèque nationale du Canada

Canadian Theses Service
Service des thèses canadiennes

Ottawa, Canada
K1A 0N4

NOTICE

The quality of this microform is heavily dependent upon the quality of the original thesis submitted for microfilming. Every effort has been made to ensure the highest quality of reproduction possible.

If pages are missing, contact the university which granted the degree.

Some pages may have indistinct print especially if the original pages were typed with a poor typewriter ribbon or if the university sent us an inferior photocopy.

Previously copyrighted materials (journal articles, published tests, etc.) are not filmed.

Reproduction in full or in part of this microform is governed by the Canadian Copyright Act, R.S.C. 1970, c. C-30.

AVIS

La qualité de cette microforme dépend grandement de la qualité de la thèse soumise au microfilmage. Nous avons tout fait pour assurer une qualité supérieure de reproduction.

S'il manque des pages, veuillez communiquer avec l'université qui a conféré le grade.

La qualité d'impression de certaines pages peut laisser à désirer, surtout si les pages originales ont été dactylographiées à l'aide d'un ruban usé ou si l'université nous a fait parvenir une photocopie de qualité inférieure.

Les documents qui font déjà l'objet d'un droit d'auteur (articles de revue, tests publiés, etc.) ne sont pas microfilmés.

La reproduction, même partielle, de cette microforme est soumise à la Loi canadienne sur le droit d'auteur, SRC 1970, c. C-30.

NL-339 (r. 88/04)

Canada

THE UNIVERSITY OF ALBERTA

THE EFFECTS OF NET CONFINING PRESSURE AND TEMPERATURE ON THE ABSOLUTE PERMEABILITY OF CONSOLIDATED CARBONATE RESERVOIR ROCKS

BY

NEIL A. PITMAN

A THESIS

SUBMITTED TO THE FACULTY OF GRADUATE STUDIES AND RESEARCH IN PARTIAL FULFILLMENT OF THE REQUIREMENTS FOR THE DEGREE OF

MASTER OF SCIENCE

IN

PETROLEUM ENGINEERING

MINING, METALLURGICAL AND PETROLEUM ENGINEERING

EDMONTON, ALBERTA

SPRING, 1988

Permission has been granted to the National Library of Canada to microfilm this thesis and to lend or sell copies of the film.

The author (copyright owner) has reserved other publication rights, and neither the thesis nor extensive extracts from it may be printed or otherwise reproduced without his/her written permission.

L'autorisation a été accordée à la Bibliothèque nationale du Canada de microfilmer cette thèse et de prêter ou de vendre des exemplaires du film.

L'auteur (titulaire du droit d'auteur) se réserve les autres droits de publication; ni la thèse ni de longs extraits de celle-ci ne doivent être imprimés ou autrement reproduits sans son autorisation écrite.

ISBN 0-315-42777-9

THE UNIVERSITY OF ALBERTA

RELEASE FORM

NAME OF AUTHOR	Neil Pitman
TITLE OF THESIS	The Effects of Net Confining Pressure and Temperature on the Absolute Permeability of Consolidated Carbonate Reservoir Rocks
DEGREE FOR WHICH THESIS WAS PRESENTED	Master of Science
YEAR THIS DEGREE GRANTED	Spring 1988

Permission is hereby granted to THE UNIVERSITY OF ALBERTA LIBRARY to reproduce single copies of this thesis and to lend or sell such copies for private, scholarly or scientific research purposes only.

The author reserves other publication rights, and neither the thesis nor extensive extracts from it may be printed or otherwise reproduced without the author's written permission.

(Signed) Neil Pitman

PERMANENT ADDRESS:

40 Wahstao Cr

Edmonton, Alberta

DATED April 22, 1988

THE UNIVERSITY OF ALBERTA

FACULTY OF GRADUATE STUDIES AND RESEARCH

The undersigned certify that they have read, and recommend to the Faculty of Graduate Studies and Research, for acceptance, a thesis entitled THE EFFECTS OF NET CONFINING PRESSURE AND TEMPERATURE ON THE ABSOLUTE PERMEABILITY OF CONSOLIDATED CARBONATE RESERVOIR ROCKS submitted by Neil Pitman in partial fulfillment of the requirements for the degree of Master of Science in Petroleum Engineering.

SUPERVISOR

EXTERNAL EXAMINER

DATE 88-04-22

ABSTRACT

The effect of elevated temperature on absolute permeability, the effect of increased net confining pressure on absolute permeability, and the combined effect of elevated temperature and net confining pressure were experimentally investigated using three different porous media.

Using thermal expansion properties of various minerals on a microscopic scale, predictions were made of the effect of increased temperature on the absolute permeability of consolidated rocks. Assuming constant net confining pressure, it was postulated that heterogeneous reservoir rocks will experience a small increase in permeability with temperature, and homogeneous rocks will show little or no effect.

The results from testing carried out on argillaceous dolomite, clean limestone and clean sandstone at temperatures up to 325°F (using nitrogen gas as the flowing fluid) agree with the theoretical predictions. Results obtained by previous researchers were reviewed as well and also agree with the theoretical results.

Matrix strength, grain orientation, bedding planes and previous stress conditions were

considered when comparing the effect of increased net confining pressure on vertical and horizontal permeability. For the argillaceous dolomite samples at low net confining pressure (below 6000 PSI), decreases in horizontal permeability were found to be much less than decreases in vertical permeability.

The hysteresis effects in previously unstressed core samples were found to be substantially greater than those in previously stressed cores.

The proposed thermal expansion model indicates that rocks which experience an increase in absolute permeability with temperature should experience a greater permeability loss due to elevated net confining pressure at high temperatures. However, test results from this type of sample at high temperatures did not indicate any noticeable change.

ACKNOWLEDGEMENTS

The author would like to give special thanks to Dr. D.L. Flock for the guidance and inspiration provided towards carrying out this study.

Appreciation is extended to AOSTRA for their financial support, to Chemical and Geological Laboratories Ltd. for their assistance and to Union Oil and the ERCB for the release of the cores.

Thanks are also due to B. Fialka for his help in preparing the apparatus and preliminary experimentation.

TABLE OF CONTENTS

LIST OF TABLES x

LIST OF FIGURES xi

NOMENCLATURE xiv

1. Introduction 1

2. Literature Search 6

   a) Pressure Effects

   b) Temperature Effects

   c) Summary of Literature

3. Review of Existing Correlations 14

   a) Pressure Effects

   b) Temperature Effects

4. Proposed Theory 19

   a) Pressure Effects

      i) Review

      ii) Stress Model

      iii) Horizontal vs Vertical Effects

   b) Temperature Effects

      i) Review

      ii) Homogeneous Matrix

      iii) Heterogeneous Matrix

5. Experimental Apparatus 43

a) Cell Assemblies

b) Control System

c) Sample Preparation

6. Procedure 54

a) Theory

b) Method

c) Processing of Data

d) Error Analysis

7. Results 68

a) Vertical Dolomite Cores

b) Horizontal Dolomite Plugs

c) Limestone Cores

d) Sandstone Core

8. Discussion 87

a) Effects of Changes in Net Confining Pressure

i) Hysteresis Effects

ii) Vertical versus Horizontal Permeability Effects

b) Effects of Elevated Temperature

c) Combined Temperature and Pressure Effects

9. Conclusions 102

REFERENCES 103

APPENDIX A1 FORTRAN PROGRAM 106

APPENDIX A2 DARCY FLOW EQUATION 108

APPENDIX A3 SAMPLE CALCULATION 110

APPENDIX A4 REYNOLDS NUMBER CALCULATION 113

APPENDIX B1 CORE 90: 3" DOLOMITE 116

APPENDIX B2 CORE 133A: 3" DOLOMITE 127

APPENDIX B3 CORE 92: 3" DOLOMITE 135

APPENDIX B4 HORIZONTAL PLUG 93B:
1" DOLOMITE 144

APPENDIX B5 HORIZONTAL PLUG 133A:
1" DOLOMITE 151

APPENDIX B6 VERTICAL PLUG 133A:
1" DOLOMITE 159

APPENDIX B7 CORE 1L: 3" LIMESTONE 166

APPENDIX B8 CORE 3L: 3" LIMESTONE 174

APPENDIX B9 CORE 4L: 3" LIMESTONE 183

APPENDIX B10 CORE 6L: 3" LIMESTONE 191

APPENDIX B11 CORE 2S: 3" SANDSTONE 200

LIST OF TABLES

TABLE	DESCRIPTION	PAGE
1.	Coefficients of Thermal Expansion	31
2.	Summary of Successful Tests	62

LIST OF FIGURES

FIGURE	DESCRIPTION	PAGE
1.	a) Grain Orientation Before Compaction	22
	b) Grain Orientation After Compaction	23
2.	Temperature Effects - Homogeneous Matrix	34
3.	Temperature Effects - Heterogeneous Matrix	37
4.	a) Plan View of 3" Cell	44
	b) Top Platen (3" Cell)	45
	c) Bottom Platen (3" Cell)	46
5.	Plan View of 1" Horizontal Cell Assembly	48
6.	Schematic of Experimental Apparatus	49
7.	Typical Klinkenberg Plot	55
8.	K/K_{ATM} versus Net Confining Pressure -3" Dolomite Cores	69
9.	Core 92 Absolute Permeability versus Net Confining Pressure	71
10.	K/K_{75} versus Temperature-3" Dolomite Cores	72

11.	Core 90 K/K_{75} versus Temperature (w/net confining pressure as cross-parameter)	73
12.	Core 90 K/K_{ATM} versus Net Confining Pressure (w/ temperature as cross-parameter)	75
13.	K/K_{ATM} versus Net Confining Pressure-Horizontal Dolomite Plugs	77
14.	K/K_{75} versus Temperature-Horizontal Dolomite Plugs	78
15.	K/K_{100} versus NCP-Vertical Dolomite Plug	80
16.	K/K_{75} versus Temperature-Vertical Dolomite Plug	81
17.	K/K_{atm} versus NCP-Vertical Limestone Cores	82
18.	K/K_{atm} versus NCP-Core 6L	83
19.	K/K_{75} versus Temperature-Vertical Limestone Cores	85
20.	K/K_{75} versus Temperature-Core 2S	86
21.	K/K_{100} versus NCP-Core 133A and Horizontal Plug 133A	90

22.	K vs $1/P_m$ (temperature as cross-parameter) - Core 133A	94
23.	K vs $1/P_m$ (temperature as cross-parameter) - Core 4L	95
24.	Klinkenberg Slip Factor vs Temperature-Core 133A	98
25.	Slip Factor vs Temperature-Core 6L	100

NOMENCLATURE AND ABBREVIATIONS

Absolute Permeability (K_{abs} or K_ℓ): The permeability of a porous medium when saturated with a single fluid. Units are length squared.

Klinkenberg Plot: Reciprocal Mean Pressure vs Apparent Permeability, for gas flowing through porous media. The laminar flow regime appears as a linear portion which may be extrapolated to zero reciprocal mean pressure to determine K_ℓ.

Net Confining Pressure (NCP): The difference between overburden (or confining pressure) and internal pore pressure.

Slip Factor (b): Correction factor to account for gas slippage when calculating absolute permeability where gas is the flowing fluid.

Diagenesis: The conversion of sediment to rock.

Mean Pressure (P_m): The average of the inlet and outlet pressures of a fluid flowing through a sample.

Mean Free Path (λ): The average path length of a gas molecule between collisions. Slip factor is dependent on mean free path.

Homogeneous Rock - Rocks composed essentially of one mineral such as quartz or limestone.

Heterogeneous Rock - Rocks containing impurities such as shale.

Silicates - Family of minerals based on SiO_4 tetrahedron. Includes clays, shales.

Carbonates - Calcium compounds, primarily dolomite ($CaMg(CO_3)_2$ and limestone ($CaCO_3$).

Consolidated Rock - solid rock mass with grains cemented together.

Isotropic stress - condition where stress along any axis in a body is uniform, such as would be found in a body submerged in a fluid.

Anisotropic stress - condition where stress differs between axes.

Elastic modulus - The ratio of stress to corresponding strain.

Clay Swelling - Some clays, particularly montmorillonite, will take on water when in contact, and can swell to many times original size.

Migration of Fines - Liquid flowing through pores may dislodge clays from the pore walls, which in turn will cause blockages to flow.

Mineral Dissolution - As sediments are buried, the increased temperature and pressure will result in some minerals dissolving.

Recrystalization - The formation of new minerals from minerals in solution. Usually in the form of intergranular cement.

Macroscopic - Considered in terms of units which can be seen by the naked eye.

Elastic Deformation - Deformation which is instantaneously reversible when the stress is released.

Plastic Deformation - Permanent deformation occurring when a material is stressed beyond its elastic limit.

Hysteresis - Change in properties at original conditions due to outside forces having acted on a body.

Pore Pressure - Pressure exerted by the fluid contained in the rock pores.

Overburden Pressure - Pressure exerted on a rock by the weight of the overlying strata.

Rock Matrix - Solid portion of a rock surrounding the pore spaces.

Argillaceous - rocks containing clays or shales.

1. INTRODUCTION

Absolute permeability, a basic parameter in reservoir engineering, is traditionally measured at room temperature and a low confining pressure. As a result, the same value of permeability is generally applied at all temperatures and pressures from the time a reservoir is initially developed until it is depleted. During this time large changes in net confining pressure could occur. Implementation of a steamflood or fireflood could result in large temperature variations as well. Although substantial research has already been carried out on both the effects of increased net confining pressure and elevated temperature on the absolute permeability of consolidated reservoir rocks, further research was justified for the following reasons:

1. Little of the work done in this field has been with carbonate rocks. Although the effect of increased net confining pressure on vertical and horizontal permeability has been compared for sandstone samples, these effects have apparently not been investigated for carbonates. Research on the effect of elevated temperature is lacking for carbonates as well. A substantial amount of Alberta's hydrocarbon reserves are found in carbonate reservoirs.

2. Many of the previous researchers used liquids as the flowing fluid in their investigations. Reactions between the fluid and the rock matrix such as clay swelling, mineral dissolution and migration of fines are all dependent on time as well as temperature, and could have affected the results of any research which utilized liquids.

3. Existing formulations, developed to predict the effects of net confining pressure and temperature on absolute permeability, all contain rock specific parameters which must be determined by further testing (see Chapter 3, Review of Existing Correlations). A method of making reasonable qualitative predictions concerning the absolute permeability of a reservoir and utilizing known geological properties and history was felt to be lacking. In this investigation, it was hoped that, by studying the effects of net confining pressure and temperature on absolute permeability, and by correlating the results to what was physically happening to the individual grains in the rock matrix, logical and simple explanations for the results obtained could be formulated.

Flow tests were carried out on a variety of limestone and dolomite samples at isotropic net confining pressures up to 6000 psi and at temperatures ranging from 75°F to 325°F. Nitrogen gas was used as the flowing fluid to eliminate the possibility of reactions occurring with the rock matrix, as well as to minimize particle migration. In all cases conventional Klinkenberg Plots* were used to determine absolute permeability and slippage.

Net confining pressure is traditionally defined as the overburden pressure minus the pore pressure. For the purposes of this study the mean flowing pressure through each sample was assumed to be the pore pressure. In typical reservoirs the net confining pressure would seldom exceed 6000 psi.

Since normal cores are cut from a reservoir with the longitudinal axis of the core having a vertical orientation, the majority of studies carried out on the effects of net confining pressure on permeability measured the effects on vertical permeability only. In order to study the effects of net confining pressure on horizontal permeability, it was necessary to cut a small plug with the longitudinal axis oriented 90° to the longitudinal axis of the core from which it is cut.

* See nomenclature

This type of sample will be referred to as a "horizontal" sample in this study while the conventional core will be referred to as a "vertical" sample.

In a typical reservoir the longitudinal axis of the horizontally oriented sample would be parallel to the bedding planes and be situated at right angles to the major principal stress, while the vertically oriented sample would cut across the bedding planes and would have its longitudinal axis parallel to the major principal stress. Studies which investigated the effects of net confining pressure on horizontal permeability indicated that the results differed somewhat from those found on the vertically oriented samples. Although most fluid flow in reservoirs is in the horizontal direction, both types of permeability are of interest to the reservoir engineer.

Both vertically and horizontally oriented samples were tested to determine if the two permeability types would react differently due to previous reservoir stress conditions, grain orientation, or bedding effects. Tests were also conducted on both types of samples to determine if hysteresis effects on absolute permeability would result from high net confining pressures.

The temperature range chosen for this study was

intended to cover the range of temperatures which would be experienced in a reservoir undergoing a steamflood. In most steamfloods the reservoir would eventually be invaded by the steam itself, however the object of this investigation was to determine the effects from elevated temperature only.

One dolomite core was subjected simultaneously to elevated net confining pressures and temperatures to determine if the combined effect on the absolute permeability differed from the additive effects of each variable.

2. LITERATURE SEARCH

Numerous laboratory studies have been carried out on the topic of the effects of net confining pressure and/or temperature on the absolute permeability of consolidated rock. Much of the work was conducted using oil or water as the saturating fluid, however some of the tests utilized gas. Regardless of the fluid saturating the core, the results are all of interest to reservoir engineering, since oil, gas and water may all exist in any given reservoir.

a) Effects of Net Confining Pressure

As a reservoir is depleted the pore pressure decreases while the overburden remains constant, resulting in an increase in the net confining pressure on the rock matrix. As net confining pressure is increased it would be expected that both plastic and elastic deformation would occur, resulting in decreased permeability as well as porosity. Conversely, it could be expected that cores removed from reservoirs at reservoir conditions would undergo some expansion prior to permeability measurements being taken in the laboratory at low net confining pressures.

Early work in this area concentrated on determining the effect of radial and/or axial stress

on the permeability and porosity of consolidated rock. In 1952 Fatt and Davis[1] made one of the first advances in this area when they found that permeability measured (with nitrogen) at confining pressures of 15,000 psi was 25 to 60% lower than that measured at zero confining pressure. At net confining pressures of 3,000 psi (20 MPa) (equivalent to about 5,000 feet (1,500 m) of overburden and hydrostatic pore pressure), they found decreases in permeability of 10 to 40% in sandstone core plugs. Gray et al.[2] continued this work in 1963 and determined that uniform stress resulted in the maximum decrease in permeability. However it was recognized that horizontal stress would only be approximately one-third of vertical stress under normal reservoir conditions. They carried out horizontal and vertical flow tests on sandstone samples and found that, accordingly, the horizontal flow results were affected to a much lesser degree by isotropic net confining pressure than were the vertical results. As well as attributing their results to the anisotropic stress conditions in the reservoir, Fatt and Gray suggested that bedding effects and grain orientation were also responsible for the different results they recorded in the vertical and horizontal samples tested.

In 1969 Afinogenov[3] carried out research on sandstone rock samples using transformer oil as the flowing fluid. He observed permeability decreases up to 40% at 1,500 psi net confining pressures, and concluded that the compressibility of the rock is dependent on the amount and type of cement binding the grains together. He postulated a formula for determining permeability under increased pressures which contained two rock specific parameters, both of which had to be determined experimentally.

Vairogs, Hearn, Dareing and Rhoades[4] carried out a study in 1971 which included several carbonates. They observed that, in general, the lower permeability cores were affected more by high net confining pressures, regardless of the rock type. They also found that the presence of shale streaks and hairline fractures drastically increased a rock's degree of permeability reduction due to stress. Dolomites tested differed from sandstones only in that they displayed more pronounced hysteresis effects.

In 1975 Jones[5] found a significant loss of permeability in fractured carbonates with net confining pressures of the magnitude found in depleted reservoirs deeper than 2,000 feet. He developed a nomograph for predicting permeability reduction with increased net confining pressure in

fractured dense carbonates. Rock specific parameters were not required to use the nomograph, and it appeared to be accurate to within 10%, however it could only be used for fractured reservoirs.

In 1978 Gangi[6] also studied the effect of overburden pressure on fractured and unfractured porous rock. Empirical equations which he developed for each case required knowledge of rock characteristics which had to be determined through testing.

Low permeability sands were studied by Jones and Owens[7] in 1980 to determine the effect of net confining pressure and gas slippage on their permeability. Tests carried out on 3/4" (1.9 cm) horizontal plug samples indicated that generally, lower permeability samples are affected to a greater degree by stress than are higher permeability samples. Absolute permeability decreases as high as 30% were measured at 6,000 psi net confining pressure (NCP). When Jones and Owen plotted the cube root of permeability against the logarithm of the NCP, a straight line relationship was found, with different samples having varying slopes depending on their response to increased NCP.

b) Effects of Elevated Temperature

The study of the effect of temperature on

absolute permeability started in the late 1960's when Greenberg et al.[8] carried out tests (with no conclusive results) on artificially consolidated porous media. Their work was followed by a number of researchers who reported various results. Afinogenov[3], in 1969, examined the effects of temperature on the permeability of sandstone rock samples and found a large decrease in permeability to oil with increased temperatures up to 200°F.

In 1972, Weinbrandt, Casse and Ramey[9] studied the effect of temperature on absolute as well as relative permeability of sandstones. At temperatures of 175° F they found the absolute permeability to water decreased as much as 50% over the absolute permeability at room temperature. They also observed that when the temperature of the sample was returned to room temperature the absolute permeability increased to the initial value, suggesting little hysteresis effect.

Casse and Ramey[10] carried out further testing at elevated temperatures with distilled water, mineral oil, and nitrogen, and in 1979 reported that they believed the decrease in permeability found in sandstones previously was due to a temperature dependent reaction between the clay or sandstone and the distilled water. Tests carried out using oil and gas resulted in a slight increase and no change

in permeability respectively, for a range of temperatures up to 300°F.

Aruna [11] in 1976 and Aruna et al.[12] in 1977 carried out permeability determinations, for naturally consolidated sandstones at elevated temperatures. Their testing showed little or no temperature dependence when white mineral oil, nitrogen and 2-octanol were used as the flowing fluids. A reduction in permeability to water with increased temperature was attributed to an interaction between water and silica. A limestone sample, tested with water, showed no temperature dependence of permeability.

In 1978 Aktan and Farouq Ali[13] studied thermal stresses induced by hot water injection using a mathematical model. They assumed that horizontal stress would be 60% of vertical stress in the reservoir, but that to accurately determine the existing state of stress, the elastic moduli at the prevailing temperature had to be used. As well, they concluded that thermally induced stresses would dominate pore and mechanical stresses at higher temperatures (up to 500°F). Aktan and Farouq Ali also predicted that microfractures produced by thermal stresses caused by heating would increase permeability.

After carrying out extensive tests on Berea

sandstone cores in 1980, Sydansk[14] concluded, as did Casse and Ramey[10], that sandstone distilled water permeability (measured at a specific amount of distilled water injected) decreases with increasing flooding temperature. He found, however, that the permeability using 3% NaCl water was not affected significantly by increased flooding temperature. Sydansk also showed that a plug fired at 1000°C displayed less permeability reduction than did plugs fired at 450°C, and explained the result as being due to the additional clay stabilization resulting from the higher temperature. He reasoned that clay-particle migration, as well as clay swelling, resulted in the permeability damage measured.

c) Summary of Literature

Research carried out on the effects of net confining pressure on absolute permeability may be summarized as follows:

1) A decrease in absolute permeability occurs with increased net confining pressure for all rock types. Lower permeability rocks seemed to be affected to a greater degree.

2) The effect on horizontal and vertical permeability from increased net confining pressure appears to differ somewhat in sandstone rock samples, with horizontal permeability being affected to a lesser degree

then vertical.

3) The presence of fractures in a sample increased the degree of permeability reduction due to stress.

Literature on the effects of elevated temperature on absolute permeability may be summarized as follows:

1) The selection of the flowing fluid used is very important, as many liquids appeared to react with clays contained in the rock matrix.
2) Where reactions with the flowing fluid were not evident, temperature effects appeared to be very minimal, although few tests were carried out on carbonates.

3. REVIEW OF EXISTING CORRELATIONS

a) Pressure Effects

In 1969 Afinogenov[3] referred to the following empirical formula, derived by previous researchers, which may be used to represent the change in permeability which occurs with changes in net confining pressure:

$$K/K_o = 1 - \Psi\beta_{por}^{max} F(\sigma) \qquad (3\text{-}1)$$

Where:

Ψ = value dependent on pore compressibility and pore space configuration, determined experimentally.

β_{por}^{max} = compressibility of the pores at 16-20 atm, units are atm^{-1}.

$$F(\sigma) = \sigma min + (\sigma/\log \frac{\sigma max}{\sigma min}) \{\log \frac{\sigma max}{\sigma min} + .434 - \frac{\sigma min}{\sigma max} (\log \frac{\sigma max}{\sigma min} + .434)\}$$

where, σ_{min}, σ_{max}, and σ are the minimum NCP, maximum NCP, and the NCP of interest, in atm. Mean values of σ_{min} and σ_{max} are taken to be 13.5 atm and 1700 atm respectively.

Afenogenov continues to say that the pore compressibility is dependent on the amount and type

of cement binding the mineral grains, and may vary from 1.7×10^{4} to 7.0×10^{-4} atm^{-1} or more. It is apparent that although this equation may be used to predict absolute permeability with some accuracy, it would be necessary to first ascertain the values of Ψ and β_{por}^{max}, which would require testing of the same sort that is carried out in this investigation. After results had been obtained from testing, use of the equation would no longer be necessary. If these rock specific parameters could be estimated for various rock types with some consistency, however, this formula would be useful in predicting permeability losses with increased net confining pressure.

Gangi[6] devised the following model for whole porous rock:

$$K/K_o = \{1-C_o\{(P+P_i)/P_o\}^{2/3}\}^4 \qquad (3-2)$$

where:

K_o = initial permeability of loose grain packing

C_o = a constant (approximately = 2) dependent on packing

P_i = "equivalent pressure" due to cementation and permanent deformation of grains

P_o = effective elastic modulus of grains

This model was derived assuming spherical grains, and P_i was introduced to correct for deviations from this. As in Equation 3-1, however, it is still necessary to have reasonably accurate values for C_o, P_i, and P_o before meaningful estimates of permeability at different confining pressures can be made. Again the simplest method of obtaining these parameters would be to carry out permeability tests (on samples from the reservoir of interest) at various net confining pressures, and match the equation to the curve.

b) Temperature Effects

Somerton and Udell [15] suggested the general empirical formula

$$K/K_o = (T/T_o)^{A(P/P_o)^b K_o^c} \qquad (3\text{-}3)$$

where:

K = absolute permeability at temperature T and pressure P

K_o = absolute permeability at reference temperature T_o and pressure P_o

A,b,c, = constants which are to be determined experimentally for given rocks.

Values of A = -0.004, b = 1, c = -1.5 were felt by the authors to be representative numbers for an outcrop sandstone.

It is interesting to note that this formula contains a pressure term, which suggests that changes in permeability with temperature are dependent on stress conditions as well. Inclusion of this term is also misleading, as it may give the false impression that the formula could be used for predicting changes in permeability with changes in pressure as well. As can be seen, at $T = T_o$, the T/T_o term is equal to one. Since one raised to any power is one, it is obvious the equation is invalid for predicting changes in permeability with pressure.

Somerton and Udell have further stated that research has shown that sandstones under stress experience decreased permeability with increased temperature. This has not always been found to be true, as indicated by Casse and Ramey [10]. By setting the constant "A", equal to a negative value, the authors are insuring that a decrease in permeability will always be predicted for an increase in temperature. Finally, it was not felt

that such complex reactions such as clay particle migration, quartz dissolution, and thermal expansion can be accounted for in a simple formula, as these authors were suggesting.

4. Proposed Theory

a) Pressure Effects

i) Review

In a buried reservoir, the weight of the overlying rock acts to compress the pore space: The effect of this overburden is partially offset by the pressure of the fluid in the pore space, however. The difference between these pressures is referred to as the net confining pressure or effective stress. Effective stress (or net confining pressure) is defined by Skempton[16] using the formula:

$$p' = P_c - (1-C_s/C)P_p \qquad (4\text{-}1)$$

where

p' = effective stress or net confining pressure

P_c = confining stress

P_p = pore pressure

C_s = compressibility of solid rock matrix

C = compressibility of porous rock

For consolidated rocks the value of C_s/C typically falls between 0.1 and 0.5. This fraction is somewhat dependent on porosity, and for low porosity samples, such as would be

found in dolomite, would probably be quite small. Where pore pressure is significantly less than confining pressure, and for low values of C_s/C, net confining pressure may be approximated by the equation:

$$P' = P_c - P_p \qquad (4\text{-}2)$$

This formula is quite widely used in the petroleum industry, and since an exact determination of net confining pressure was not critical for evaluating the results of this study, this approximation for net confining pressure was used for the purpose of plotting results.

It has long been known that increasing net confining pressure causes compaction which results in decreased absolute permeability as well as porosity. Conversely, cores removed from the reservoir will expand prior to permeability measurements being made in the laboratory. It has also been shown that the loss of permeability experienced with increased net confining pressure varies with rock type, as well as with the rock's stress history. Rock specific parameters such as clay content, cement composition, crystal structure, grain

size and orientation, pore space distribution and the presence of fractures could all be expected to affect a reservoir rock's response to increased net confining pressure as well.

The primary concerns of this investigation relating to the effects of net confining pressure changes (for a specific reservoir) were to determine:

1. How close to in situ reservoir permeabilities are the permeabilities established in the laboratory (i.e. how much will the permeability change with a large decrease in net confining pressure and;
2. Will there be a significant decrease in horizontal permeability as the reservoir is depleted, or as pressure is drawn down around the wellbore.

ii) Stress Model

To develop an understanding of what is happening in a reservoir on a macroscopic scale, a microscopic model showing individual grains will be considered (Figures 1A and 1B). For simplification, grains are assumed to be 'tablet' shaped with the long axis oriented in the horizontal direction, as a normally deposited particle in a sedimentary sequence would lie. In carbonate reservoirs this

FIGURE # 1A

GRAIN ORIENTATION

BEFORE COMPACTION

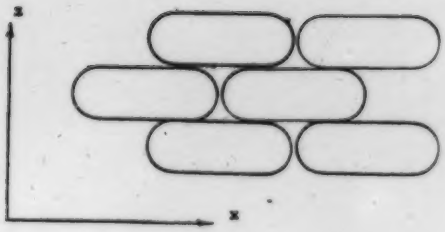

SIDE VIEW

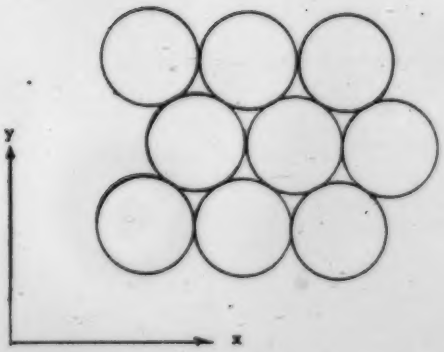

TOP VIEW

FIGURE #18

GRAIN ORIENTATION

AFTER COMPACTION

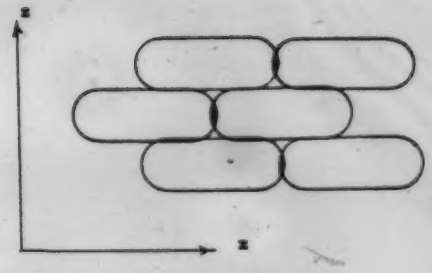

SIDE VIEW

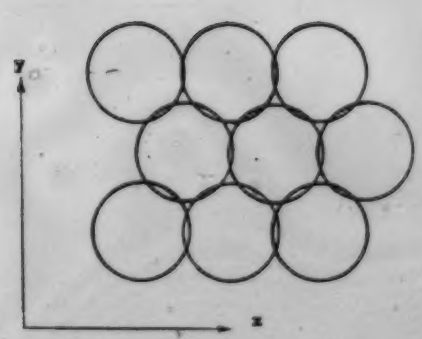

TOP VIEW

configuration could result from distortion due to overburden stress or recrystalization (dolomitization). Since it is commonly accepted that the effective horizontal stress in a reservoir is approximately 60% of the effective vertical stress, depending on the elastic moduli of the reservoir rock, it is probable that some plastic deformation of the individual grains (or crystals) would have occurred, resulting in a larger load bearing surface in the vertical direction, as depicted in figures 1A and 1B.

Upon removal of net confining pressure (as would occur when bringing a core to the surface), it is reasonable to assume some expansion of the rock matrix would occur in all three dimensions. The amount of expansion in each dimension would undoubtedly depend on the rock type and its stress history. A rock which had experienced high net confining pressure and had undergone stress failure and/or recrystallization would expand insignificantly. A rock sample which had deformed primarily in its elastic range however, would likely expand more with the same change in net confining pressure.

The hypothesis could therefore be made that

cores from deep reservoirs would likely exhibit relatively smaller changes in absolute permeability with changes in net confining pressure. Conversely, cores from shallow reservoirs would exhibit relatively larger changes in permeability for a comparable drop in net confining pressure. In general, the geologic history of the formation will play a large role in determining a sample's reaction to changes in stress. Formations which had previously undergone deep burial and subsequent erosion and uplift, for example, would show little change in permeability with changes in net confining pressures.

In this study, hysteresis effects, as well as changes in permeability with <u>decreasing</u> net confining pressure, were investigated to evaluate the relationship between permeability measured in commercial laboratories at low net confining pressures and permeabilities found at greater net confining pressures, such as would occur under reservoir conditions.

iii) Horizontal vs Vertical Effects

As previously stated, the effective horizontal stress (P_h') would be approximately 60% of the effective vertical stress (P_v') in a

typical reservoir. Since porous materials experience a decrease in compressibility with increased stress, it is reasonable to assume that the compressibility along the horizontal axis (C_h) would be significantly larger than the compressibility along the vertical axis (C_v). Considering that some plastic deformation had occurred, these compressibilities would differ at varying stress levels as well.

By relating these observations to changing stress conditions in reservoir, it may be theorized how vertical and horizontal permeability will be affected.

Initially, assuming typical reservoir conditions:

Overburden or Vertical
Confining Pressure (P_{cv}) = 5000 psi
Pore Pressure (P_p) = 2000 psi

and

$C_s/C_v = 0.50$
$C_s/C_h = 0.35$

therefore

$$\text{Effective Vertical Stress } (P_v') = P_{cv} - (1-C_s/C_v)P_p$$

$$= 5000 - (1-.5)2000$$

$$= 4000 \text{ psi}$$

and

$$\text{Effective Horizontal Stress } (P_h') = 0.6\ (P_v')$$

$$= 0.6\ (4000)$$

$$= 2400 \text{ psi}$$

and, by equating

$$P_h' = P_{ch} - (1-C_s/C)P_p$$

the horizontal confining pressure (P_{ch}) may be solved for (since in the reservoir it will not equal P_{cv}).

$$P_{ch} - (1-.35)\ 2000 = 2400 \text{ psi}$$

$$P_{ch} = 3700 \text{ psi}$$

Now, assuming P_{cv} and P_{ch} remain constant, and decreasing reservoir pore pressure to 1000 psi, new values for P_v' and P_h' may be determined.

$$P_v' = 5000\ (1-.5)\ 1000$$
$$= 4500 \text{ psi}$$
(an increase of 500 psi)

and

$$P_h' = 3700-(1-.35)\ 1000$$
$$= 3050 \text{ psi}$$
(an increase of 650 psi)

As this would result in a localized stress anomaly in the area where the pore pressure was reduced, it may not be an exact determination, however, it appears that the stress along the horizontal axis would tend to increase at a greater rate than along the vertical axis. Since the compressibility factor is also greater along the horizontal axis, these two factors would both work toward decreasing vertical permeability at a faster rate than horizontal permeability would decrease with declining pore (or reservoir) pressure.

In the determinations carried out in this study, the confining pressure was isotropic in

nature and was held constant. To determine how horizontal and vertical permeability would be affected under these conditions, the changes in stress along the principal axes may again be calculated.

Initially, setting

$$P_{cv} = P_{ch} = 4000 \text{ psi}$$
$$P_p = 1000 \text{ psi}$$

and assuming, as before

$$C_s/C_v = 0.5$$
$$C_s/C_h = 0.35$$

$$P_v' = 4000-(1-0.5)1000$$
$$= 3500 \text{ psi}$$

$$P_h' = 4000-(1-0.35)1000$$
$$= 3350 \text{ psi}$$

Now, increasing confining pressure to 5000 psi,

$$P_v' = 5000 - (1-0.5)\ 1000$$
$$= 4500 \text{ psi}$$

(an increase of 1000 psi)

and

$$P_h' = 5000 - (1-0.35)\ 1000$$
$$= 4350 \text{ psi}$$
(an increase of 1000 psi)

Under these conditions it is apparent that the effective stress is increasing the same amount along all principal axes, although the percentage increase along the horizontal axes is slightly larger. Taking into account the differences in compressibility between the axes, however, a larger decrease in vertical permeability would still be expected at low stress levels. At higher effective stresses it is probable that the compressibility factors would equalize resulting in similar responses for vertical and horizontal permeability.

b) Temperature Effects

i) Review

Most substances expand when heated, whether they are solid, liquid, or gaseous. Tests carried out on the major components of rock matrixes, (quartz, carbonates, and silicates) have shown that they all expand when heated (see Table 1). It is interesting to note that sandstone and limestone have coefficients of

TABLE 1

COEFFICIENTS OF THERMAL EXPANSION

EXPERIMENTALLY DETERMINED:

Sandstone = 7.9×10^{-6}/°F (1.43×10^{-5}/°C)

Limestone = 7.6×10^{-6}/°F (1.36×10^{-5}/°C)

Dolomite = $2.2 - 6.3 \times 10^{-6}$/°F ($.39 - 1.14 \times 10^{-5}$/°C)

(Dirty)

DOCUMENTED:

*Sandstone = $5.5 \pm 1 \times 10^{-6}$/°F ($1 \pm .2 \times 10^{-5}$/°C)

*Limestone = $4.4 \pm 2 \times 10^{-6}$/°F ($.8 \pm .4 \times 10^{-5}$/°C)

Dolomite = Not documented

*Silicates (Avg.) = 2.8×10^{-6}/°F ($.5 \times 10^{-5}$/°C)

*As documented in GSA Memoir 97, edited by Sidney P. Clark[17]

expansion approximately double that of silicates.

For simplification of the temperature model it was assumed that since both pore pressure and overburden pressure remained constant, the net confining pressure would remain constant in a reservoir. Although reservoir conditions will differ somewhat from laboratory conditions, it was felt that the difference in stress conditions would only affect the results to a small degree. This effect was investigated by Aktan and Farouq Ali[13], who observed that expansion in the horizontal plane would be inhibited to some extent by the surrounding rock mass.

Once again, the rock matrix can be investigated on a microscopic scale to determine how it is changing with temperature. Since silicates have lower expansion coefficients, rocks containing significant amounts will have to be examined separately. Henceforth they will be referred to as "heterogeneous" rocks. Reservoir rocks containing primarily limestone, dolomite, or sandstone will be referred to as "homogeneous".

ii) Homogeneous Matrix

For simplicity of calculations and as shown in Figure 2, spherically shaped grains are assumed for the temperature model. Once again, the effective stress will be as defined in equation 4-1. If all of the grains in this matrix expand equally, the packing pattern (tetrahedral) should remain the same and therefore the porosity will remain constant. Since the overburden pressure and pore pressure will remain constant, the effective stress should remain relatively constant with the exception of boundary effects, as previously discussed. It is therefore expected that, as shown in Figure 2, the cross section of the pore spaces will increase proportionately with the expansion experienced by the rock particles which will be:

$$\Delta r = r_1 C (T_2 - T_1) \qquad (4\text{-}3)$$

or

$$\Delta r = r_1 C \Delta T$$

where

r = radius of rock grain

C = coefficient of thermal expansion

T_1, T_2 = initial and final temperature

$\Delta T = T_2 - T_1$

$r_2 = r_1 + \Delta r$

Figure 2

TEMPERATURE EFFECTS - HOMOGENEOUS MATRIX

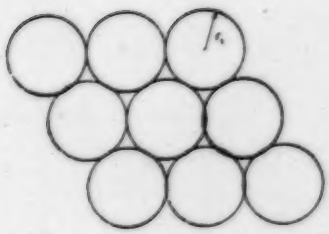

Matrix at ambient temperature, T_1
Average radius of grains = r_1

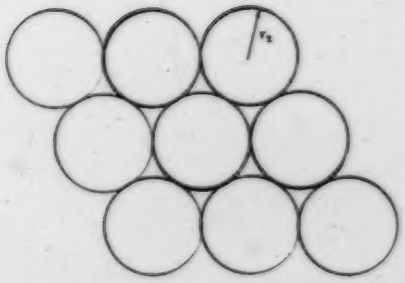

Matrix at elevated temperature T_2

Average radius of grains, $r_2 = r_1 + \Delta r$

Now, finally the change in permeability can be determined. Using Poiseuilles Equation: $K_\ell \propto r^2$ (since radius of pores is proportional to grain radius) and,

$$K_2/K_1 = r_2^2/r_1^2 = (r_1 + \Delta r)^2/r_1 \qquad (4\text{-}4)$$

$$= (r_1 + r_1 C\Delta T)^2/r_1^2 = (1 + C\Delta T)^2$$

where

K_1, K_2 = initial and final absolute permeability, respectively

For a relatively large change in temperature, say 140°C, a typical increase in absolute permeability can be estimated:

For sandstone:

$$C = 1 \times 10^{-5}/°C$$

therefore

$$K_2/K_1 = (1 + C\Delta T)^2 = \left(1 + \frac{1 \times 10^{-5}}{°C} \times 140°C\right)^2$$

$$= 1.002$$

Likewise for limestone:

$$C = 8 \times 10^{-6}/°C$$

and

$$K_2/K_1=(1 + 8 \times 10^{-6} \times 140)^2 = 1.002$$

In both cases this calculation results in a 0.2% increase in permeability, which would be hardly measurable. It is interesting to note, however, that the increase in permeability predicted is a function of the change in temperature squared. Further increases in temperature should therefore result in proportionately larger increases in permeability.

iii) Heterogeneous Matrix

Initially it will be assumed again that the matrix is composed of spherical particles (Figures 3A, 3B, and 3C). As the matrix is heated, the different materials will expand at different rates. As can be seen in Figures 3B and 3C, there are two possible outcomes, depending on whether silicates are the imbedded material or form the matrix. A <u>decrease</u> in permeability would be expected if the <u>matrix</u> was <u>silica</u> and the imbedded particles were sandstone or carbonate, as the greater

FIGURE #3

TEMPERATURE EFFECTS-HETEROGENEOUS MATRIX

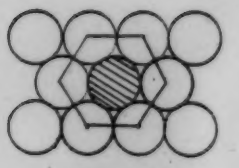

FIGURE 3A

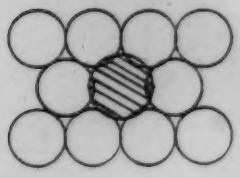

FIGURE 3B

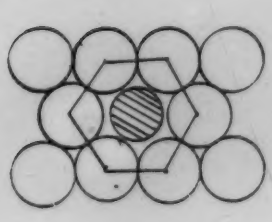

FIGURE 3C

MATRIX MATERIAL (COEFFICIENT OF THERMAL EXPANSION = C_1)

IMBEDDED MATERIAL (COEFFICIENT OF THERMAL EXPANSION = C_2)

IF $C_2 > C_1$,
A DECREASE IN Ø, K, AROUND IMBEDDED MATERIAL OCCURS

IF $C_2 < C_1$,
AN INCREASE IN Ø, K, AROUND IMBEDDED MATERIAL OCCURS

expansion of the imbedded particles would result in decreased porosity. Conversely, if the imbedded particles were silicates (which would be more common, such as in a dirty dolomite or sandstone) an increase in porosity, as well as permeability, would be expected.

In the case of a reservoir rock composed of sandstone with embedded silicates, what change in K_ℓ would be expected to happen when it was heated? Referring to Figures 3A and 3C, the change in the cross-sectional area of the pore space can be determined for an increase in temperature. Since permeability is proportional to the cross-sectional area available for flow this should give an indication of the change in permeability which may be expected.

Referring to Figure 3A, the initial cross-sectional area of pore space can be determined by subtracting the area covered by sand grains from the total area. The area of a hexagon (A_h) is given by the equation,

$$A_h = 3(3^{\frac{1}{2}}/2)X^2 \qquad (4\text{-}5)$$

Where X is the length of each side. Since the

length of each side of the hexagon is equal to twice the radius of the sandstone grains (r_{sd}),

$$A_h = 3(3^{\frac{1}{2}}/2)(2r_{sd})^2 = 6(3^{\frac{1}{2}})\ r_{sd}^2 \qquad (4\text{-}6)$$

The area covered by grains (where radius of the silica grains = r_{sl}) may be determined by summing the areas of the sandstone and silica grains.

$$A_g = A_{sd} + A_{sl} = 6(\pi r_{sd}^2)/3 + \pi r_{sl}^2 = 3\pi r_1^2, \qquad (4\text{-}7)$$

(where r_1 is the initial average grain radius and $r_1 = r_{sd} = r_{sl}$)

Now, subtracting the grain cross-sectional area from the total area, the initial cross-sectional area of the pore spaces (A_{po}) can be determined.

$$A_{pol} = A_h - A_g = 6(3^{\frac{1}{2}})\ r^2 - 3\pi r_1^2, = 0.96753\ r_1^2 \qquad (4\text{-}8)$$

Upon heating by 140° C, the particles will expand as shown in Figure 3C.

$$r_{sd} = r_1 (1+C_{sd}\Delta T)$$
$$r_{sl} = r_1 (1+C_{sl}\Delta T)$$

Where C_{sd} and C_{sl} are the coefficients of thermal expansion for sandstone and silica.

Substituting $C_{sd} = 8X10^{-6}\ {}^{o}C^{-1}$ and
$C_{sl} = 5X10^{-6}\ {}^{o}C^{-1}$

$$r_{sd} = (1+8X10^{-6}X140)r_1$$
$$= 1.00112\ r_1$$

and

$$r_{sl} = (1+5X10^{-6}X140)r_1$$
$$= 1.00070\ r_1$$

Now the area inside the hexagon in Figure 3C will be:

$$A_h = 6(3^{\frac{1}{2}})\ r_{sd}^2$$
$$= 6(3^{\frac{1}{2}})\ (1.00112)^2\ r_1^2$$
$$= 10.41560\ r_1^2$$

And the area covered by grains can be determined by adding the cross-sectional areas

of the expanded silica and sandstone grains.

$$\begin{aligned} A_g &= A_{sd} + A_{sl} \\ &= 6(\tfrac{\pi}{3} r_{sd}^2) + \pi r_{sl}^2 \\ &= 2\pi(1.00112\ r_1)^2 + \pi(1.00070 r_1)^2 \\ &= 9.44326\ r_1^2 \end{aligned}$$

Therefore the cross-sectional area of the pore space may be calculated:

$$\begin{aligned} A_{po2} &= A_h - A_g \\ &= 10.41560\ r_1^2 - 9.44326\ r_1^2 \\ &= 0.97234\ r_1^2 \end{aligned}$$

If we assume, as before, that permeability is proportional to the cross-sectional area of the pore space, the theoretical change in permeability may be ascertained

$$\begin{aligned} K_2/K_1 &= A_{po2}/A_{po1} \\ &= 0.97239\ r_1^2/0.96753\ r_1^2 \\ &= 1.005 \end{aligned}$$

For this extreme case, where the sample contained 25% silicates, a 0.5% increase in permeability would therefore be expected. Although this is greater than in the

homogeneous model, it is still not significant.

c) Combined Effects of Increased Temperature and Net Confining Pressure.

Due to the more or less uniform (and insignificant) expansion of most minerals over the temperature range studied in this investigation, the change in the microstress state within a typical reservoir rock would be relatively small. At elevated temperatures it would therefore be expected that, since the stress state would be similar to normal temperatures, the effects of increased net pressures on a rocks permeability would not differ significantly from those experienced at normal (or ambient) temperatures. Depending on the rock type however, it is possible that a change in the elastic moduli of the rock matrix with temperature could result in a small change in behavior.

Similarily, at high net confining pressures, it would not be anticipated that the effects on permeability from increasing temperature would differ from the effects measured at low net confining pressures. This is thought to be the case particularly since the expansion due to temperature has been shown to be relatively independent of the existing stress conditions, providing the net confining pressure remains constant.

5. Experimental Apparatus

a) Cell Assemblies -

Two high pressure cells were used to carry out all flow tests: a three-inch cell for the vertical cores, and a one-inch cell for the horizontal plugs.

The three-inch cell (shown in Figure 4A) was constructed from a cylinder of stainless steel nine inches in diameter and incorporated walls two inches thick and capable of withstanding over 7000 psi. The entrance to the chamber was threaded to a depth of approximately three inches to accomodate the six-inch diameter cell cap. A three-inch diameter platen (Figure 4B) was fastened to the bottom of the cell cap to distribute gas evenly over the end of the core samples. A second platen (Figure 4C) was situated at the bottom of the core and held in place by means of a holding plate. Both top and bottom platens incorporated two ports: one for fluid flow, and one for pressure measurement. Sintered steel plates were designed to separate the core from the caps and further enhance fluid distribution over the core ends. A two-part membrane consisting of a heat shrinkable teflon sleeve and a thick silicone sleeve isolated the core sample from the overburden fluid in the cell chamber.

FIGURE 4A

PLAN VIEW OF 3" CELL ASSEMBLY

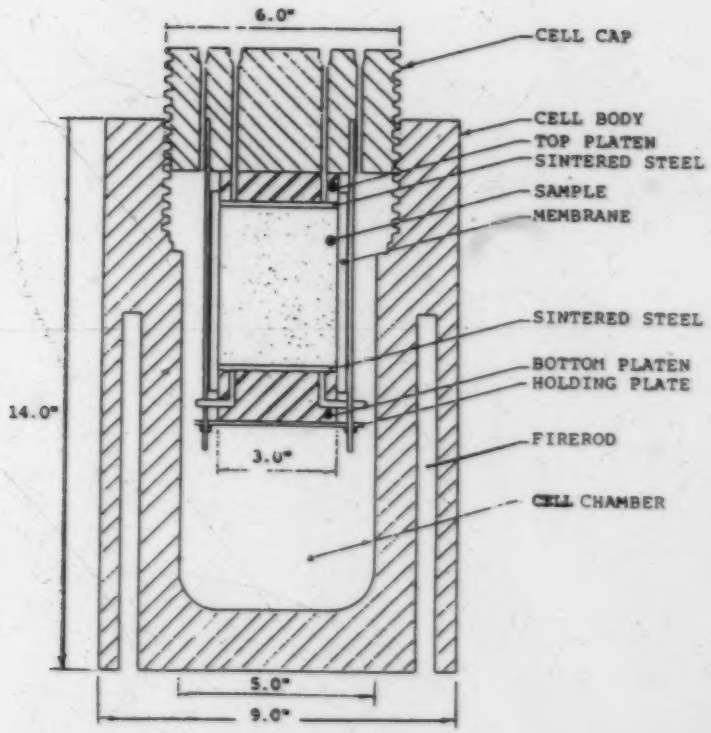

FIGURE 4B

TOP PLATEN - 3" SAMPLES

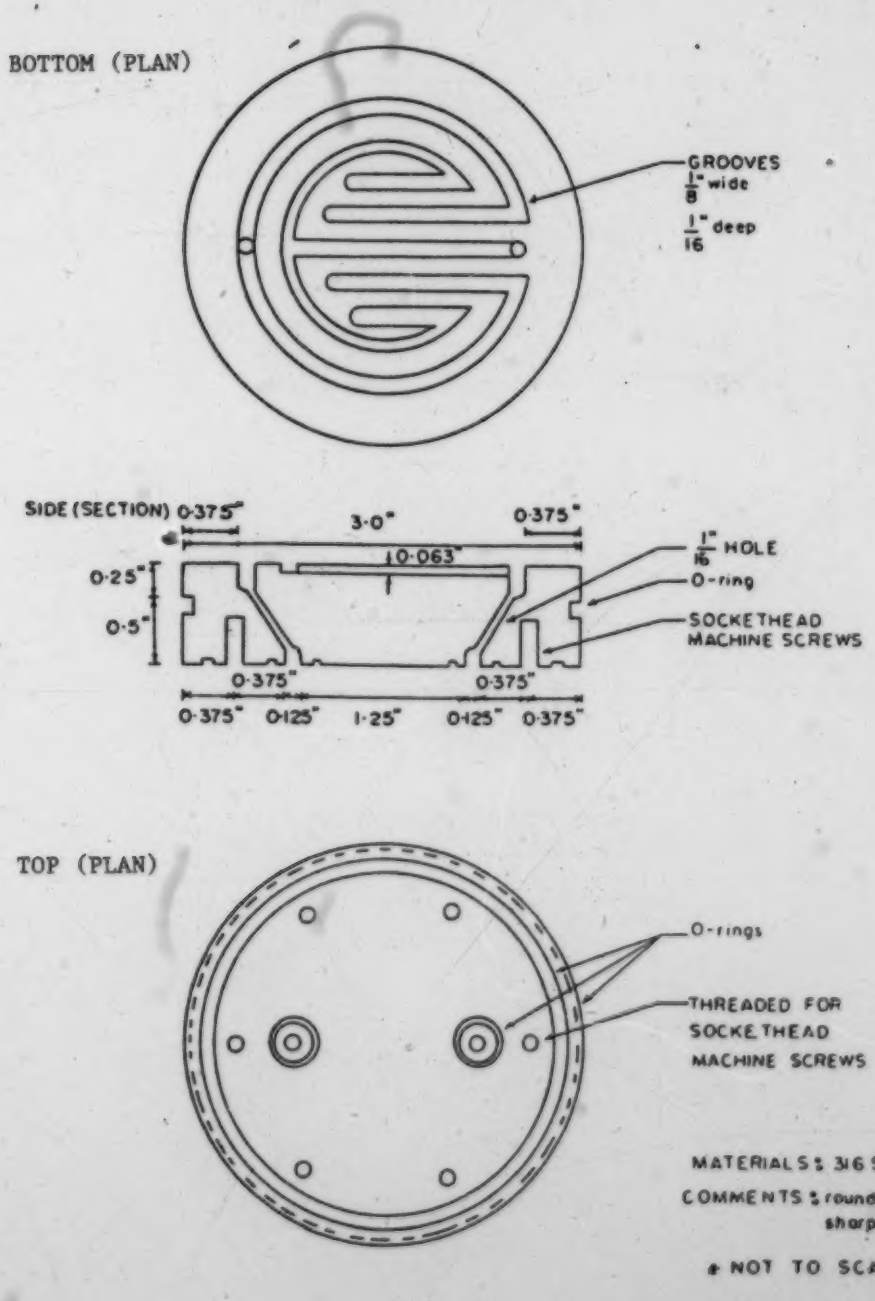

FIGURE 4C

BOTTOM PLATEN - 3" SAMPLES

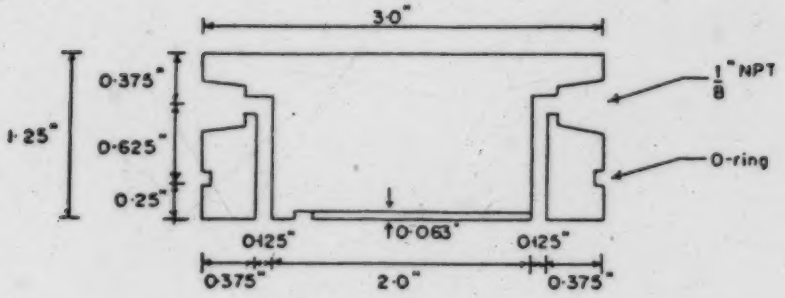

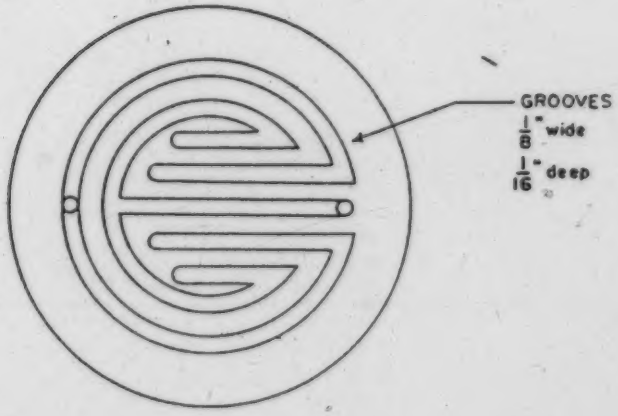

materials: 316 SS

comments: round off sharp corners

* NOT TO SCALE

Two stainless steel coiled tubes provided communication to the bottom platen through holes in the cell cap. The cell was heated by means of firerods inserted in holes within the cell walls.

The one-inch cell assembly used for testing the plugs (Figure 5) was similar in design to the three inch cell assembly, except that it was smaller, and the cell cap was flanged rather than threaded. The top and bottom platen were not grooved (due to their smaller size) and it was not necessary to clamp them in place, as the one-inch samples were much lighter than the three-inch samples.

b) Control System

The apparatus used to control and measure flowrates, as well as to control conditions in the cell, is depicted in Figure 6.

Temperature in the cell was controlled by means of a temperature controller which received input from a thermocouple inserted into the cell fluid through an opening in the cell cap. A temperature readout attached to the thermocouple was used to ensure that an accurate and constant temperature was attained.

Initially mineral oil was used as a cell fluid to transmit overburden pressure to the samples. Water was later substituted for overburden fluid as it greatly simplified cleaning the core sample if a

FIGURE 5

PLAN VIEW OF HORIZONTAL
CELL ASSEMBLY

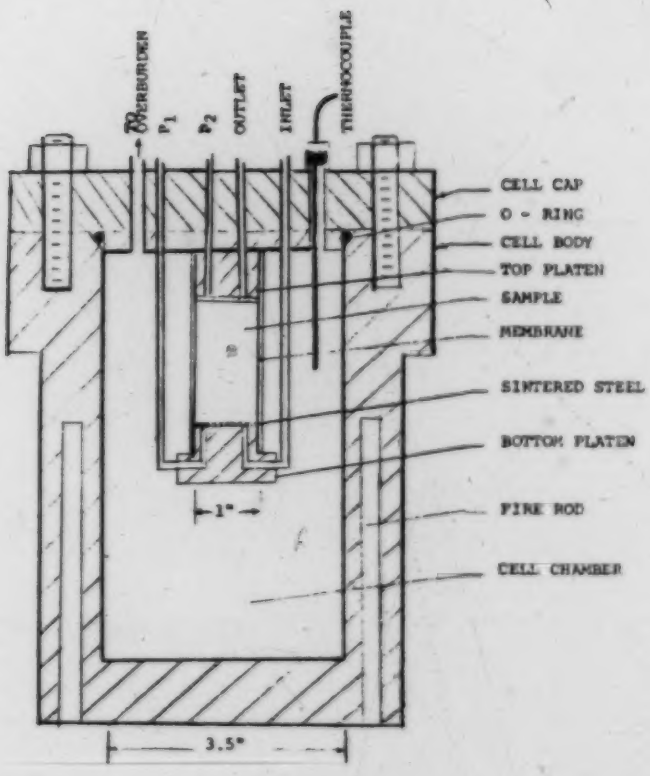

FIGURE 6
SCHEMATIC OF APPARATUS

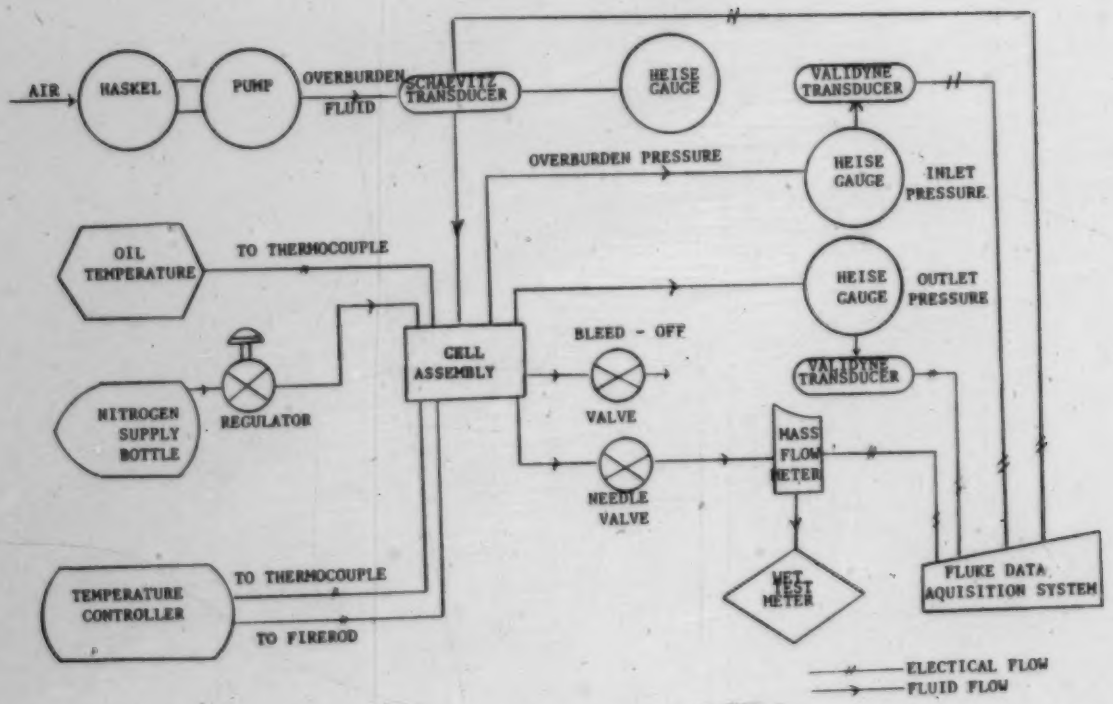

leak in the membrane occurred. Overburden pressure was supplied by a positive displacement Haskel Pump, which was in turn driven by compressed gas. Overburden pressure was recorded by means of a Schaevitz pressure transducer connected to a Fluke Datalogger. A Heise pressure gauge was used to monitor overburden pressure, as well as calibrate the pressure transducer at any time. A bleed off valve on the cell was used for decreasing the overburden pressure.

Nitrogen gas was utilized as a flowing fluid to avoid reactions with the sample matrix as well as to minimize any particle migration within the cores. A 2500 psi cylinder of compressed nitrogen equipped with double adjustable regulators was used as a source. Gas was channelled through stainless steel tubing into the inlet port on the cell cap. The gas was then passed through coiled stainless steel tubing (where it was brought to system temperature) into the bottom end platen and through the sample. Outlet pressure was set by means of a fine metering needle valve. Both inlet and outlet pressures were measured at the sample face by means of Validyne transducers. Precalibrated Heise gauges were used with the transducers as a means of calibration, as well as for quick visual readout of inlet and outlet flow pressures.

Instantaneous flow rates were measured downstream of the needle valve (at essentially atmospheric pressure) using a Matheson Mass Flowmeter (Figure 6). A precalibrated precision wet test meter was utilized to calibrate the flowmeter, as well as to measure very low flow rates encountered while testing the one-inch horizontal plugs. Cleaning and recalibration of the mass flow meter was periodically necessary, as it became contaminated with overburden fluid whenever a leak occurred in the membrane surrounding the core.

Output from the Validyne pressure transducers and the mass flowmeter was monitored by the Fluke Datalogger, which incorporated a visual LED readout and provided a printed summary of all readings. Calibration of each of the inputs was carried out using a calibration factor (for example, a readout of 0 to 10 mv from the transducer translated to a pressure change of 0 to 1000 psig, with a calibration factor of 100). The Fluke Datalogger allowed for both resetting of the calibration factor for greater precision and for substitution of pressure transducers with different ranges.

c) Sample Preparation

Most of the tests in this investigation were carried out on samples of vuggy dolomite reservoir

rock taken from the Grosmont Formation in Northern Alberta.

The three-inch cores were cut into lengths of approximately 4.25 inches and cleaned of residual oil and other fluids with a distillation apparatus utilizing boiling toluene. The ends of the cores were sandblasted to open any plugged pores and the circumference was coated with a thin layer of thermoset resin to fill any vugs. The core sample was then fitted between the sintered plates and cell caps and an impermeable heat shrinkable teflon sleeve was shrunk over the sample and caps. A thick silicone sleeve was fitted over the teflon sleeve and clamped in place with hose clamps for added protection against leakage of overburden fluid. The coiled tubing was attached and the bottom plate was clamped to the top cell cap. Upon inserting the sample into the cell body and fastening the top cell cap in place, the apparatus was ready for a test run to be carried out.

The procedure for preparing the one-inch horizontal plugs was essentially the same as for the three-inch cores. The length of the horizontal plugs were determined by the diameter of the cores from which they were taken, which in this case resulted in approximately 2.4 inch-long samples. The heat-shrinkable teflon sleeves were deleted from

the installation of the one-inch plugs as a leak-proof seal around the platens could not be obtained. (The larger platens incorporated a rubber O-ring, the smaller ones did not.) As the silicone sleeves were found to be impermeable to water, water was used as an overburden fluid from this point on and teflon sleeves were no longer required.

6. Procedure

a) Theory - Evaluation of Absolute Permeability

For each permeability determination at a specific temperature and net confining pressure it was necessary to construct a Klinkenberg[18] Plot (Figure 7) since permeability values determined using gas as a flowing fluid are affected by a phenomenon known as slippage.

Gas slippage can best be understood by studying fluid flow in a small capillary. If a liquid is flowing in the capillary the molecules touching the capillary walls will have zero, or almost zero velocity, while the molecules in the centre of the capillary will have the maximum velocity. When a gas is flowing in the capillary (with a mean free molecular path equivalent to or greater than the capillary diameter), the velocity of all the molecules will be the same. If the mean free path of the molecules is decreased to less than half the diameter of the capillary (due to increased pressure) the molecules near the walls of the capillary will slow down due to friction. At infinite pressure the gas will theoretically behave like a liquid. This difference in behavior is known as slippage, and the correction factor is known as the Klinkenberg Slip Factor (b). Anything which affects either the mean free path of the gas

FIGURE 7
TYPICAL KLINKENBERG PLOT

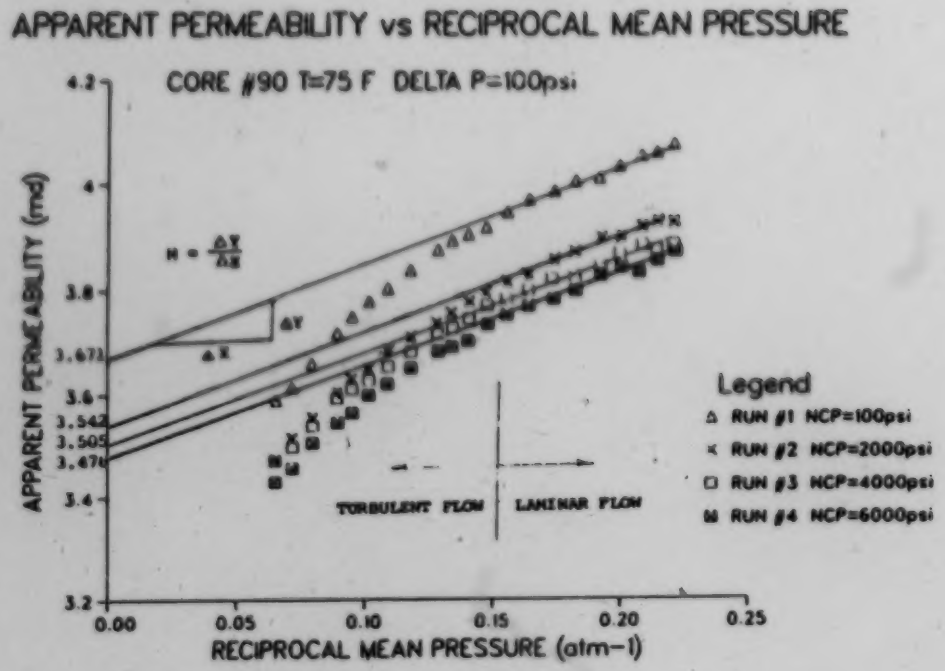

molecules or the diameter of the capillary will result in a change in this slip factor, since it is directly proportional to λ and inversly proportional to d, i.e.,

$$b \propto \lambda/d$$

where

λ = mean free path of gas molecule

d = diameter of pore throat

As can be seen in Figure 7, a Klinkenberg Plot is constructed by correlating a number of apparent permeabilities (K_a) (measured over a range of mean flowing pressures), against the inverse of the mean flowing pressures ($1/P_m$). The linear portion of the resulting plot may then be extrapolated to infinite mean pressure (at the Y-intercept) to obtain an equivalent liquid permeability (K_ℓ). This permeability is unique to each sample and represents the fluid independent absolute permeability of the sample. Units of permeability are length squared, usually expressed in μm^2 or darcies.

The straight line portion of the Klinkenberg Plot indicates laminar flow, while at higher flowing pressures the effects of vesco-inertial flow are manifested by the curved portion of the plot.

The equation for the linear portion is known as

the Klinkenberg Equation:

$$K_a = K_\ell \ (1+b/P_m) \qquad (6\text{-}1)$$

Writing the Klinkenberg Equation in the form of a straight line equation ($y = M X + b$),

$$K_a = K_\ell b \ (1/P_m) \ K_\ell$$

the slope of the line (M) can be equated to $K_\ell b$ and the slip factor (b) may be solved for, i.e.,

$$M = K_\ell b$$

and

$$b = M/K_\ell \qquad (6\text{-}2)$$

Both the slope M and the y-intercept (K_ℓ) are easily obtainable from the graph.

In addition to the slippage effect, the tortuous path followed by gas through porous media results in an inertia effect. As this phenomenon is thought to be related to the velocity of the gas, a number of flow tests using various pressure drops were investigated as follows:

1. The simplest method of conducting the flow tests would have been to set the upstream pressure at a constant level and lower the

outlet pressure, thereby obtaining apparent permeabilities over a range of mean flowing pressures. This procedure resulted in large increases in flowrates, as well as gas velocities, which in turn resulted in an early incidence of visco-inertial flow conditions.

2. Conversely, holding downstream pressure constant at atmosphere pressure and increasing upstream pressure was considered. Again, this procedure results in large increases in gas flow rate and velocities during the course of a test run. Due to ensuing changes in inertia effects and slippage this method was discounted.

3. By varying upstream and downstream pressure while maintaining a constant pressure drop, the velocity of the gas flowing through the core is held essentially constant, and inertia and slippage effects should therefore remain relatively constant. This method resulted in the best range of permeabilities in the laminar flow regime (straight line portion of the Klinkenberg Plot), therefore it was adopted for this investigation.

To further investigate if visco-inertial effects were present, data from the linear portion of a Klinkenberg plot was graphed using

a quasilinearization approach suggested by Casse and Ramey[10]. A linear plot could not be obtained by this method, however, and it was abandoned. A Reynolds number determination was carried out as well, using a method outlined in Denevers[19], and is included in Appendix A4. The Reynolds number obtained using this method was unrealistically low, however, possibly because the particle diameter determination method used may not have been applicable to porous media such as dolomite.

b) Method

For each test run carried out to obtain a Klinkenberg Plot, the net confining pressure (NCP) was maintained at a constant level. Since net confining pressure (NCP) is defined as the overburden pressure minus the pore pressure, the overburden pressure applied to the core had to be varied with the mean flowing pressure (pore pressure) in order to maintain the predetermined level of NCP.

Essentially the tests carried out on the samples could be categorized into five different groups as follows:

Group 1 - Pressure Effects

Flow tests carried out at room temperature over a

range of NCP's ranging from several hundred psi to 6000 psi.

Group 2 - Hysteresis Losses - Pressure Effects

Flow tests carried out at room temperature starting at a low NCP and working stepwise up to an NCP of 6000 psi, then decreasing stepwise to the initial low NCP.

Group 3 - Temperature Effects

Flow tests carried out at a constant NCP starting at room temperature, and progressing to higher temperatures after each flow test, to a maximum temperature of 320°F.

Group 4 - Hysteresis Losses - Temperature Effects

After carrying out the temperature tests, the sample was cooled to room temperature and a permeability determination was conducted to determine if any permanent deformation had occurred due to heating.

Group 5 - Combined - Temperature & Pressure Effects

Flow tests carried out over range of NCP's up to 6000 psi at room temperature. The temperature was then increased in stepwise fashion up to 320°F and flow tests repeated over range of NCP's after each temperature increase.

Extensive tests were run on three-inch Indiana limestone cores as well as on the Grosmont carbonate and an unidentified sandstone. A summary of the

successful tests which were carried out is shown in Table 2.

Cores were weighed before and after each run to determine if any overburden fluid had invaded. If any weight gain was experienced the results of the test runs were discarded.

Sandstone, limestone, and dolomite core samples were measured and heated to 320°F, then remeasured to determine the amount of thermal expansion experienced by each rock type.

TABLE 2

SUMMARY OF SUCCESSFUL TESTS

Core #	PROPERTIES	SIZE	TESTS RUN
1L	Limestone 2.55 md	3" x 4½"	Group 1
3L	Limestone 1.85 md	3" x 4½"	Group 5
4L	Limestone 2.00 md	3" x 4½"	Group 1, Group 4
90	Dolomite 3.63 md	3" x 4½"	Group 2, Group 3
92	Dolomite .728 md	3" x 4½"	Group 2, Group 4
133A	Dolomite 59.3 md	3" x 4½"	Group 2, Group 3
6L	Limestone 3.18 md	3" x 4½"	Group 2, Group 3
25	Sandstone 218 md	3" x 4½"	Group 3
*93B	Dolomite 23.8 md	1" x 2½"	Group 2, Group 3
*133A	Dolomite 452.5 md	1" x 2½"	Group 2, Group 3
**133A	Dolomite 5.9 md	1" x 2½"	Group 2, Group 3

* Horizontal Plug - extracted from 3" core sample at right angles to the longitudinal axis of the source sample.

** Vertical Plug - extracted from 3" core sample at same orientation as the source sample.

c) Processing of Data

As previously stated, a number of flow tests conducted over a range of mean flowing pressures were required to determine an adequate range of apparent permeabilities in order to construct a Klinkenberg Plot which could be used to obtain an accurate K_ℓ (or liquid absolute permeability). Each set of flow tests was referred to as a 'run' and resulted in one value of absolute permeability for the core at a specific temperature and net confining pressure.

In general, a 'run' consisted of approximately 25 flow tests with the first flow test carried out at an inlet pressure of eight or nine hundred psig. Consecutive tests were carried out at progressively lower inlet pressures, while maintaining a constant pressure drop across the sample. The lower limit of flowing pressure was reached when the outlet pressure approached atmospheric pressure. (See Appendix B for flow test data for all cores).

After each flow test had been allowed to stabilize, a printout of inlet pressure, outlet pressure, flow rate and overburden pressure (all in millivolts) was recorded with the Fluke Datalogger. Upon completion of each run this raw data was entered into a Fortran data file. The data was in turn interpreted by means of a Fortran program

(Appendix A1), which read the data and converted the transducer readings into pounds per square inch absolute and the mass flow meter readings into milliliters per second. The calibration factors required for these conversions were input into the program each time as required, along with the sample temperature.

Values for permeability for each flow test were calculated using the Darcy Flow Equation for steady state, isothermal, laminar flow (Appendix A2). Nitrogen viscosity was calculated using the correlation by Kestin and Wang[21]. Output from the program in tabular form included: input pressure, outlet pressure, mean flowing pressure, overburden pressure, and net confining pressure (all in psia); as well as the flow rate at atmospheric pressure, the flow rate at mean flowing pressure, and values for the inverse mean pressure and permeability (see Appendix B for tables of all runs). Values for inverse pressure and apparent permeability were also output to a data file which was used to create the Klinkenberg Plots with a plotting program. A sample calculation of an apparent permeability is included in Appendix A3.

Using the extrapolated permeabilities from the resulting Klinkenberg Plots, graphs were constructed showing: K/K_{atm} versus net confining pressure,

$K/K_{75°F}$ versus temperature, and slip factor versus temperature for each core. (Figures 8,10 and 22 are examples which will be discussed later).

d) Error Analysis

Extrapolating the linear portion of the Klinkenberg plots to the ordinate to obtain the absolute liquid permeability (K_ℓ) at infinite mean pressure required some personal judgement, and introduced the possibility of some error into the investigation. By plotting a group of consecutive runs for one sample on the same Klinkenberg Plot (as shown in Figure 7), it was felt that some consistency between extrapolated valves of K_ℓ would be maintained, diminishing the inherent experimental error. In addition to maintaining consistency between runs, it was felt that this method was superior to using a least-squares function on the computor, since it allowed for disregarding extraneous data points as well as an individual examination of each run to determine at what pressure visco-inertial effects became apparent.

Other considerations regarding experimental error involved limitations of the experimental apparatus. The mass flow meter was precise to within 1/100 of a ml/sec and very accurate within its designed flow range. Below 10 ml/sec and above 400 ml/sec accuracy dropped off rapidly, however.

For tests where the flow rate dropped below 10 ml/sec the wet test flow meter was used. Since the wet test flow meter measured the total volume of gas flowed during a flow period, more accurate flow rates could be obtained by utilizing longer flow periods.

Accuracy over the range of the pressure transducers depended on how well the calibration was carried out and the condition of the transducer. The transducers used were generally accurate to within 1 or 2 psi over the range used. Although this represents a significant amount of error it was not felt to be too detrimental to the tests, since the primary concern was the difference between absolute permeabilities determined at various conditions, rather than the specific permeability of any one sample at some specific set of conditions. If the procedure used was consistent in each flow test, a comparative analysis could be made between a series of flow tests. If consistency was maintained throughout, the effect of experimental error could therefore be neglected for the investigation as a whole.

The Fluke Datalogger utilized a four digit readout, and therefore could cover a range from 0 to 9,999. When used in conjunction with a 1000 psi transducer, pressure readings could be obtained to a

precision of one tenth of a psi. (For example: a reading of 5331 on the datalogger would correlate to a pressure of 533.1 psi)

During runs which required small pressure drops (5 psi) the precision of data readings became a significant consideration. For these runs 250 psi range transducers were used. The error in the pressure drop due to precision was calculated as follows:

Range = 0-250 psi

Readout = 0-10 milliamps,

therefore 1 milliamp = 25 psi

Precision to 1/1000 milliamps

or to 25 x 1/1000 = .025 psi

Since $\Delta P = P_1 - P_2$, error = .025 + .025 = .05 psi

and for ΔP = 5 psi, % error = $\frac{.05 \text{ psi}}{5 \text{ psi}} \times 100\% = 1.0\%$

It was therefore necessary to consider that, when determining absolute permeability of a sample for which a 5 psi pressure drop had been used, variations in readings as high as 1% existed due to data precision. Most of the cores tested utilized pressure drops of 100 psi however, for which an error of only 0.2% was calculated.

7. Results

Successful flow tests were carried out on essentially four different types of cores; vertically oriented dolomite, horizontally oriented dolomite, homogeneous limestone, and homogeneous sandstone (see core summary, Table 2). The results for each type of core were grouped together for comparison, as cores of the same type generally displayed similar results.

a) Vertical Dolomite Cores

Three three-inch diameter dolomite cores with a wide range of vertical permeability were studied to investigate the effects of net confining pressure (NCP) and temperature on absolute permeability. Complete results for these three samples are in Appendices B1, B2 and B3.

Since two of the cores, core #133 A and core #90 had been subjected to high NCP in previous tests, a comparison between the effects of NCP on permeability prior to hysteresis effects could not be made.

Figure 8 represents the relative changes in absolute permeability (K_ℓ) with NCP by correlating K/Katm (K_ℓ at any pressure over K_ℓ at a low NCP) versus NCP for the three samples after hysteresis losses. It may be observed that for all three samples a decrease in permeability with increased

FIGURE 8

K/Katm vs NET CONFINING PRESSURE

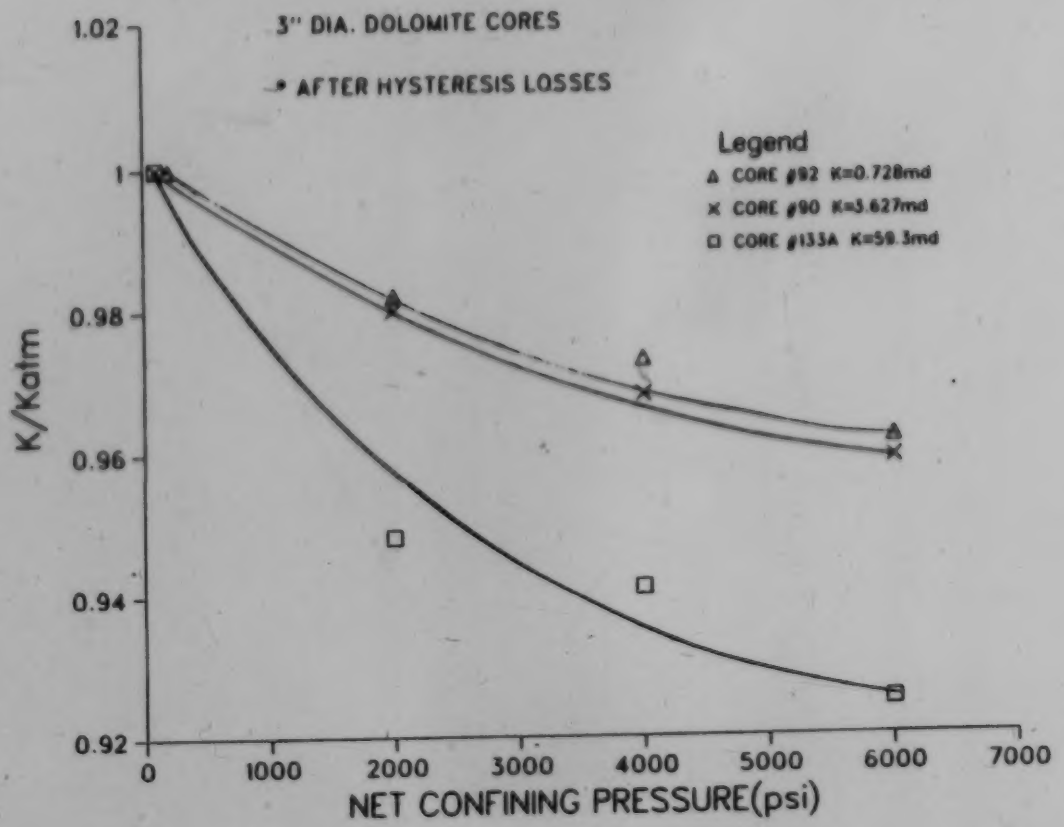

NCP occurs, the greatest change being observed for the highest permeability sample.

Hysteresis effects are illustrated in Figure 9 for core #92 which had not been previously stressed. To determine the effect of NCP on permeability before and after hystersis losses, permeability determinations were carried out at progressively higher NCP, then at progressively lower NCP. Prior to hysteresis losses core 92 initially displayed a 15% loss in permeability at 6000 psi NCP, while after hysteresis losses only a 4% difference was apparent.

As shown in Figure 10, increasing the temperature of the dolomite cores (while keeping the NCP constant) in all cases caused an apparent increase in absolute permeability. Again the effect was the greatest in core #133A, which had the highest permeability, and the least in core #92 which had the lowest permeability. A run carried out on core # 92 after it had cooled off (run #15) showed the absolute permeability to be the same as it was prior to being heated, indicating no hysteresis effects as a result of temperature change.

In Figure 11, K/K75 was plotted for various net confining pressures, while in Figure 12 K/Katm was plotted at various temperatures. As can be seen in

FIGURE 9

ABSOLUTE PERMEABILITY vs. NET CONFINING PRESSURE

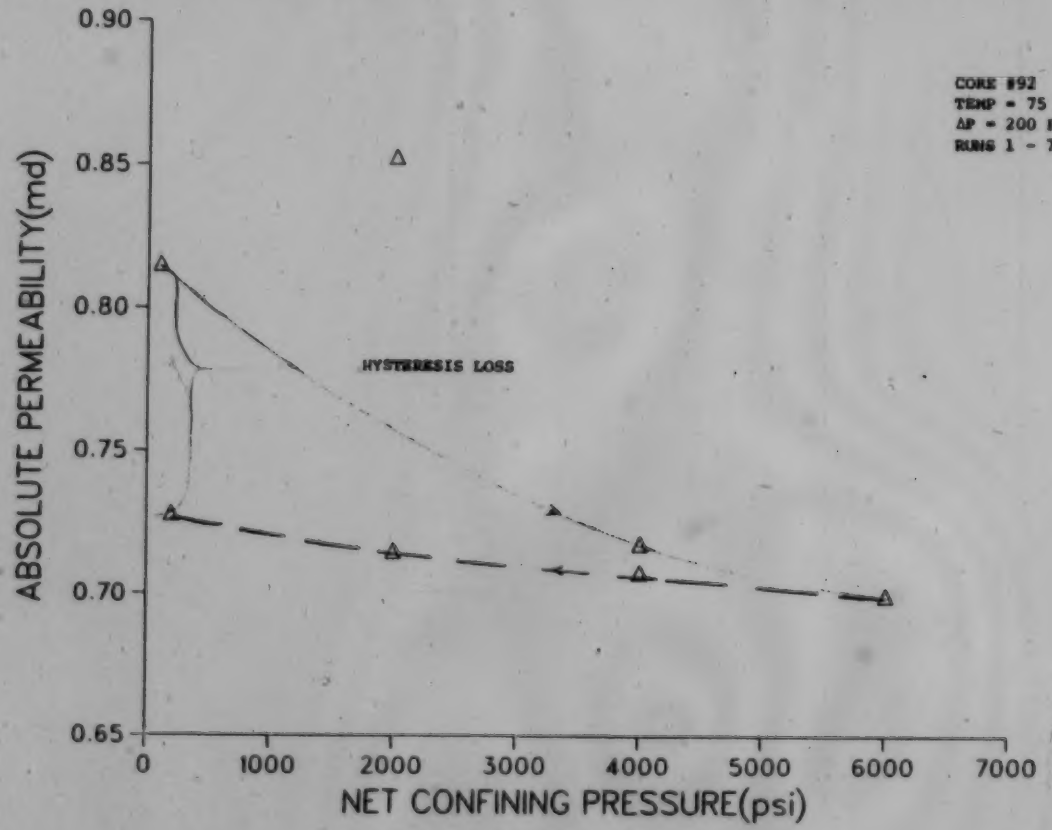

FIGURE 10

K/K(75 F) vs TEMPERATURE

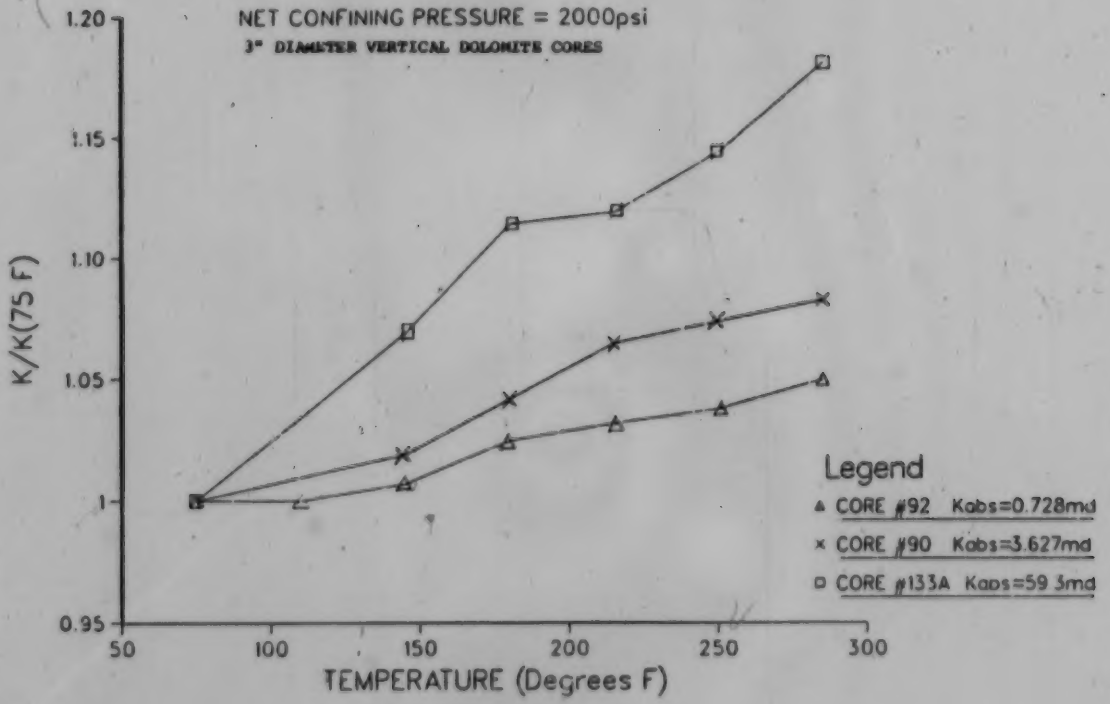

FIGURE 11

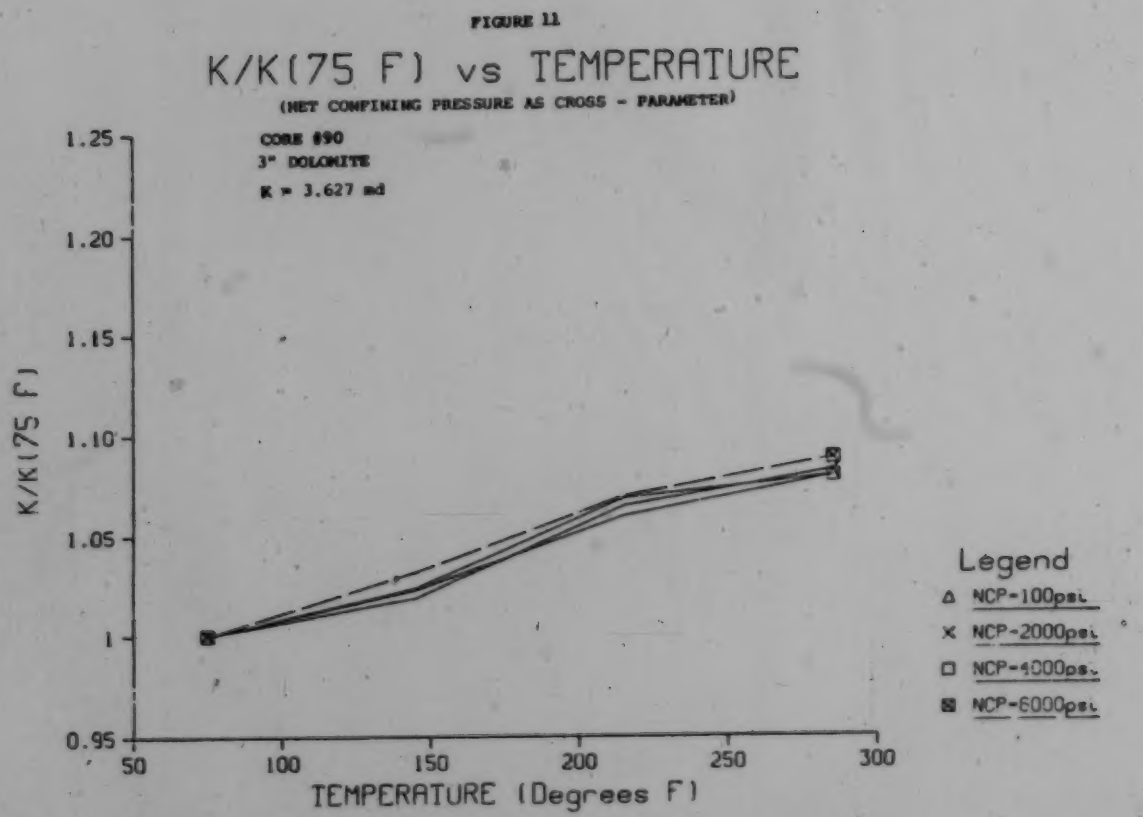
K/K(75 F) vs TEMPERATURE
(NET CONFINING PRESSURE AS CROSS - PARAMETER)
CORE #90
3" DOLOMITE
K = 3.627 md
1.25
1.20
1.15
1.10
1.05
1
0.95
K/K(75 F)
50
100
150
200
250
300
TEMPERATURE (Degrees F)
Legend
NCP-100psi
NCP-2000psi
NCP-4000psi
NCP-6000psi

Figure 11, the relative increase in absolute permeability with elevated temperature was approximately the same at all net confining pressures. In Figure 12 the relative decrease in absolute permeability with increased NCP was also the same at all temperatures.

As discussed in the theory section of the procedure, the slip factor (b) is proportional to λ/d, and is therefore indicative of the size of flow channels open to flow (d) and, since the mean free path of the gas molecules (λ) will increase with temperature, the slip factor is also indicative of the temperature of the flowing gas. Although the slip factor is calculated by dividing the slope of the Klinkenberg Plot by K_ℓ, the slope of the plot itself is probably more representative of the degree of slippage occurring during each run. This is thought to be so, since, although the degree of slippage may be increasing due to the greater mean free path of the gas molecules at higher temperatures (as indicated by the increased slope of the Klinkenberg Plot), the absolute permeability of the sample may be increasing faster due to new flow channels being opened up at higher temperatures, resulting in a decrease in the calculated slip factor.

FIGURE 12

K/Katm vs NET CONFINING PRESSURE

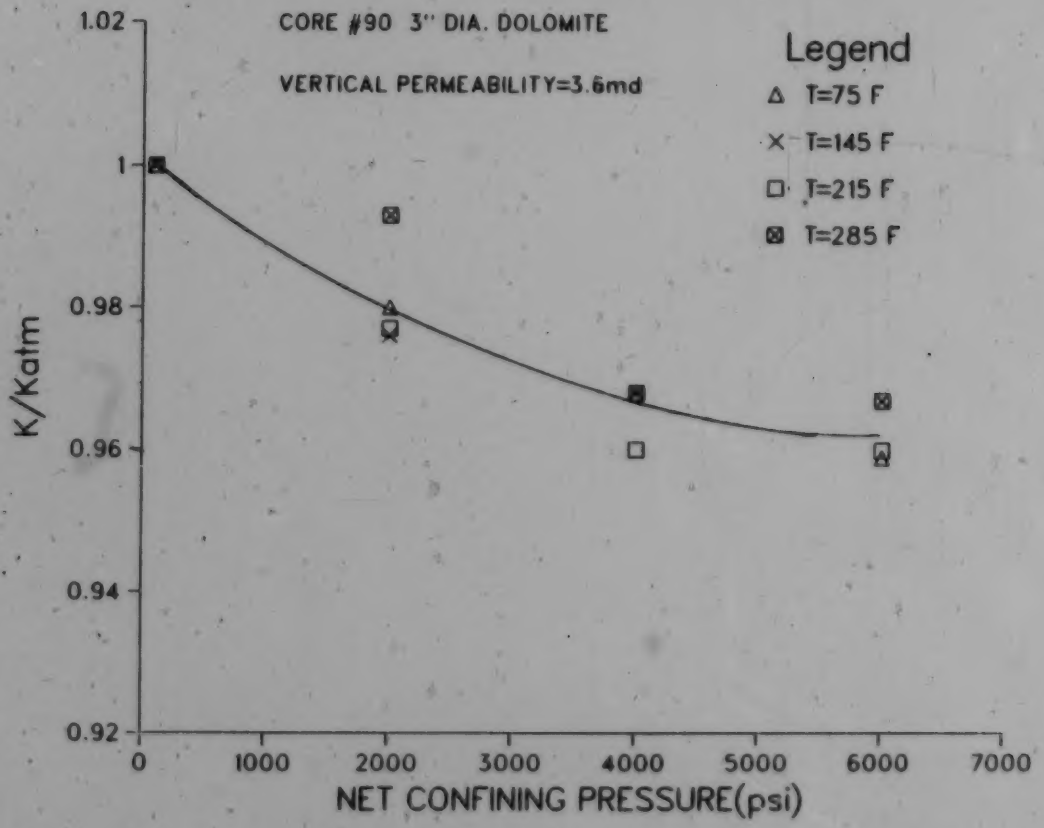

This appeared to be the case for the dolomite samples, where slip factors calculated for cores 90 and 133A (Appendices B1 and B2) decreased with increased temperature while the slip factor for core 92 (Appendix B3) increased with increasing temperature. The slope of the Klinkenberg Plots increased or remained constant with increasing temperature for all three dolomite samples tested, as expected, since the mean free path of the gas molecules was increasing with temperature.

b) Horizontal Dolomite Plugs

Figure 13 depicts results from flow tests performed on two one-inch diameter horizontal dolomite plugs (#93B and #133A) of 23 and 463 millidarcies permeability, respectively. As previously mentioned, these plugs were removed at right angles from conventional vertically oriented cores and characterize horizontal permeability. The plug from core #133A had been previously stressed, while the plug from core #93B had not. It may be observed that there was a small decrease (<4%) in permeability with increasing NCP for both samples.

The effects of increased temperatures are shown in Figure 14, where the horizontal plugs displayed absolute permeability gains near 20% at 320°F. As with the two vertical cores (#90 and #133A), the horizontal cores displayed a decrease in slip

FIGURE 13

K/K100 versus NET CONFINING PRESSURE

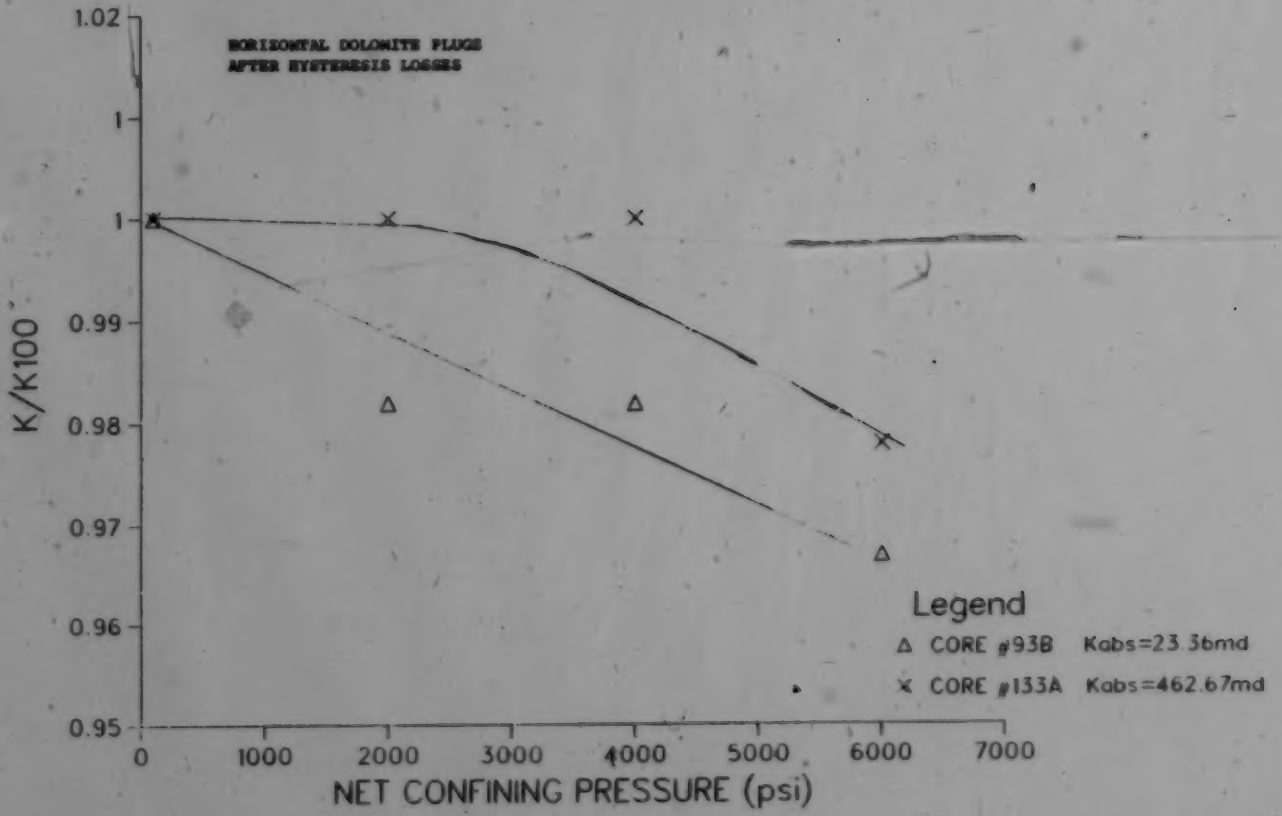

FIGURE 14

K/K75 versus TEMPERATURE

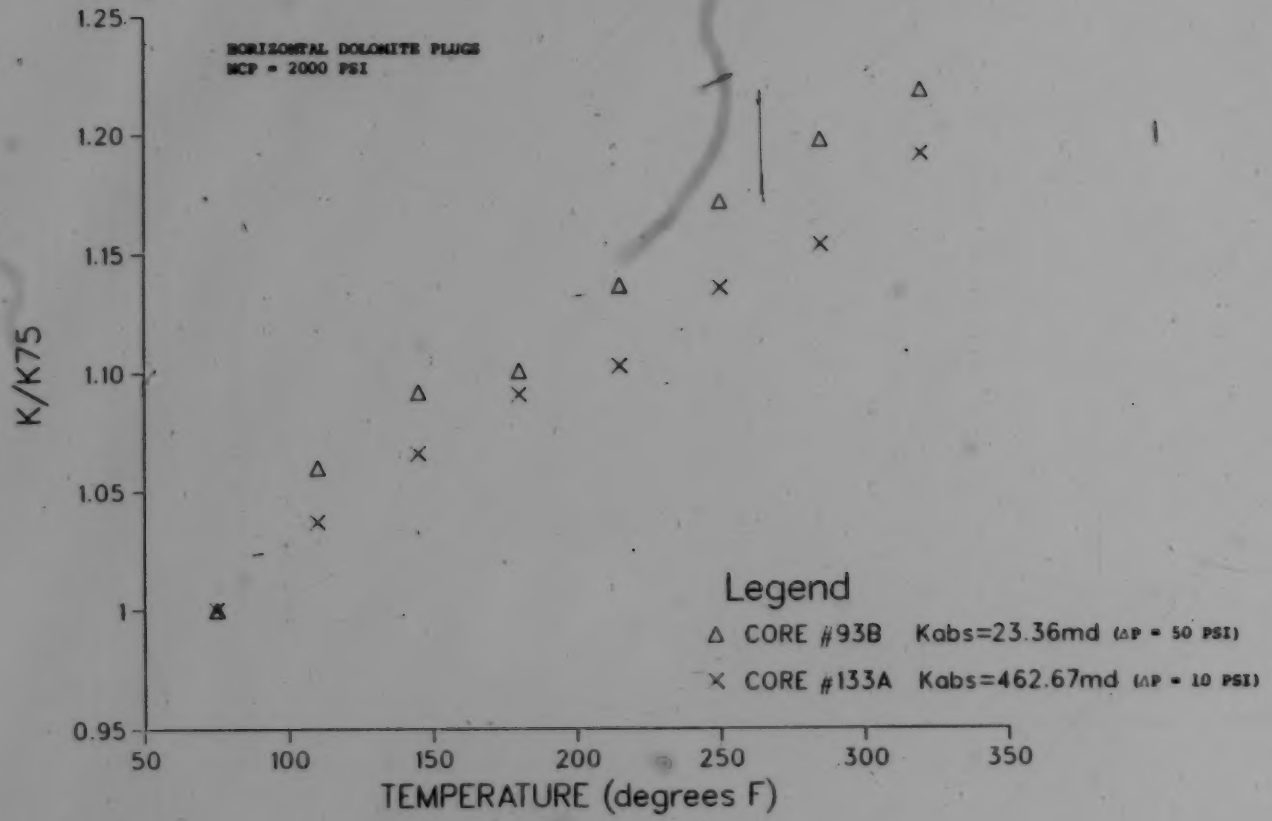

factor, with the slope of the Klinkenberg Plots remaining approximately the same with increasing temperature. Complete test results for plugs #93B and #133A are documented in appendices B4 and B5.

Due to the unusual results obtained with the one-inch horizontal dolomite plugs, tests were carried out on a one-inch vertical dolomite plug from core 133A to determine if sample size was a factor. Results from this plug are shown in Figures 15 and 16 and documented in Appendix B6. The effects of net confining pressure on the vertical plug were similar to those of the vertical core, however the elevated temperature runs indicated increases in absolute permeability approaching 50% at 320°F.

c) Limestone Cores

The four three-inch limestone cores tested (Figure 17) experienced decreases in absolute permeability ranging from 7% to 9% at net confining pressures up to 6000 psi. Since the initial tests for cores 1L, 3L and 4L were carried out at 6000 psi, hysteresis effects could not be determined for these cores. As shown in Figure 18 hysteresis losses in core 6L were determined to be approximately 7%.

FIGURE 15

K/K100 versus NET CONFINING PRESSURE

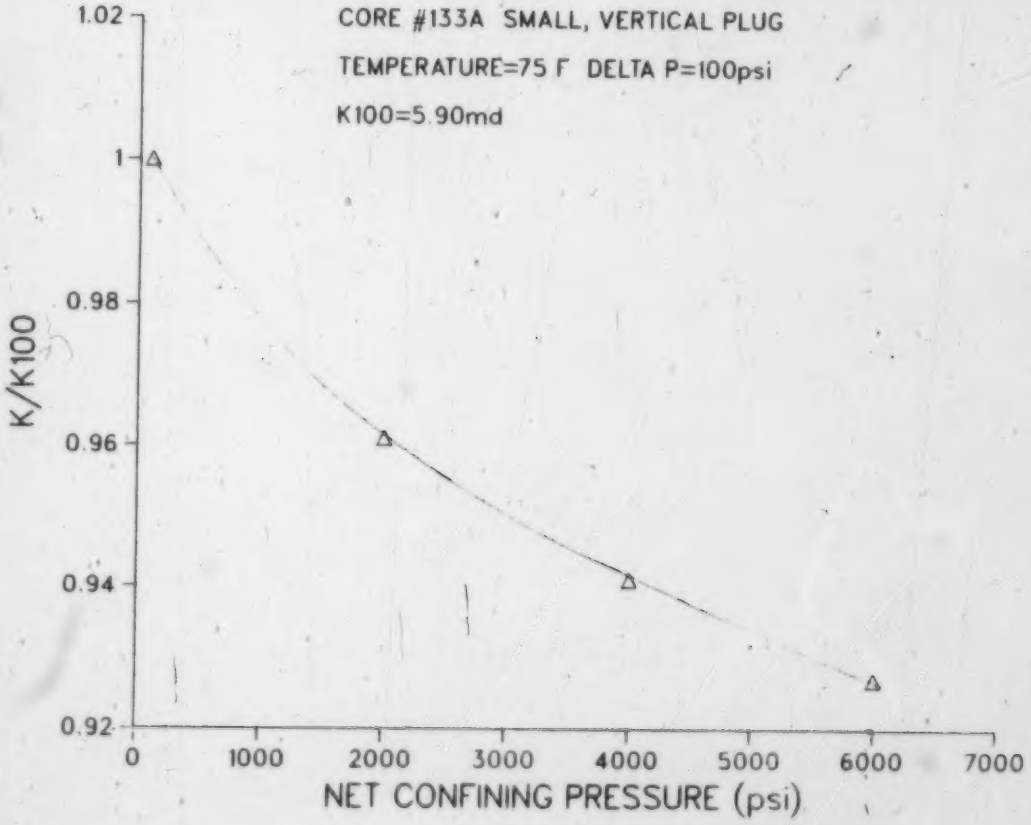

FIGURE 16

K/K75 versus TEMPERATURE

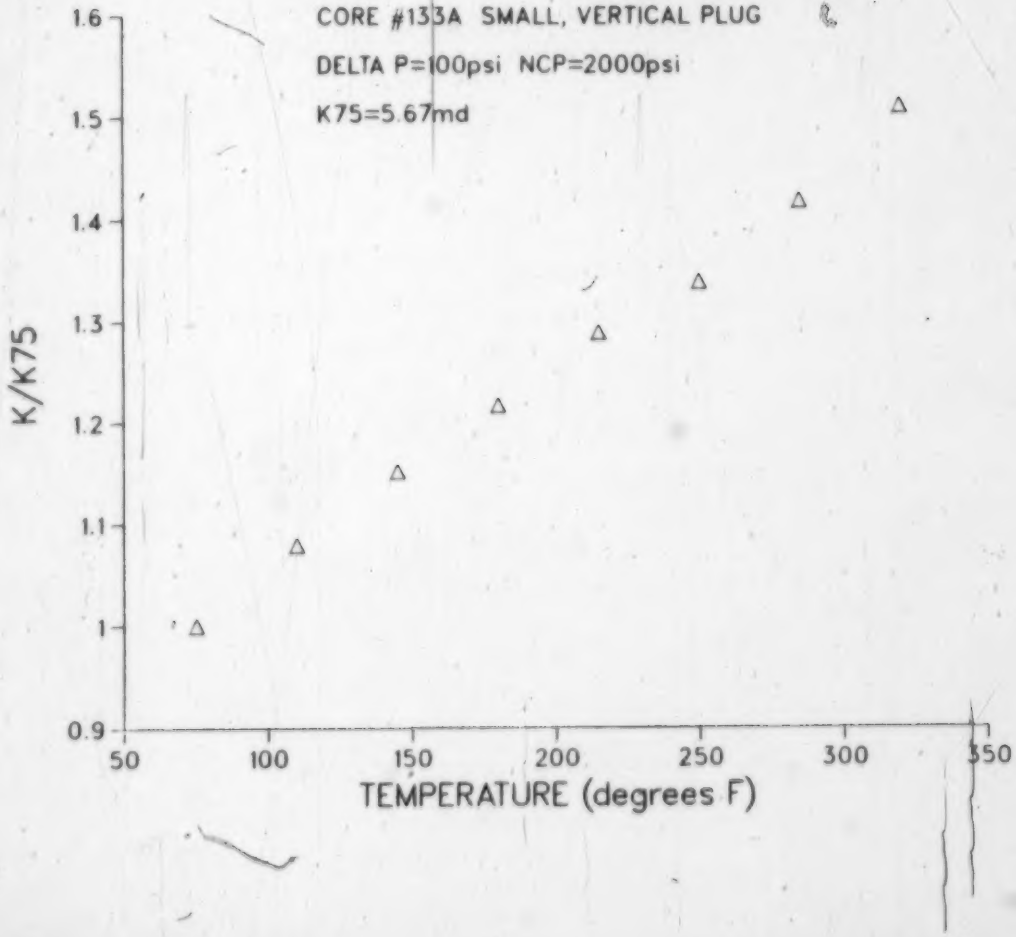

FIGURE 17

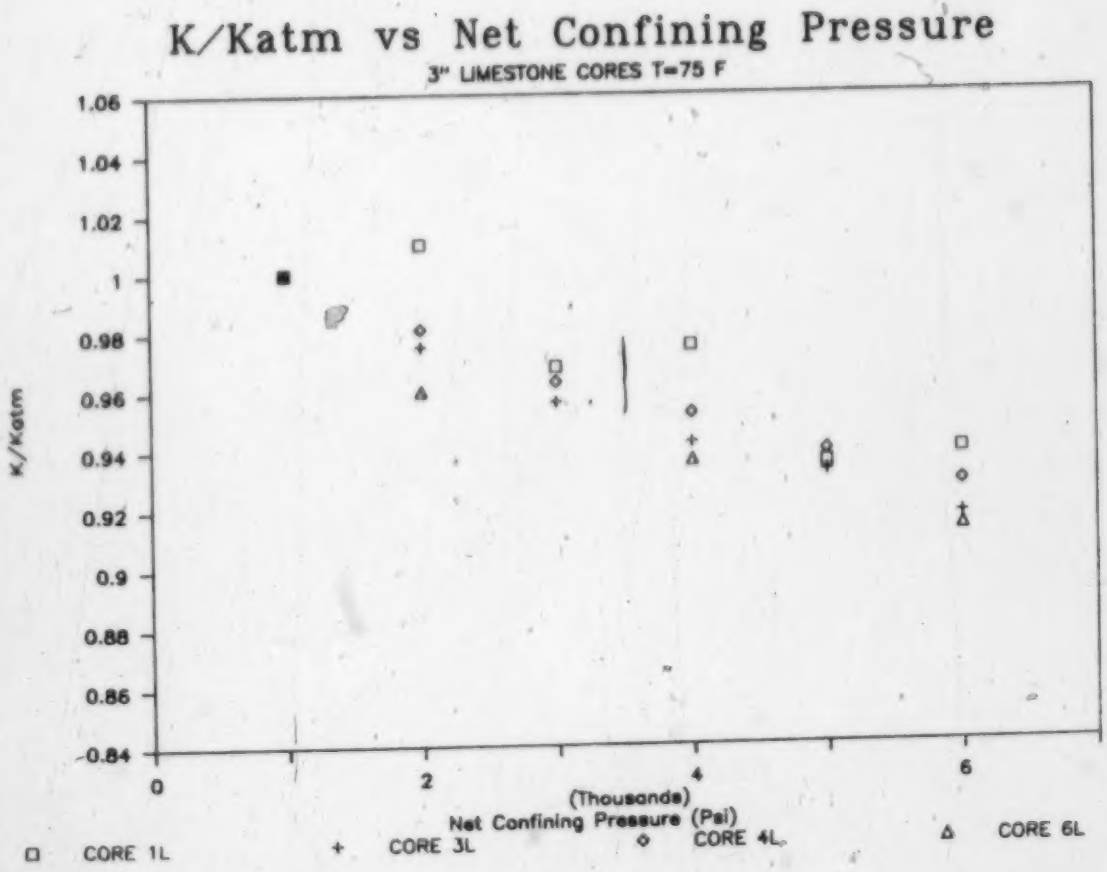
K/Katm vs Net Confining Pressure
3" LIMESTONE CORES T=75 F
K/Katm
1.06
1.04
1.02
1
0.98
0.96
0.94
0.92
0.9
0.88
0.86
0.84
0
2
4
6
(Thousands)
Net Confining Pressure (Psi)
CORE 1L
CORE 3L
CORE 4L
CORE 6L

FIGURE 18

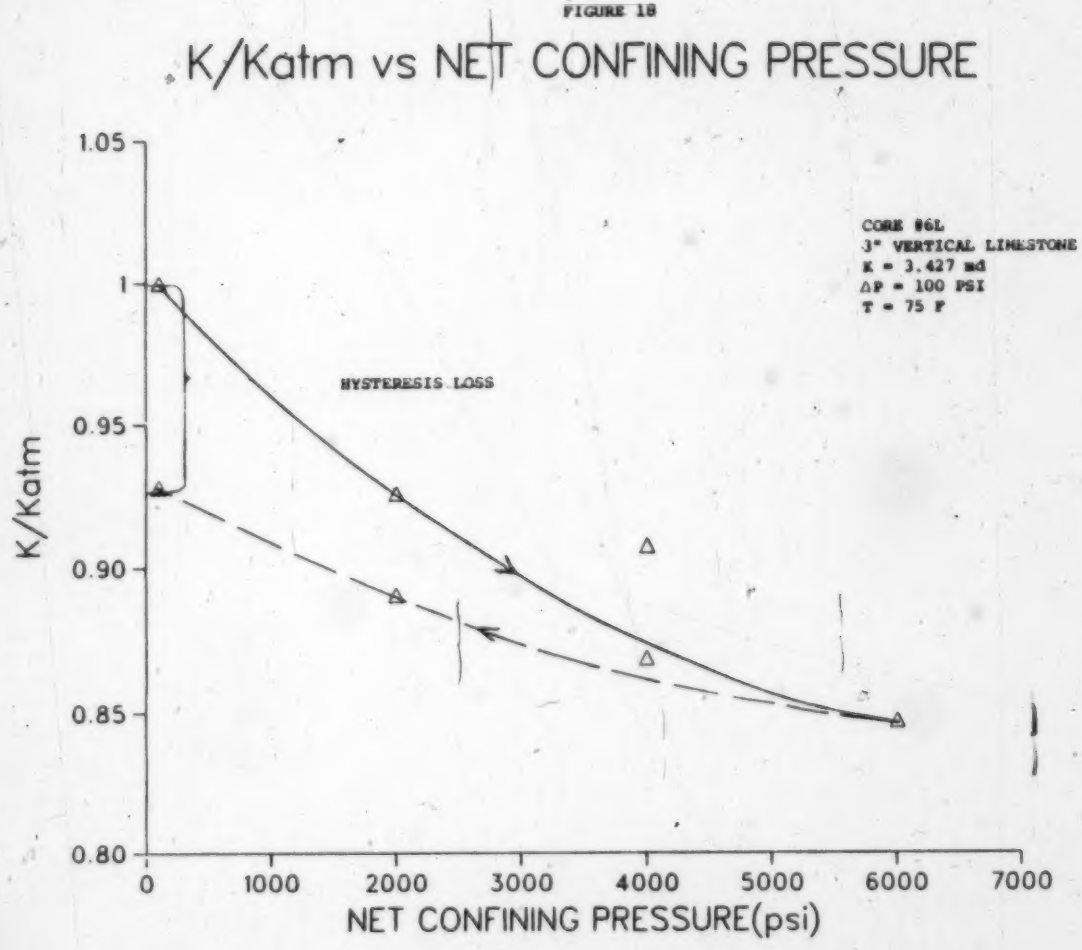
K/Katm vs NET CONFINING PRESSURE
CORE #6L
3" VERTICAL LIMESTONE
K = 3.427 md
ΔP = 100 PSI
T = 75 F
HYSTERESIS LOSS
K/Katm
1.05
1
0.95
0.90
0.85
0.80
0
1000
2000
3000
4000
5000
6000
7000
NET CONFINING PRESSURE(psi)

During the elevated temperature runs (Figure 19) core 4L's absolute permeability remained constant up to 250°F, then increased by about 2% at 325°F. Core 6L experienced a continuous gain in absolute permeability with a total increase of about 4% at 325°F. As expected slip factors calculated for both cores increased with temperature. Temperature runs for core 3L were not considered, as a sudden drop in permeability for all runs at 325°F suggested that the overburden fluid (oil) had invaded the core through the membrane. Some staining of the core was evident upon removal from the cell.

d) Sandstone Core

One set of temperature runs (Figure 20) was carried out for comparison on a vertical clean homogeneous sandstone core (2S) with a permeability of 218.7 md at 75°F (Appendix B11). An increase in K_ℓ of around 2% at 285°F was recorded, while a constant increase in slip factor with increased temperature occurred. Fluctuations in Kabs recorded at lower temperatures may have been due to the error in reading the low pressure drop across the core (only 5 psi), as discussed under "Error Analysis" in the Procedure Section.

FIGURE 19

K/K(75 F) vs TEMPERATURE

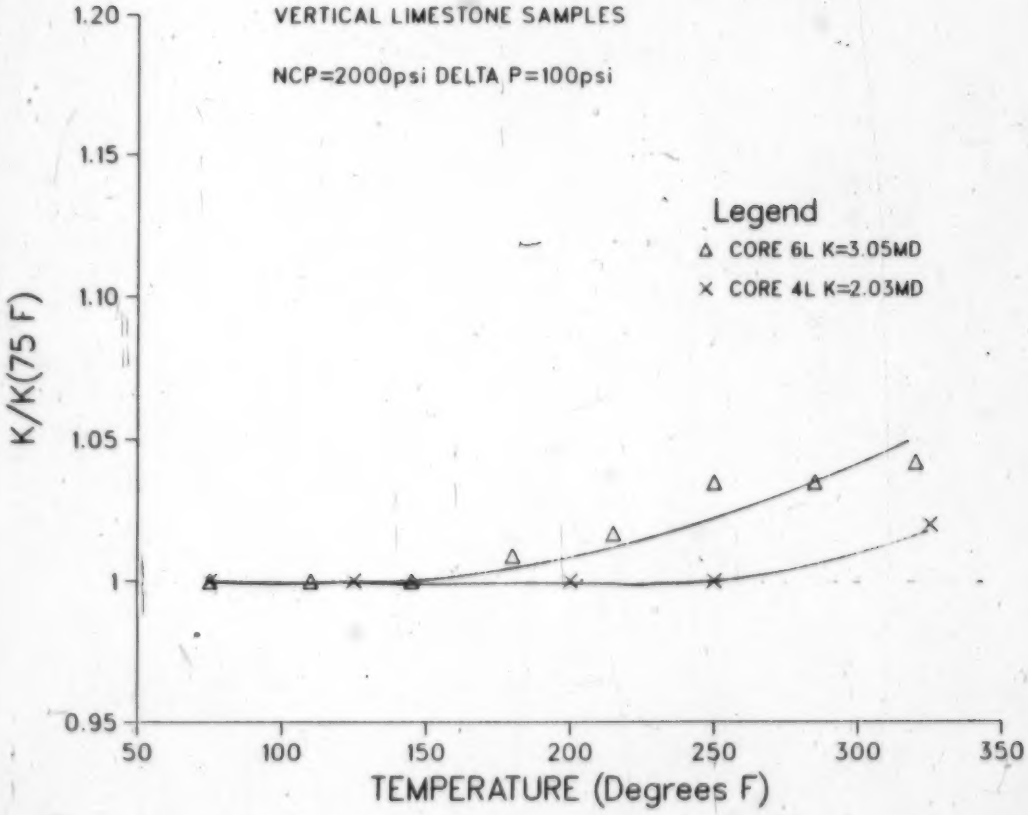

FIGURE 20

K/K(75 F) vs TEMPERATURE

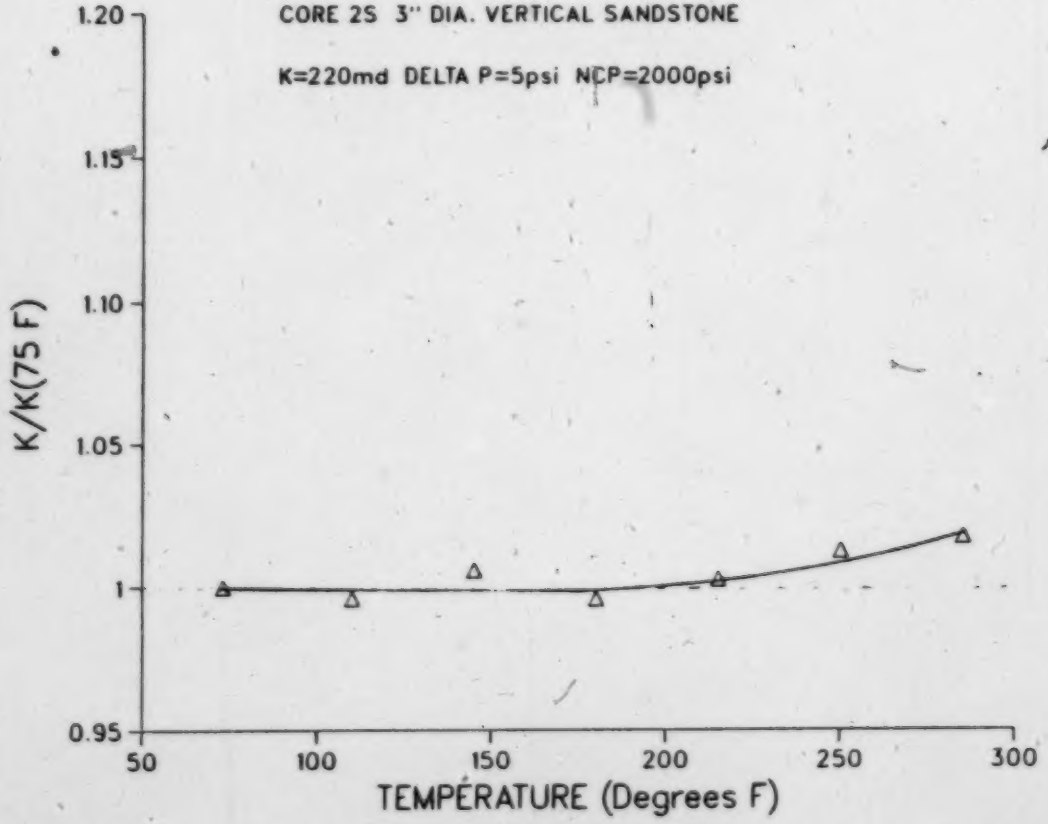

8. Discussion

a) Effects of Changes in Net Confining Pressure

The effects of increased net confining pressure (NCP) on the carbonate samples found in this investigation conformed quite well to expectations based on existing literature and on proposed theory. The most significant results of this study were:

1. large hysteresis effects were quite evident in almost all samples tested; and,
2. the effect of increased NCP on horizontal permeability was considerably less than on vertical permeability in the dolomite samples tested.

i) Hysteresis Effects

Reviewing the hysteresis effects, it was observed that the largest decreases in permeability (around 15%) were found in the previously unstressed vertically oriented dolomite and limestone cores (Figures 9 and 18). Previously stressed vertical dolomite cores experienced decreases in absolute permeability on the order of three to seven percent, while the previously stressed vertical limestone cores varied from seven to nine percent losses at net confining pressures of 6000 psi.

The presence of hysteresis losses indicates that both plastic and elastic deformation are occurring, since some of the losses were reversible,

while some were not. To further analyze the deformation occurring it is necessary to consider the stress history of the rock samples tested. Because the samples tested were removed from shallow formations, it may be assumed they had not been previously subjected to more than 1000 psi net confining pressure. At this pressure the rock sample would have undergone some elastic deformation as well as some plastic deformation. When removed from the formation only the elastic deformation would have rebounded and, accordingly, when restressed in the pressure cell, only elastic deformation would occur below the maximum stress level which the sample had previously endured. Beyond that level both plastic and elastic deformation would occur.

Relating these results to a reservoir situation, it is obvious that the magnitude of permeability change with net confining pressure is dependent on the previous stress history of the reservoir. As was theorized, a reservoir which has undergone high stresses would show relatively smaller changes in permeability with changes in net confining pressures, and vice versa. A sample core being removed from a reservoir will expand elastically only, with the degree of expansion being partially rock-dependent, as well as related to the previous stress history. A formation undergoing

pressure depletion will be compressed both elastically and plastically, assuming uplift and erosion have not previously occurred. Once again, the initial NCP and the rock specific parameters will control the amount of deformation occurring.

ii) Vertical versus Horizontal Permeability Effects

Although vertical permeability is of interest to the reservoir engineer, horizontal permeability is the primary factor in determining a reservoir's productivity. A comparison of K/Katm versus NCP for a vertically oriented three inch dolomite core (#133A) and a one inch horizontally oriented plug removed from the subject core (Figure 21) shows a significant difference in the effects of the increased NCP on the permeabilities of the two samples.

At a NCP of 6000 psi the horizontal sample had experienced between 1 and 2% permeability loss while the vertical samples absolute permeability had decreased around 7%. Since both the core and the plug removed from it had the same stress history, hysteresis was not a factor in the comparison.

These results agree quite well with the sandstone results found by Gray and Fatt[2], as well as with the proposed theory. It is probable therefore, that differences in compressibility in the horizontal and vertical directions were present

FIGURE 21

K/K100 versus NET CONFINING PRESSURE

(FOR VERTICAL AND HORIZONTAL PERMEABILITY IN DOLOMITE)

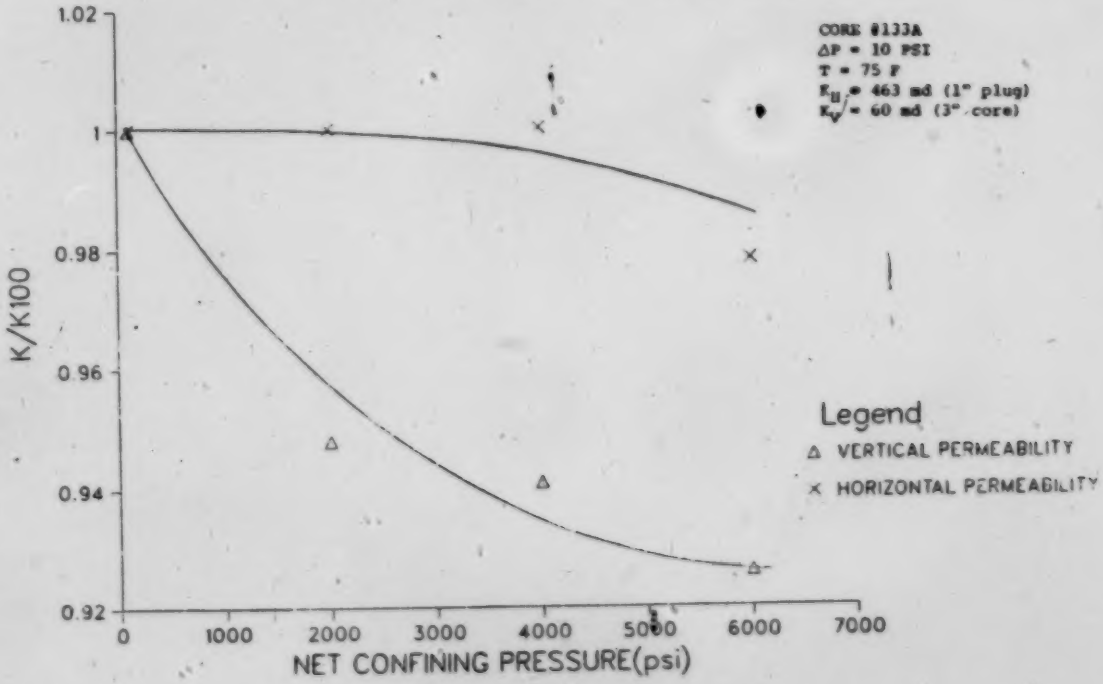

in the dolomite samples tested, and could be expected in other dolomite reservoirs. As previously stated, this condition could be the result of distortion due to the greater vertical stresses experienced in the reservoir, the orientation of sediments deposited in the carbonates, or from dissolution and recrystalization at higher temperatures and pressures.

A second observation may be made from Figure 21 with regards to the shape of the two curves. At low net confining pressures very little change in horizontal permeability is occurring, while at the same pressures large changes in vertical permeability are taking place. Conversely, as net confining pressure was increased losses in horizontal permeability became greater, while corresponding losses in vertical permeability decreased. These effects are in agreement with proposed theory, since it was postulated that under isotropic stress conditions the compressibility of in the rock samples would be initially greater in the horizontal direction due to previous conditions in the reservoir, as stated. Furthermore, as deformation of the rock grains occurs, it would be expected that the compressibilities would move toward equilibrium, as evidenced by the shape of the two curves.

b) Effects of Elevated Temperature

The effect of elevated temperature on the absolute permeability of the samples tested conformed to proposed theory for the most part, however the magnitude of the changes recorded was considerably greater than was expected. As shown in Figures 10,14,16 and 19, the homogeneous samples experienced increases varying from 2 to 4% with increases of 250°F, while the heterogeneous samples experienced increases as high as 50%. Generally the three-inch heterogeneous samples experienced smaller increases (up to 15%) while the one inch plugs displayed much greater gains.

From the results obtained, two observations were made:

1. As predicted, the increase in absolute permeability with increased temperature was greater for the heterogeneous samples and,
2. The effect of increased temperature appeared to be dependent on the size of the sample tested, as both the vertical and horizontal plugs displayed far greater gains than any of the full-size cores.

Although the magnitude of the permeability increases far exceeded the predictions made, it is believed that all increases in permeability recorded

were the result of temperature induced changes to the rock sample, and not from other effects, such as unaccounted for viscosity changes or inertial effects. Observations which support this conclusion are:

1. The effect of elevated temperature on absolute permeability varied considerably for the different types of core samples, but was relatively constant for samples of the same size and composition, even though their permeabilities were significantly different. If the effects measured were the result of uncorrected changes in gas properties with temperature, they should have been consistent for all flow tests.
2. As typified in Figures 22 and 23, the slope of the Klinkenberg Plots was essentially constant for the dolomite cores, yet a distinct increase in slope occurred between runs on the limestone samples, indicating a definite rock specific response.
3. Reynolds number calculations (Appendix A4) indicate that the flow tests were in the laminar flow regime. Laminar flow is also indicated by the linear section on each Klinkenberg Plot. As previously mentioned,

FIGURE 22

APPARENT PERMEABILITY vs RECIPROCAL MEAN PRESSURE

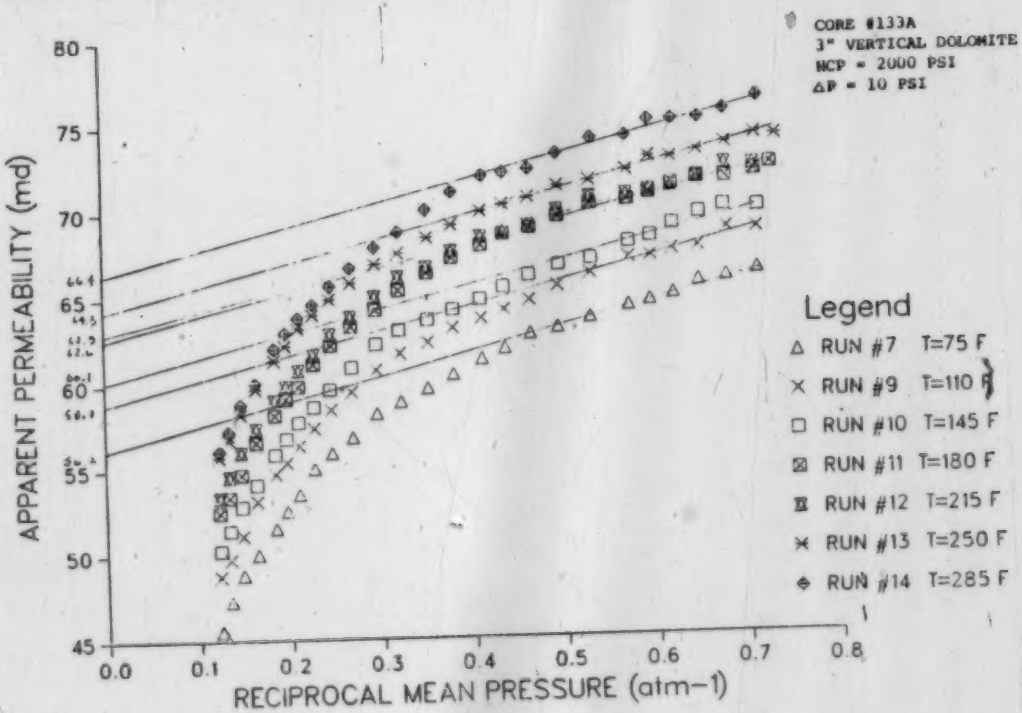

FIGURE 23

APPARENT PERMEABILITY vs INVERSE MEAN PRESSURE

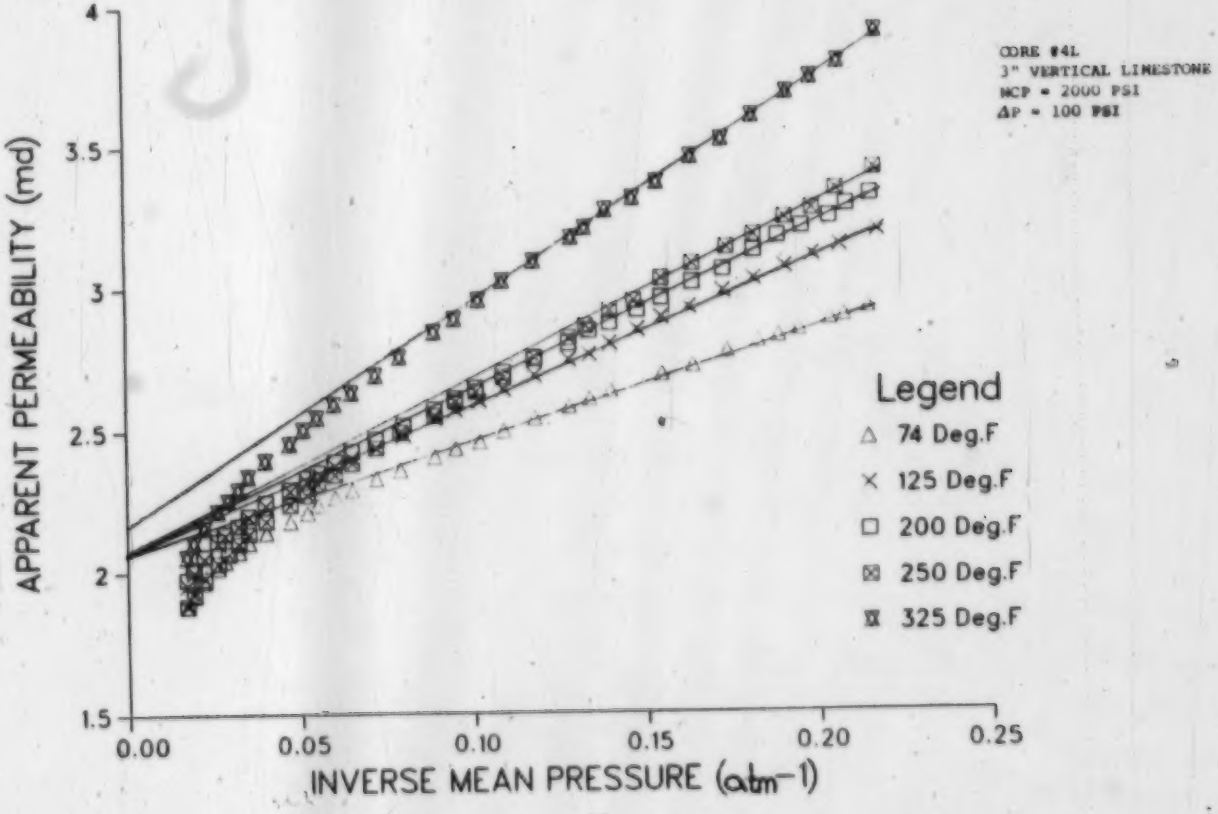

the Darcy Flow Equation is valid only for laminar flow.

Having established that the rock samples tested underwent substantial changes in absolute permeability with temperature changes, the reasons why this occurred may be investigated further. Since permeability gains were far in excess of those predicted, previously unaccounted for phenomena must have took place as the samples were heated. Two reasons postulated are :

1. The rock samples tested contained minerals with coefficients of expansion considerably different than those documented; or
2. The expansion of the matrix opened new channels for gas flow which had previously not existed.

Since the measured values for matrix expansion of several samples (Table 1), were reasonably close to the documented values, matrix expansion greater than predicted was unlikely. Mechanism two is more probable, and as discussed below, slip factor data obtained from flow tests appears to support this theory.

As detailed in the results and procedure sections, the two primary conditions affecting slippage are the size of the flow passage and the

mean free path of the gas molecules. In the course of temperature runs carried out in this investigation it was apparent that both the mean free molecular path of the gas and the cross-sectional area open to flow were affected.

For core 133A (Figure 22) it was evident from the slope of the plots that slippage effects remained relatively constant with higher temperatures, while absolute permeability increased. Resulting slip factors (Figure 24) decreased with increased temperature. It would appear then, that three possible effects were occurring as temperature was increased:

1. The mean free path of the gas molecules was increasing with temperature.

2. Pore throat size was increasing with temperature, resulting in relatively constant slippage effects as well as increased permeability.

3. New passageways were opening, causing a further increase in permeability and subsequently, a decrease in the calculated slip factor.

FIGURE 24

KLINKENBERG SLIP FACTOR versus TEMPERATURE

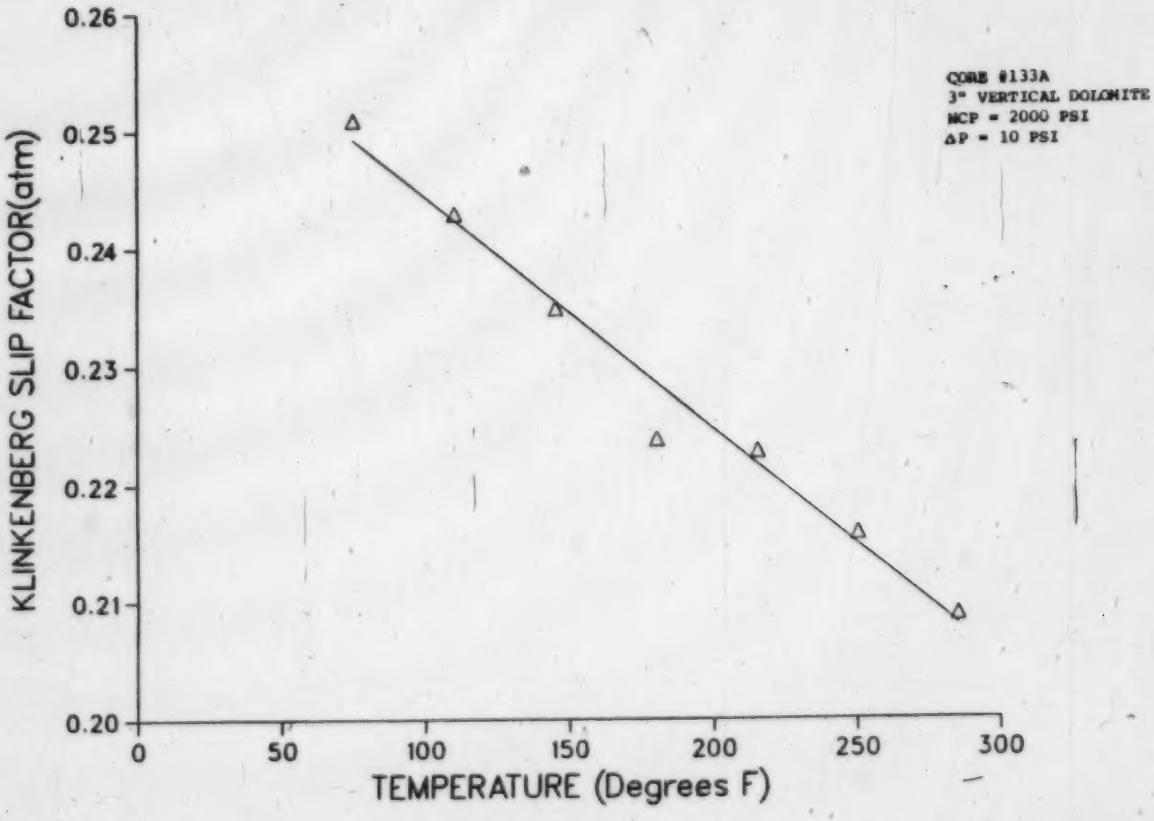

In the case of limestone core 6L (Figure 25) increasing slip factors were calculated, indicating a larger influence from the increased mean free gas molecule path. Since the dolomite core experienced relatively larger gains in absolute permeability (18% vs 4% for core 6L), this result seems logical.

Results from temperature runs on the small one-inch plugs (Figures 14 and 16) were expected to be similar to results from the larger cores of the same sample. Since both the vertical and horizontal plugs experienced greater gains in permeability than the larger vertical cores, it may be concluded that sample size was a factor in the results found on the plugs. It is thought that perhaps small discontinuities in the samples would have relatively larger effects on the much smaller samples, but this theory could not be verified. The formation of microfractures with heating, as postulated by Aktan and Farouq Ali[13], would seem to be a more plausible explanation. As the small plugs probably have less overall integrity than the larger samples they may have been more severely affected by the microfracturing.

c) Combined Temperature and Pressure Effects

As was seen in Figures 11 and 12 in the results section, the dolomite core tested reacted to temperature increases exactly the same at all net

FIGURE 25

SLIP FACTOR versus TEMPERATURE

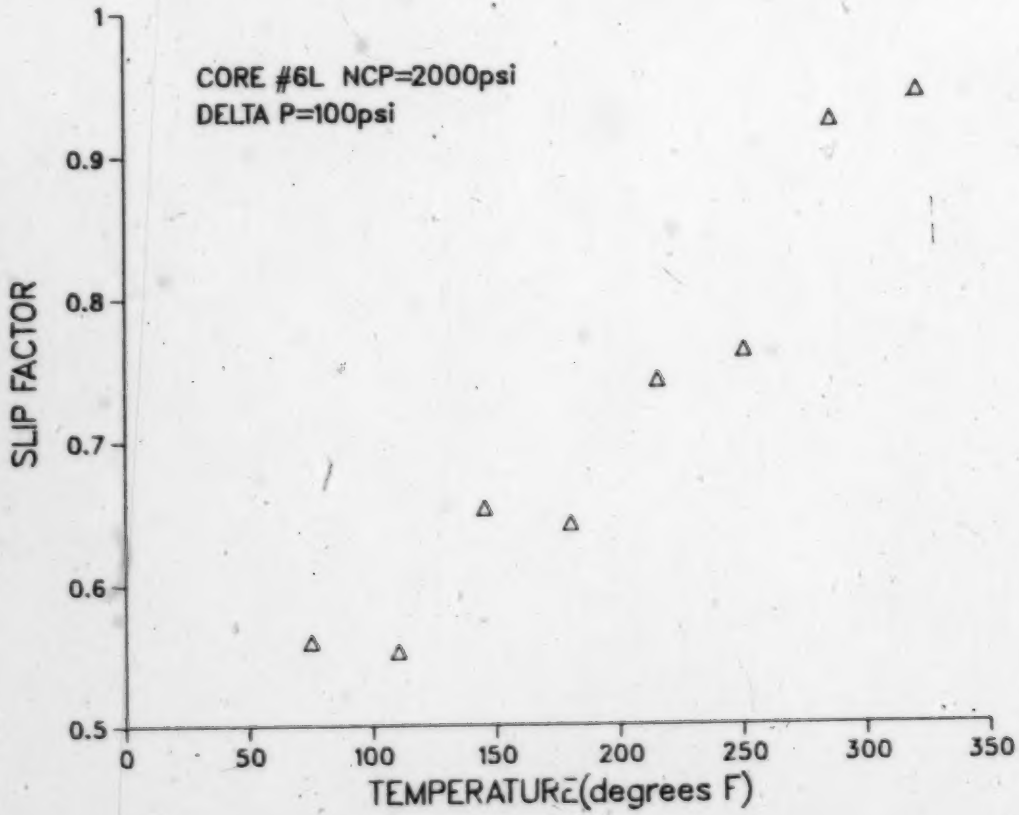

confining pressures, and conversely, reacted the same to changes in net confining pressure at all temperatures. Apparently the change in effective stress caused by the increased temperature was not significant, as a variation in the initial state of stress in a sample would be expected to result in a change in characteristics when the sample was subjected to increased net confining pressure.

9. CONCLUSIONS

Based upon experiments carried out to determine the effects of net confining pressure and temperature on the absolute permeability of consolidated carbonate rocks, the following conclusions can be made relating to the samples which were tested:

1) Dolomite cores subjected to net confining pressures up to 6000 psi will undergo insignificant changes in horizontal absolute permeability.

2) Horizontal permeabilities measured at low net confining pressures (which is normal for most commercial laboratories) will be representative of horizontal permeabilities measured under conditions of high net confining pressure.

3) Stress history, matrix strength and grain orientation are probably the most important factors to consider when estimating the effects of increased net confining pressures on the absolute permeability of a carbonate formation.

4) Carbonate reservoir rocks will experience a slight increase in absolute permeability when heated.

5) Heterogeneous carbonates will be more likely to experience increases in permeability with temperature than will homogeneous carbonates.

REFERENCES

1. Fatt, I., Davis, D.H., "Reduction in Permeability with Overburden Pressure". Trans., AIME (1952) 195, 329.
2. Gray, D.M., Fatt, I., Bergamini, G., "The Effect of Stress on Permeability of Sandstone Cores". Soc. Pet. Eng. J. (June 1963) 95-100.
3. Afinogenov, Y.A., "How the Liquid Permeability of Rocks is Affected by Pressure and Temperature". Soviet Mining Science, NG, 1969, 644-678.
4. Vairogs, J., Hearn, C.L., Dareing, D.W., Rhoades, V.W., "Effects of Rock Stress on Gas Production from Low-Permeability Reservoirs". J. Pet. Techn. (September, 1971) 1161-1167.
5. Jones, F., "A Laboratory Study of the Effects of Confining Pressure on Fracture Flow and Storage Capacity in Carbonate Rocks". J. Pet. Techn. (January, 1975) 21-27.
6. Gangi, A.F., "Variations of Whole and Fractured Porous Rock Permeability with Confining Pressure". Int. J. Rock. Mech. Min. Sci and Geomech. Abstra., V15, (1978) 249-257.
7. Jones, F.O., Owens, W.W., "A Laboratory Study of Low-Permeability Gas Sands". J. Pet. Tech. (September, 1980) 1631-1640.

8. Greenberg, D.B., Cresap, R.S., and Malone, T.A., "Intrinsic Permeability of Hydrological Porous Mediums: Variation with Temperature". Water Resources Research (August, 1968) 4, No. 4, 791.

9. Weinbrandt, R.M., Ramey, H.J. Jr., Casse, F.J., "The Effect of Temperature on Relative and Absolute Permeability of Sandstones". Soc. Pet. Eng. J. (October, 1975) 376-384.

10. Casse, F.J., Ramey, H.J. Jr., "The Effect of Temperature and Confining Pressure on Single-Phase Flow in Consolidated Rocks". J. Pet. Techn. (August, 1979) 1051-1059.

11. Aruna, M., "The Effects of Temperature and Pressure on the Absolute Permeability of Sandstones". Ph.D., Disertation, Stanford, and Disertation Abstracts International, V37, n5, P.(1976) 2451-58.

12. Aruna, M., Arihara, N., Ramey, H.J. Jr., "Effect of Temperature and Stress on the Absolute Permeability of Sandstones and Limestones". Energy Research Abstracts V3, n 16, (1977) 3868.

13. Aktan, T., Farouq Ali, S.M., "Finite-Element Analysis of Temperature and Thermal Stresses Induced by Hot Water Injection". Society of Pet. Eng. (December, 1978) 457-469.

14. Sydansk, R.D., "Discussion of the Effect of Temperature and Confining Pressure on Single-Phase Flow in Consolidated Rocks". J. Pet. Techn. (August, 1980) 1329-1330.

15. Somerton, W.H., Udell, K.S., "Thermal and High Temperature Properties of Rock Fluid Systems." Dept. of Mech. Eng., University of California, Berkley, (1981)

16. Skempton A.W., "Effective Stress in Soils, Concrete and Rocks", Butterworths (1960) 4-15.

17. Clark, S.P., "Handbook of Physical Constants", GSA Memoir 97, (1966), 78-88.

18. Klinkenberg, L.J., "The Permeability of Porous Media to Liquids and Gases". Drill. and Prod. Prac., API (1941) 200.

19. De Nevers, Noel, "Fluid Mechanics" Addison Wesley, 1977, 381-388.

20. Kestin, J., Wang, H.E., "The Viscosity of Five Gases: A Re-Evaluation". Transcript ASME: 80, (1959) 13.

APPENDIX A1

FORTRAN PROGRAM

```
      REAL DATA1,DATA2,DATA3,OVBRDN,LENGTH,PIN,POUT,PMEAN,
     * INPM,DELTAP,QFL,QFLM,CONST1,VISC,KPERM,W,DATA4,
     * PM,NCP,MINPM,MKPERM,MPM,TMEAN,TATM
C
      WRITE (6,200)
200   FORMAT (T54,'CORE 3L')
C
      WRITE (6,201)
201   FORMAT (T54,'RUN #19')
C
      WRITE (6,202)
202   FORMAT (T47,'TEMPERATURE = 163 C (325 F)')
C
      WRITE (6,203)
203   FORMAT (T37,'CONSTANT NET CONFINING PRESSURE = 2000 psi')
C
      WRITE (6,204)
204   FORMAT (T49,'PIN-POUT = 100 psi')
C
      WRITE (6,205)
205   FORMAT (/,'PIN(psi)',1X,'POUT(psi)',1X,'Q(ml/s)',1X,
     * 'Qm(ml/s)',2X,'PMEAN(psi)',2X,'OVBRDN(psi)',2X,'NCP(psi)',2X,
     * '1/Pa(atm-1)',
     * 2X,'K(md)',2X,'1/Pa(kpa-1)',2X,'K(um**2)',/)
C
      READ (5,100) LENGTH
100   FORMAT (F4.1)
C
C
      READ (5,103) W
103   FORMAT (F5.3)
C
10      READ (5,104,END=50) DATA1, DATA2, DATA3, DATA4
104     FORMAT (F5.3,2X,F5.3,2X,F7.3,F6.3)
C
        TATM=73+460
        TMEAN=325+460
C
        PIN=200*DATA1+ 14.696
        POUT=200*DATA2+14.696
        OVBRDN=DATA4*349.122
C
        PM=(PIN+POUT)/(2.0)
        PMEAN=PM/14.696
        INPM=1/PMEAN
        NCP=OVBRDN-PM
        MINPM=1/(PM*6.89476)
C
        DELTAP=(PIN-POUT)/14.696
C
        IF(W.LT.1) GO TO 11
C
        QFL=4000*DATA3/60
        QFLM=(QFL*TMEAN)/(PMEAN*TATM)
        GO TO 12
C
11      QFL=DATA3
        QFLM=DATA3*W/PMEAN
C
12      CONST1=LENGTH*4.0*1.0E-2/(3.141*7.50**2.0)
C
        VISC=1778.0*(1.0+8.958E-04*(PMEAN-1.0)
     *  +6.120E-07*(PMEAN-1.0)**2+3.997E-08*(PMEAN-1.0)**3)
     *  +4.550*(163-25)
C
4       KPERM=(QFLM*VISC*CONST1)/DELTAP
        MKPERM=KPERM/1013.25
C
        WRITE (6,206)PIN,POUT,QFL,QFLM,PM,OVBRDN,NCP,INPM,
     *  KPERM,MINPM,MKPERM
C
206     FORMAT (T2,F6.1,T11,F6.1,T20,F6.2,T28,F6.2,T39,F6.1,
     *  T52,F6.1,T64,F6.1,T75,F6.4,T85,F6.4,T94,E9.3,T106,E9.3)
C
      GO TO 10
C
50    STOP
      END
```

APPENDIX A2

DARCY FLOW EQUATION

DARCY FLOW EQUATION

For linear, steady state, isothermal laminar flow

$$Q_r = \frac{K \cdot A \cdot \Delta P}{\mu L} \frac{P_m}{P_r} \frac{T_r}{T}$$

and:

$$K = \frac{Q_r \cdot \mu \cdot L \cdot P_r \cdot T}{A \cdot \Delta P \cdot P_m T_r} = \frac{Q_m \cdot \mu \cdot L}{A \, \Delta P}$$

where:

Q_m = flow rate at a mean pressure (cc/sec)

Q_r = flow rate at room pressure (cc/sec)

ΔP = pressure drop across core (atm)

P_m = mean pore pressure (atm)

P_r = room pressure (atm)

A = cross-sectional core area (cm^2)

L = core length (cm)

T = core temperature (°K)

T_r = room temperature (°K)

K = permeability (darcies)

μ = viscosity of nitrogen (cp)

The viscosity of nitrogen is determined using the correlation developed by Kestin and Wang[20]:

$$\mu = 1778 \times 10^{-5} [1 + 8.958 \times 10^{-4} (P_m - 1) + 6.120 \times 10^{-7} (P_m - 1)^2 + 3.997 \times 10^{-8} (P_m - 1)^3 + 4.55 (T - 25)]$$

APPENDIX A3

SAMPLE CALCULATION

SAMPLE PERMEABILITY CALCULATION

Core 32, Run #9

P_{inlet} = 899.4 psig + 14.7 = 914.1 psia

P_{outlet} = 800.0 psig + 14.7 = 814.7 psia

$$\Delta P = \frac{(899.4 - 800.0)\text{psi}}{14.7\ \text{psi/atm}} = 6.76\ \text{atm}$$

$$P_{mean} = \frac{(914.1 - 814.7)\text{psia}}{2(14.7)} = 57.82\ \text{atm}$$

T_{atm} = 24°C + 273° = 297°K

T_{mean} = 52°C + 273° = 325°K

Q_{atm} = 133.67 ml/sec

$$Q_{mean} = \frac{Q_{atm} \cdot T_{mean} \cdot P_{atm}}{P_{mean} \cdot T_{atm}} \quad \text{(From Boyles Law)}$$

Substituting:

$$Q_{mean} = \frac{(133.67\ \text{ml/sec})\ (325°K)\ (1\ \text{atm})}{(57.82\ \text{atm})\ (297°K)}$$

$$= 2.53\ \text{ml/sec}$$

From Appendix A2:

$$\mu = 1778.0 \times 10^{-5} [1 + 8.958 \times 10^{-4}(57.82 - 1) + 6.120 \times 10^{-7}\ (57.82 - 1)^2 + 3.997 \times 10^{-8}(57.82 - 1)^3 + 4.55(52 - 25)]$$

$$= 2007.8 \times 10^{-5}\ \text{cp}$$

$$A = \frac{\pi D^2}{4}, \quad D = 7.5\ \text{cm}, \quad A = 44.2\ \text{cm}^2$$

$$L = 10.78\ \text{cm}$$

Now, substituting:

$$K = \frac{Q_m \mu L}{\Delta P \cdot A}$$

$$= \frac{2.53 \text{ ml/sec} \cdot 2007.8 \times 10^{-5} \text{ cp} \cdot 10.78 \text{ cm}}{6.76 \text{ atm} \cdot 44.2 \text{ cm}^2}$$

$$= 0.00183 \text{ darcies}$$

$$= 1.83 \text{ md}$$

APPENDIX A4

REYNOLDS NUMBER CALCULATIONS

REYNOLDS NUMBER DETERMINATION

To determine Reynolds number for a porous medium*

$$R = \frac{D_p V_s \rho}{\mu(1 - \emptyset)} \quad 6.72 \times 10^{-4} \text{ lbm/ft·sec·cp}$$

If R < 250 flow is considered to be laminar.

D_p = particle diameter (ft)

V_s = superficial velocity (ft/sec)

ρ = density (lbm/ft^3)

μ = viscosity (cp)

Using data from Core 92, Run #3

K = 0.729 md, $\emptyset$ = 11.1%,

Particle diameter is determined using Poiseuilles Equation:

$$K = 20 \times 10^6 \emptyset D_p^2$$

Where K is in darcies, $\emptyset$ is porosity and D_p is in inches.

Solving for D_p,

$$Dp = \sqrt{\frac{K}{20 \times 10^6 \emptyset}} = \sqrt{\frac{0.000729}{20 \times 10^6 (0.111)}}$$

$$= 1.81 \times 10^{-5} \text{ in}$$

$$= 1.51 \times 10^{-6} \text{ ft}$$

Superficial Velocity (V_s) is defined by the equation:

---

* from Denevers [18].

$$V_s = \frac{Q_m}{A}$$

where:

Q_m = flow rate at mean flowing pressure

A = total cross-sectional area of medium

Using data from Core #92, Run #3, in laminar region at $1/P_{mean} = 0.1\ atm^{-1}$:

$A = 0.049\ ft^2$

$P_m = 10\ atm = 147\ psi$

$T_m = 24°C = 535°R$

$\mu = 0.01793\ cp$ (using Kestin and Wang correlations in Appendix A3)

The density of nitrogen may be determined:

$$\rho = \frac{MP}{RT} = \frac{28(lb/lbmol)\ (10\ atm)}{0.730\ (atm \cdot ft^3/lbmol\ °R)\ 535°R} = 0.72\ lbm/ft^3$$

$Q_{atm} = 24.2$ ml/sec (from data)

$$Q_{mean} = Q_{atm} \cdot \frac{P_{atm}}{P_{mean}} = \frac{24.2}{10} = 2.42\ ml/sec$$

therefore:

$$V_s = \frac{2.42\ ml/sec}{0.048\ ft^2} \times 35.14\ ft^3/m^3 \times 1 \times 10^{-9}\ m^3/ml$$

$$= 1.77 \times 10^{-6}\ ft/sec$$

And substituting, R_e may now be determined

$$R_e = \frac{1.51 \times 10^{-6}\ ft \times 1.77 \times 10^{-6}\ ft/sec \times 0.72\ lbm/ft^3}{0.01793\ cp\ (1 - 0.111)\ 6.72 \times 10^{-4}\ (lbm/ft \cdot sec \cdot cp)}$$

$$= 1.8 \times 10^{-7}$$

APPENDIX B1

Core 90: 3" Dolomite

ABSOLUTE PERMEABILITY versus NET CONFINING PRESSURE

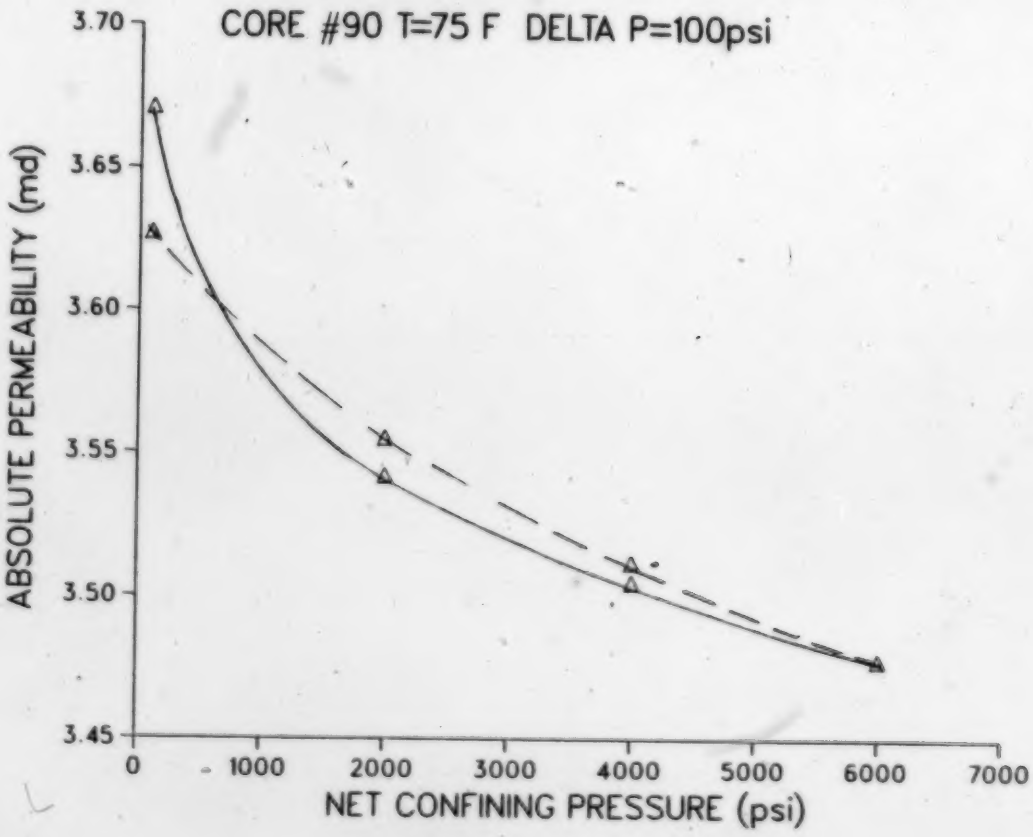

K/Katm vs NET CONFINING PRESSURE

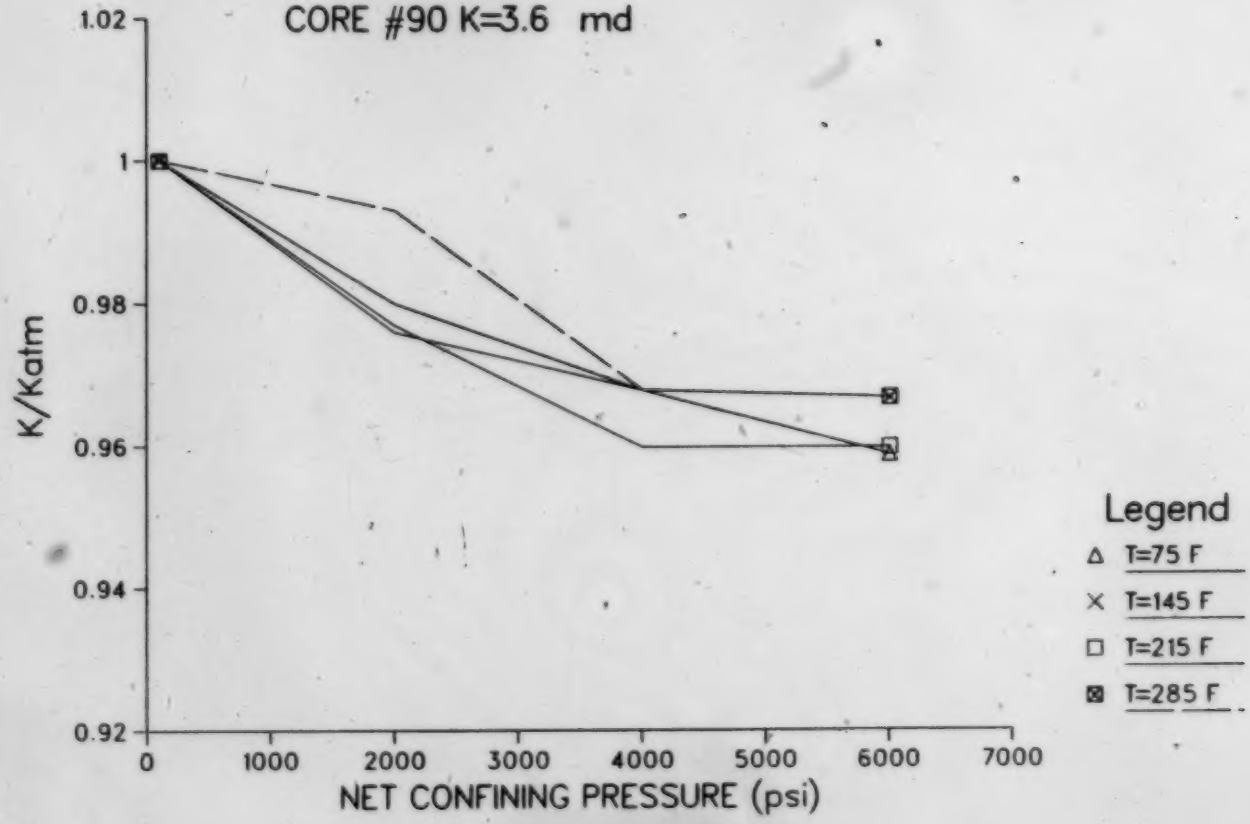

K/K(75 F) vs TEMPERATURE

(NET CONFINING PRESSURE AS CROSS - PARAMETER)

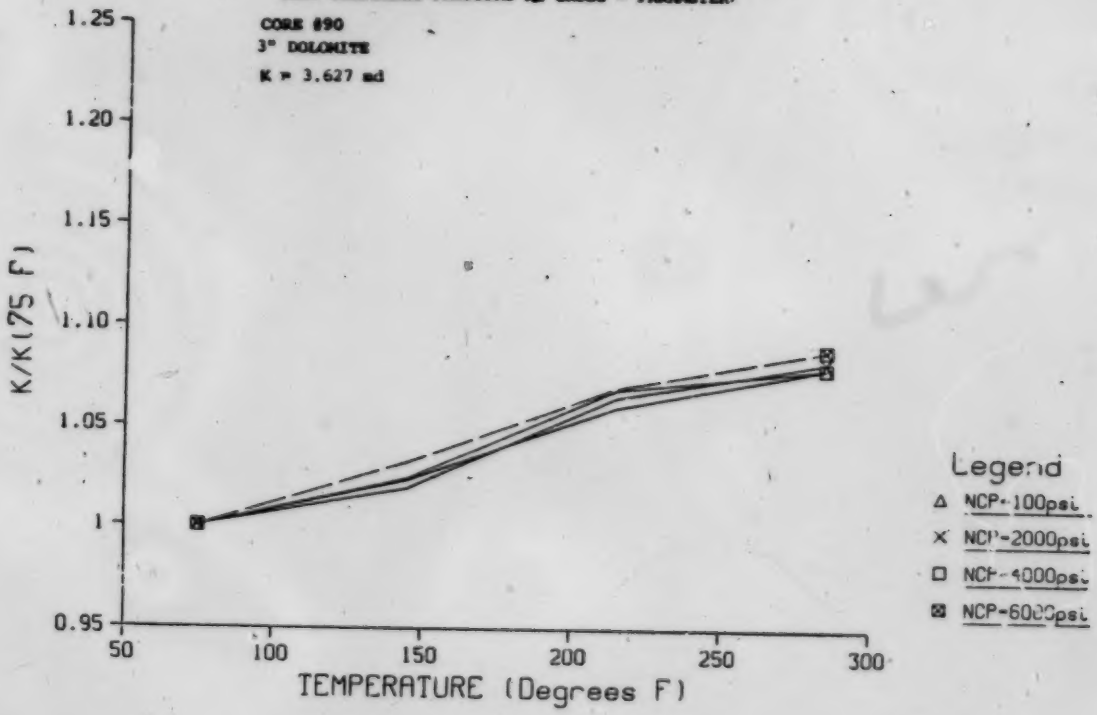

SLIP FACTOR vs TEMPERATURE

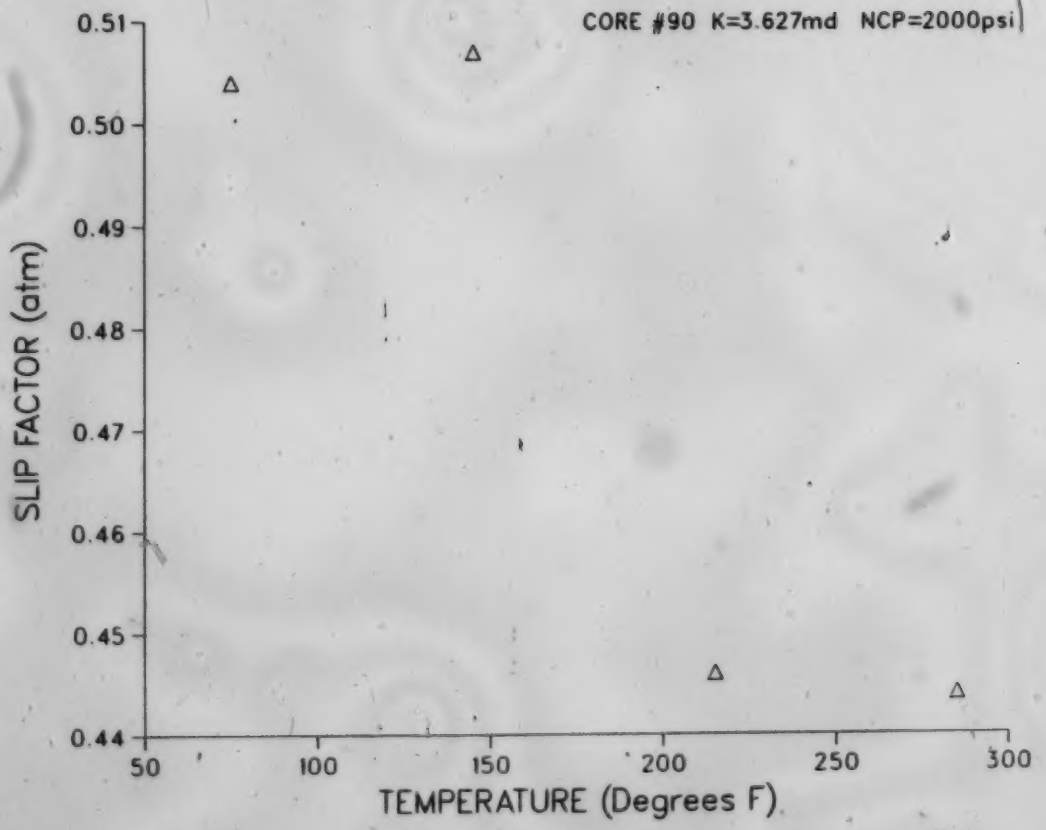

APPARENT PERMEABILITY vs RECIPROCAL MEAN PRESSURE

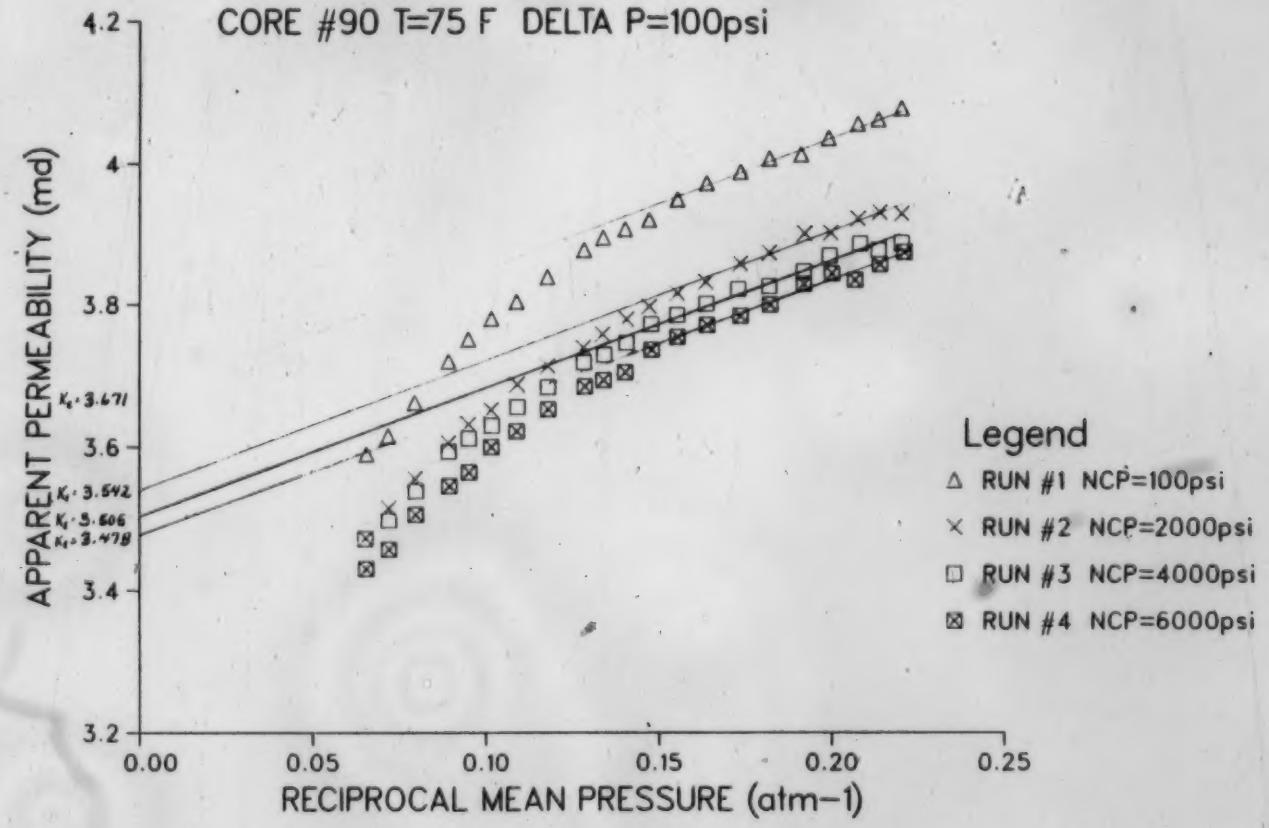

APPARENT PERMEABILITY vs RECIPROCAL MEAN PRESSURE

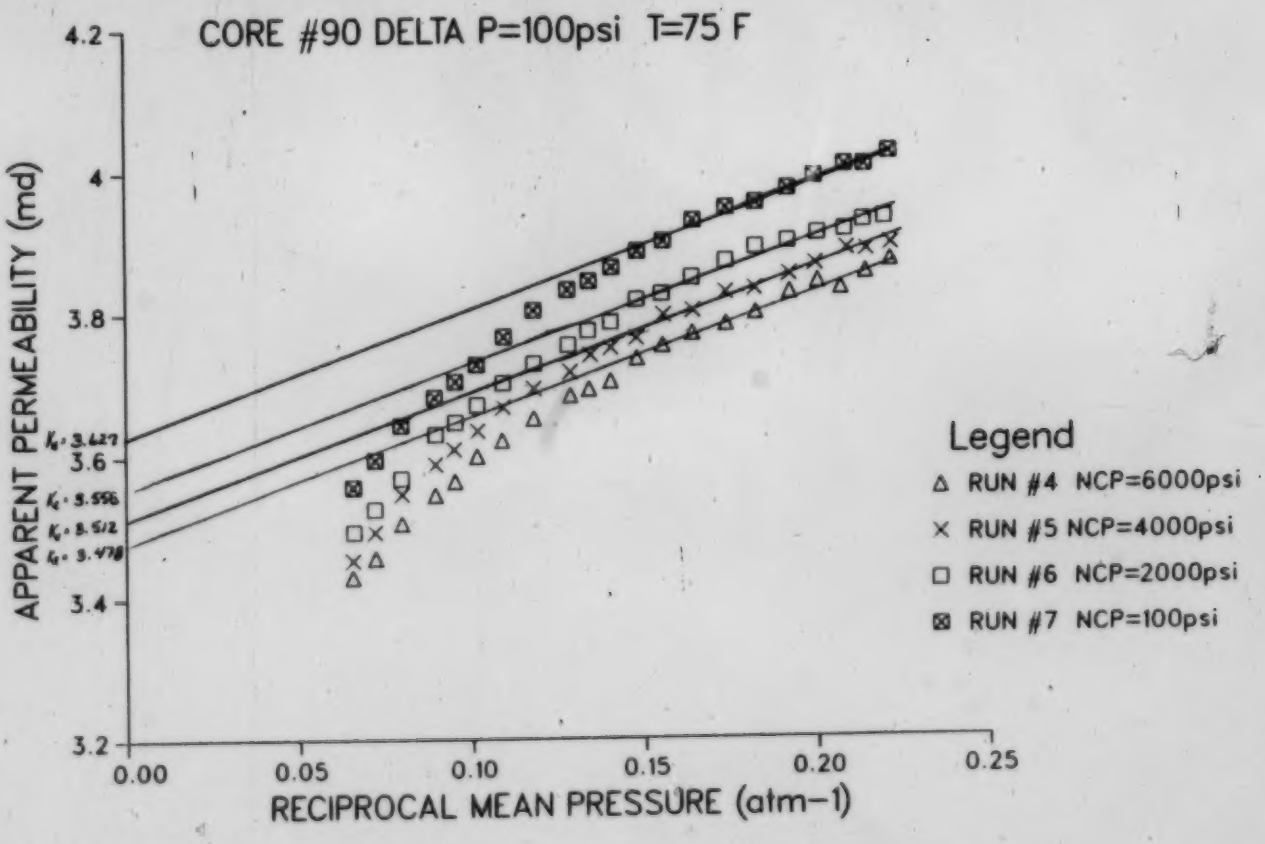

APPARENT PERMEABILITY vs RECIPROCAL MEAN PRESSURE

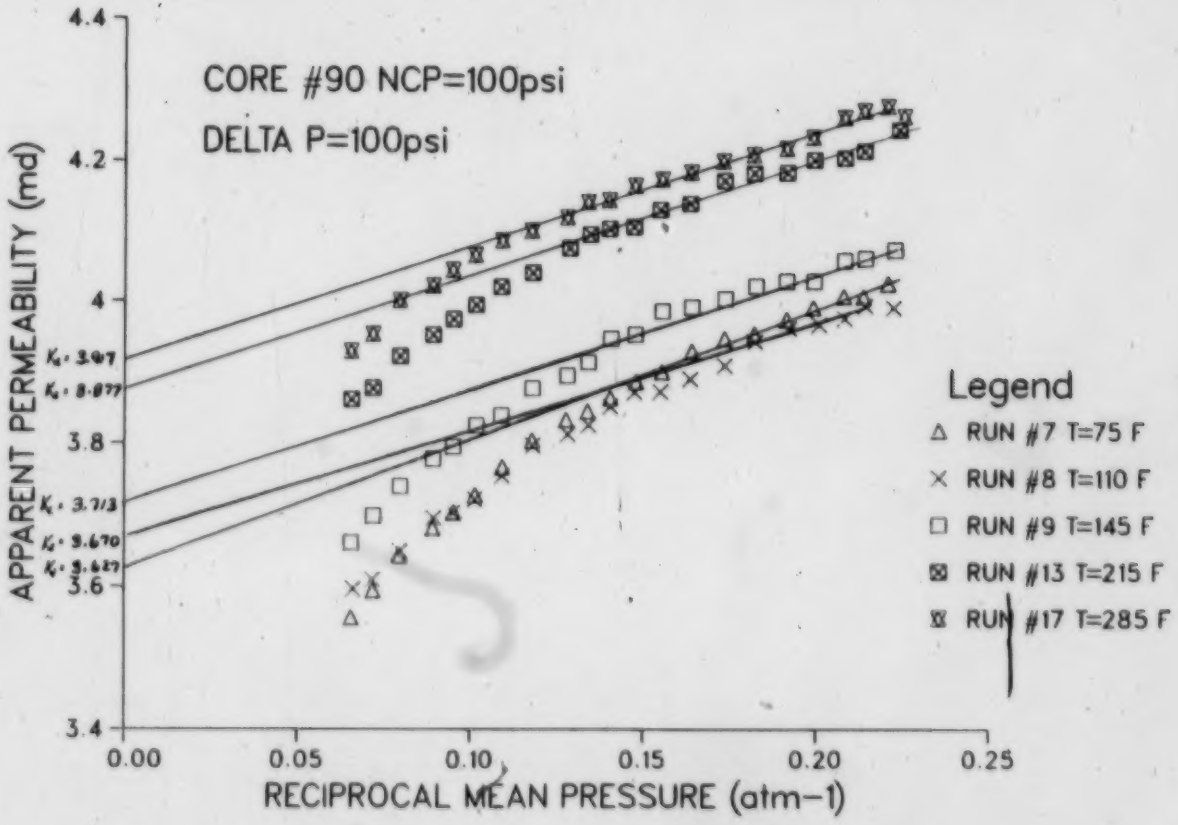

APPARENT PERMEABILITY vs RECIPROCAL MEAN PRESSURE

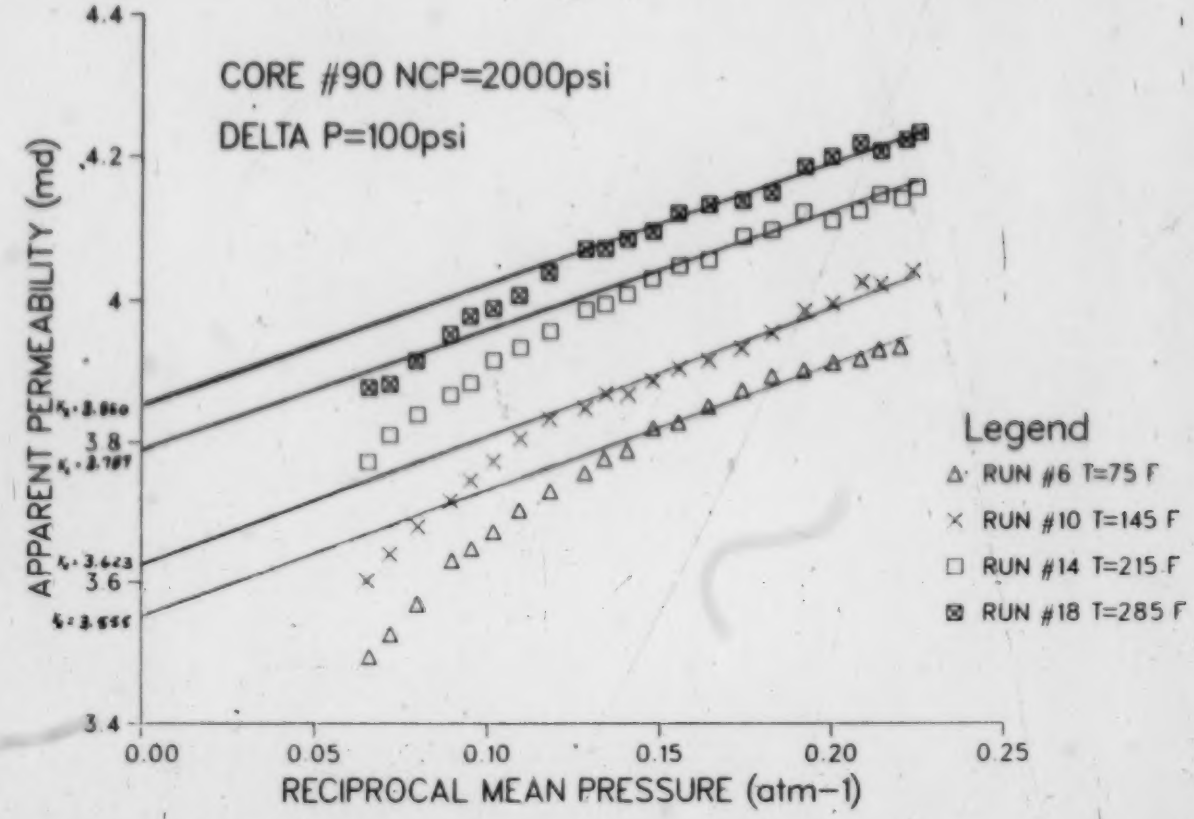

APPARENT PERMEABILITY vs RECIPROCAL MEAN PRESSURE

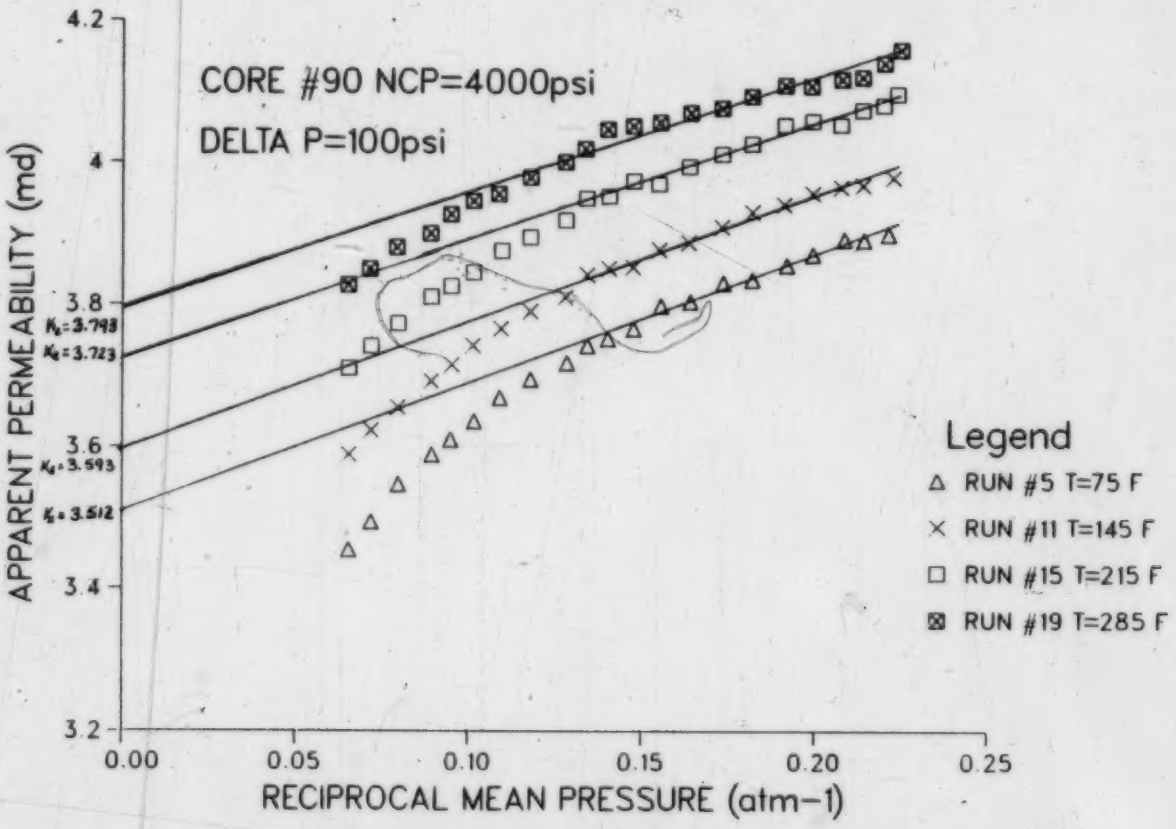

APPARENT PERMEABILITY vs RECIPROCAL MEAN PRESSURE

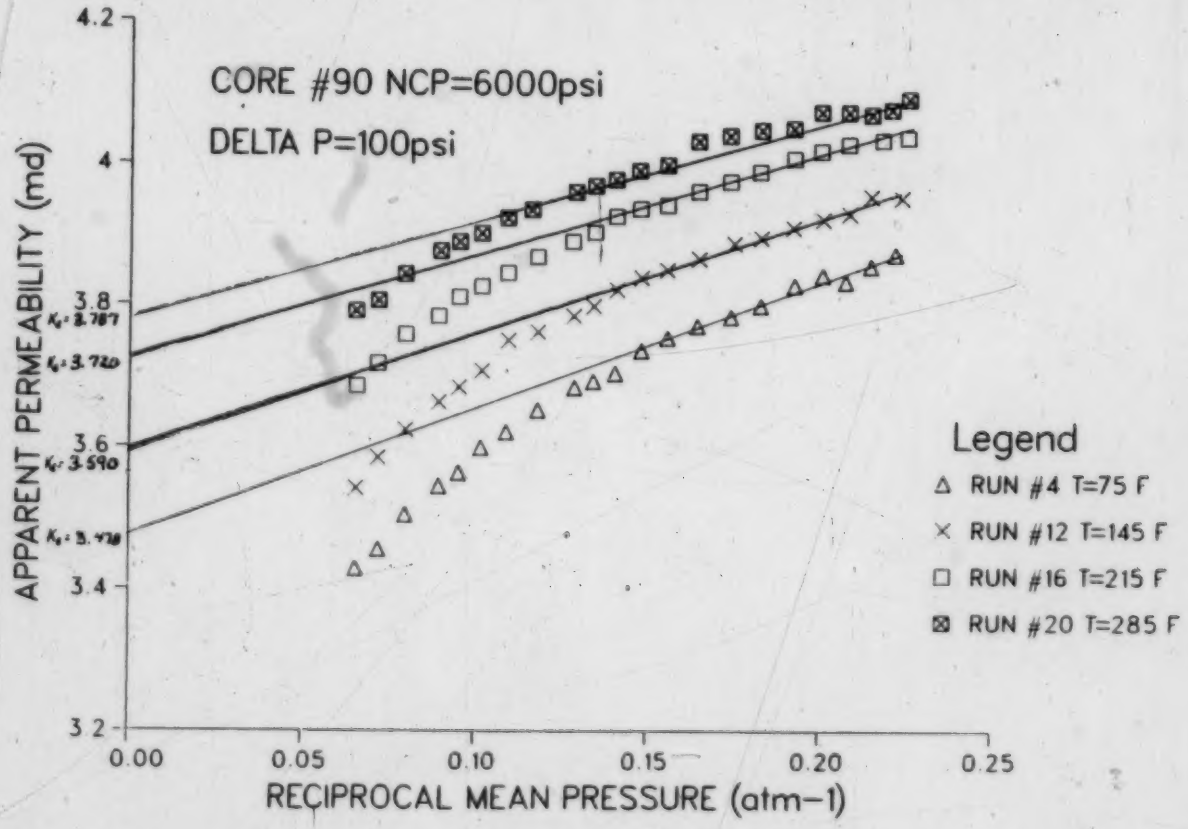

APPENDIX B2

CORE 133A: 3" Dolomite

ABSOLUTE PERMEABILITY versus NET CONFINING PRESSURE

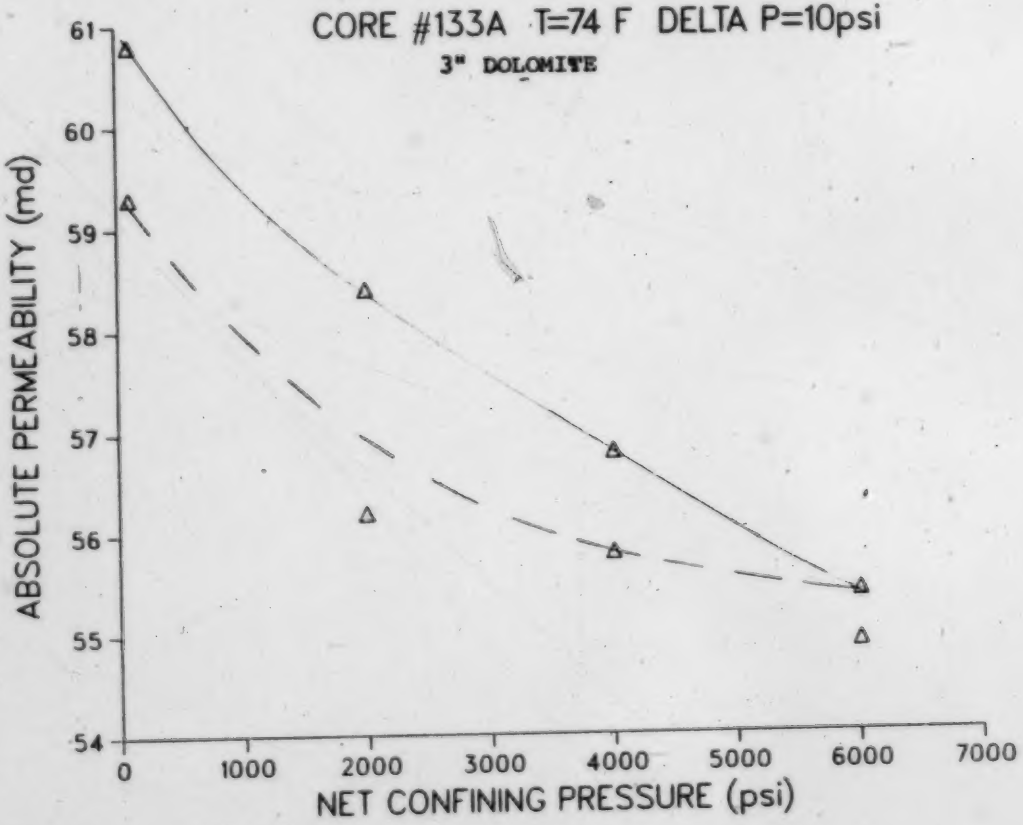

Kabs/Kabs(at 75 F) vs TEMPERATURE

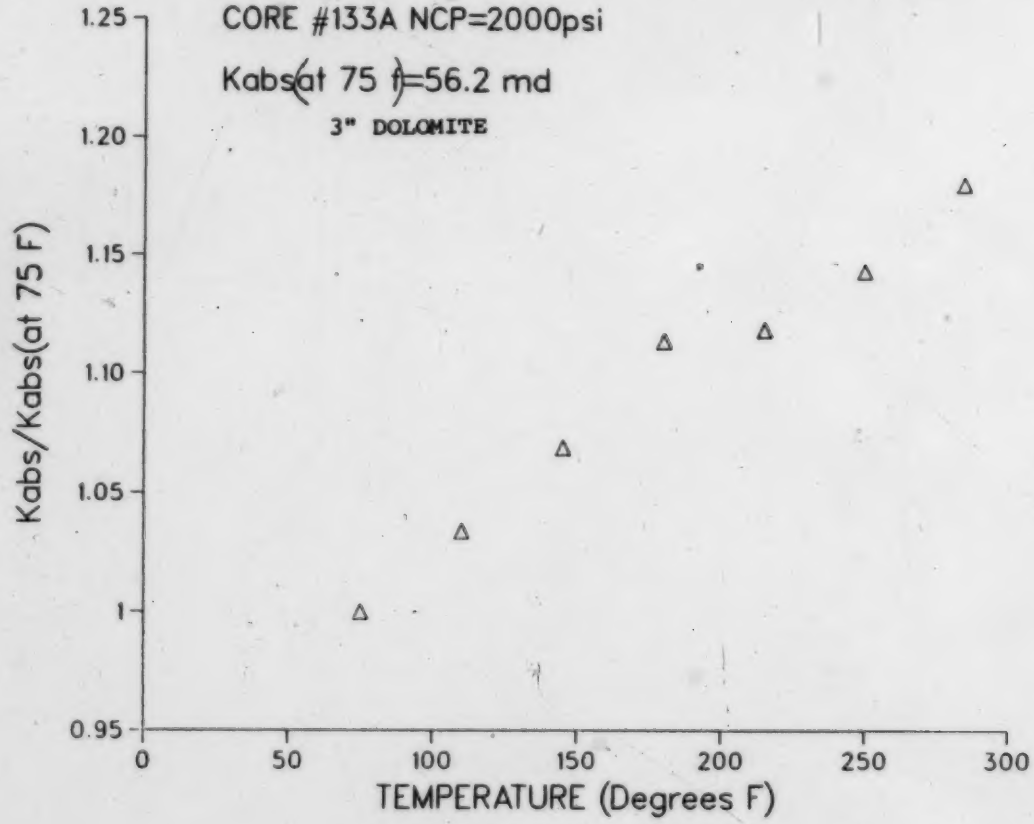

ABSOLUTE PERMEABILITY versus TEMPERATURE

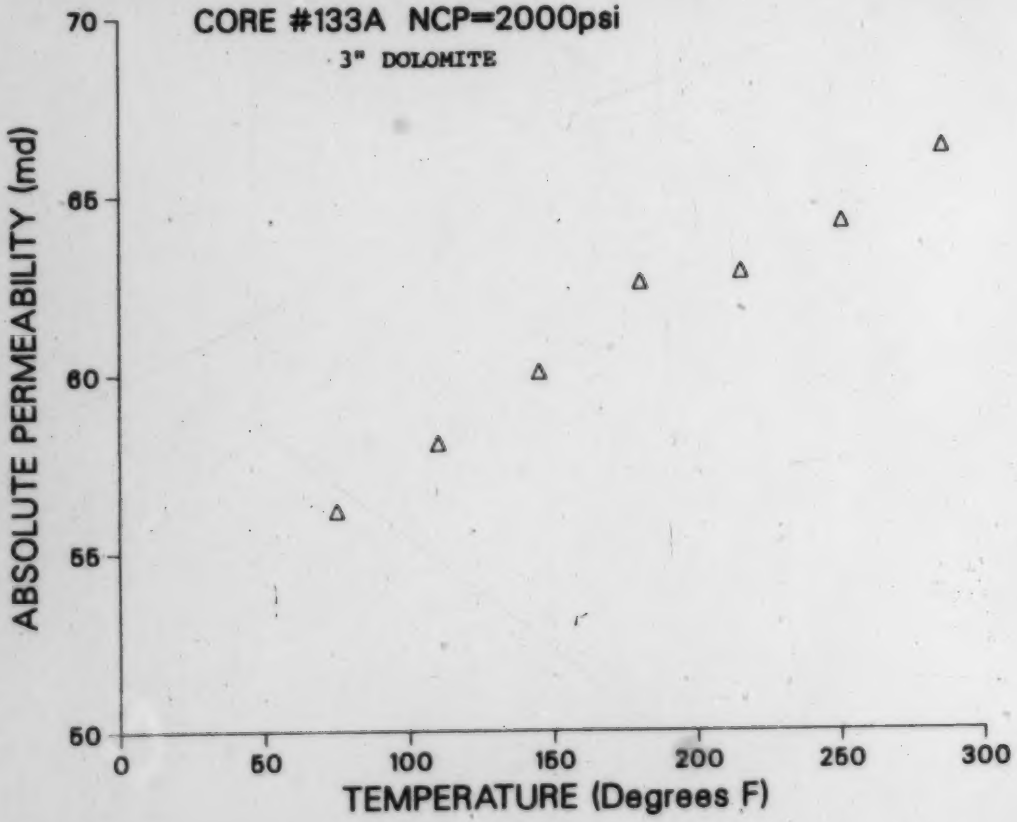

KLINKENBERG SLIP FACTOR versus TEMPERATURE

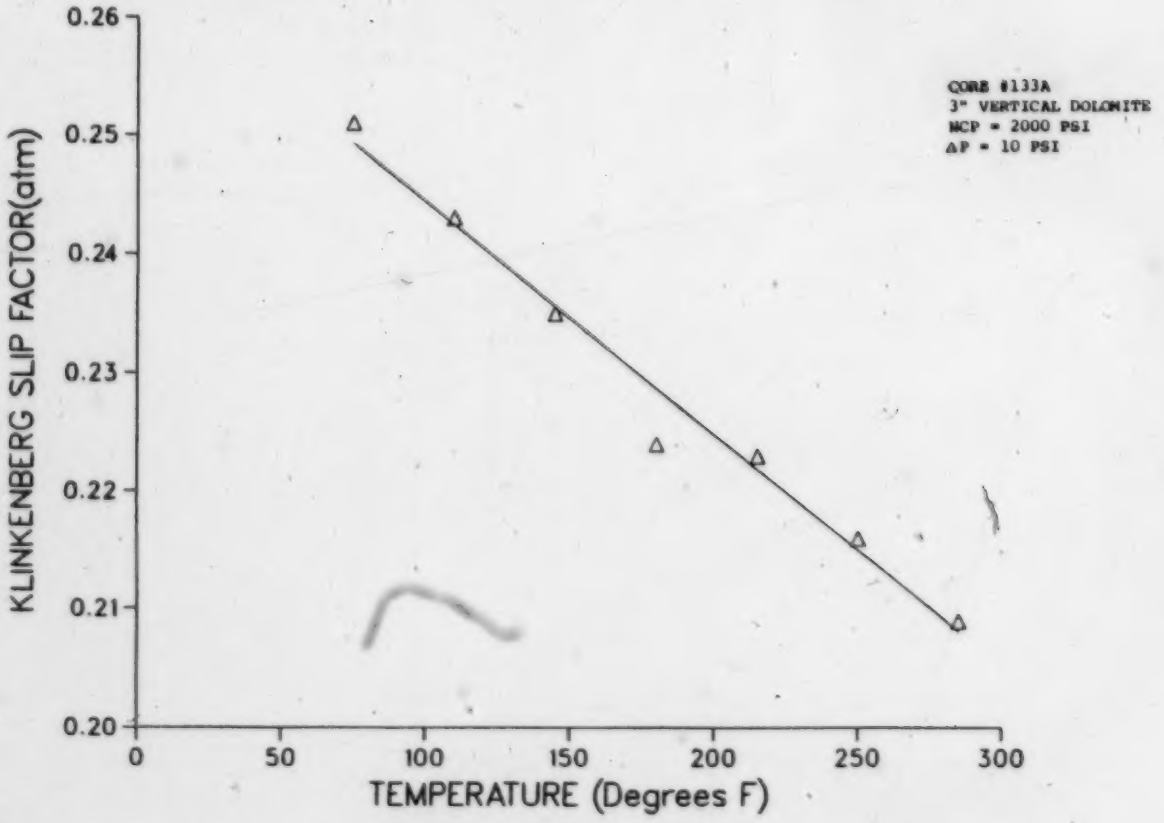

APPARENT PERMEABILITY vs RECIPROCAL MEAN PRESSURE

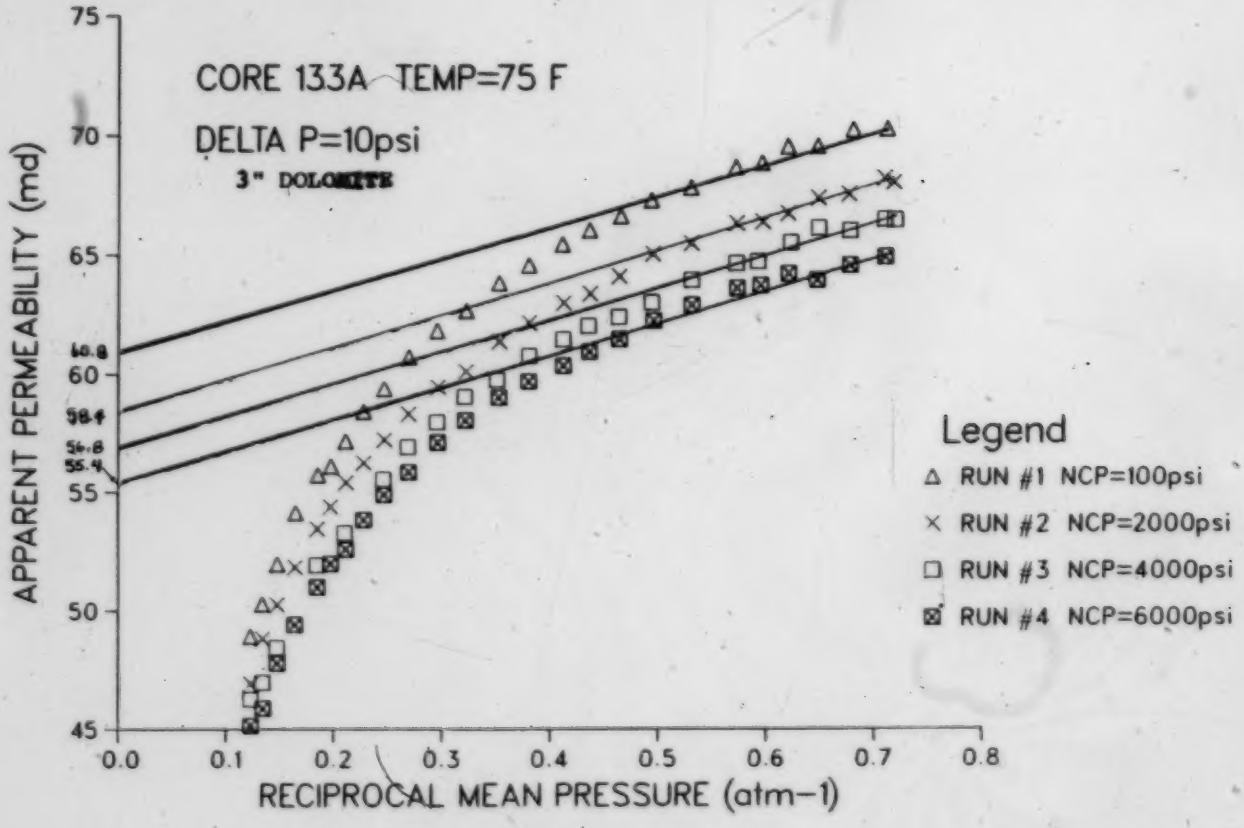

APPARENT PERMEABILITY vs RECIPROCAL MEAN PRESSURE

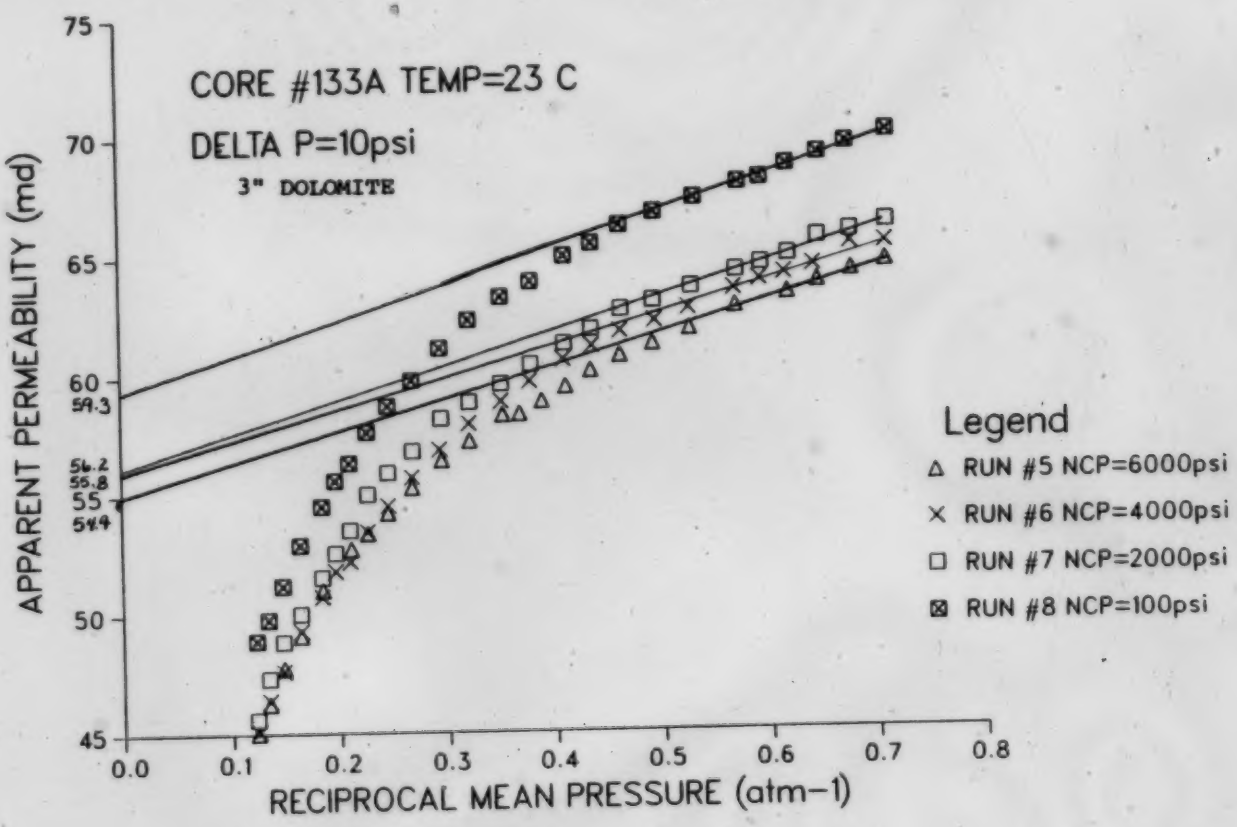

APPARENT PERMEABILITY vs RECIPROCAL MEAN PRESSURE

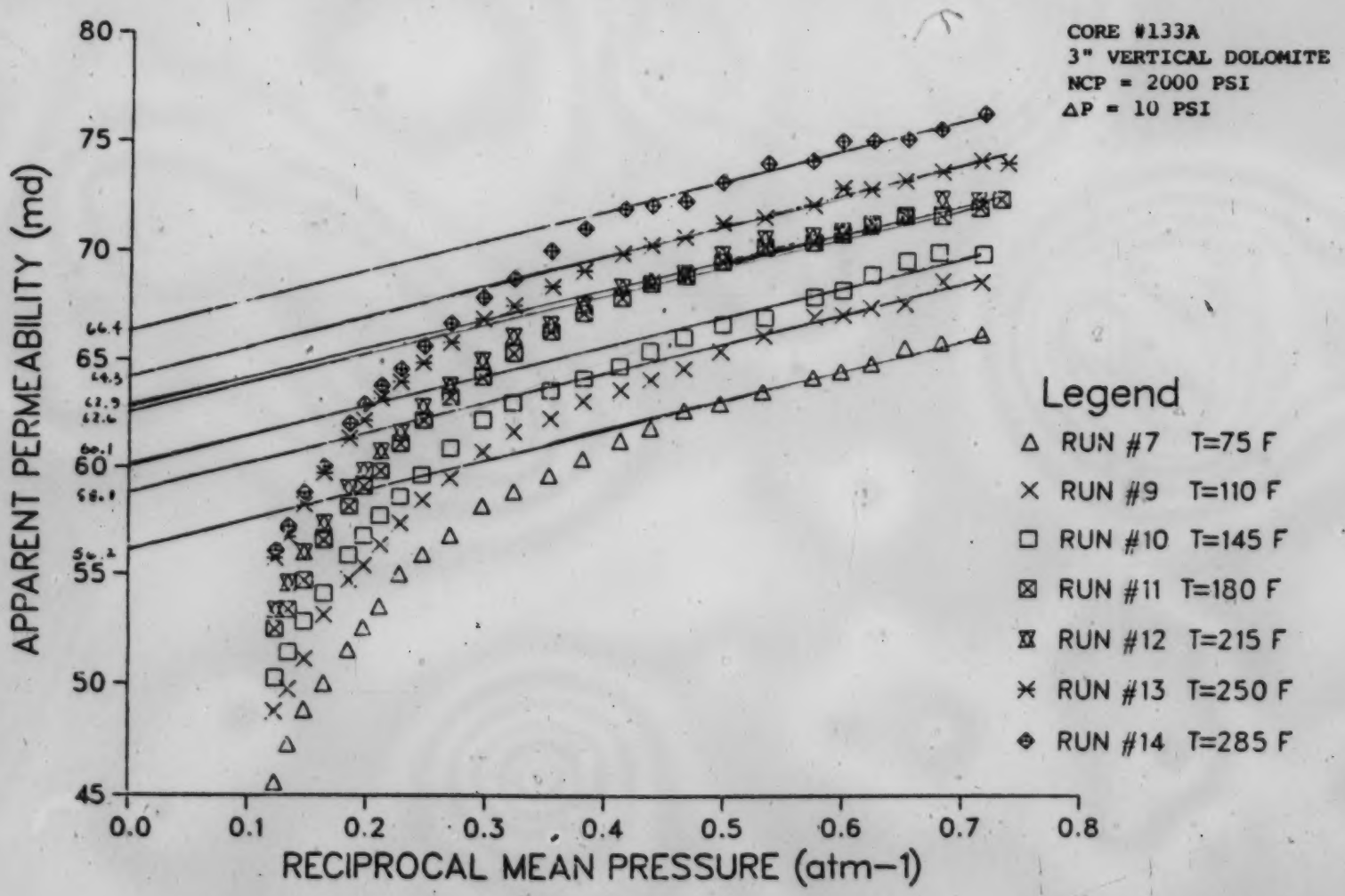

APPENDIX B3

CORE 92: 3" Dolomite

ABSOLUTE PERMEABILITY vs. NET CONFINING PRESSURE

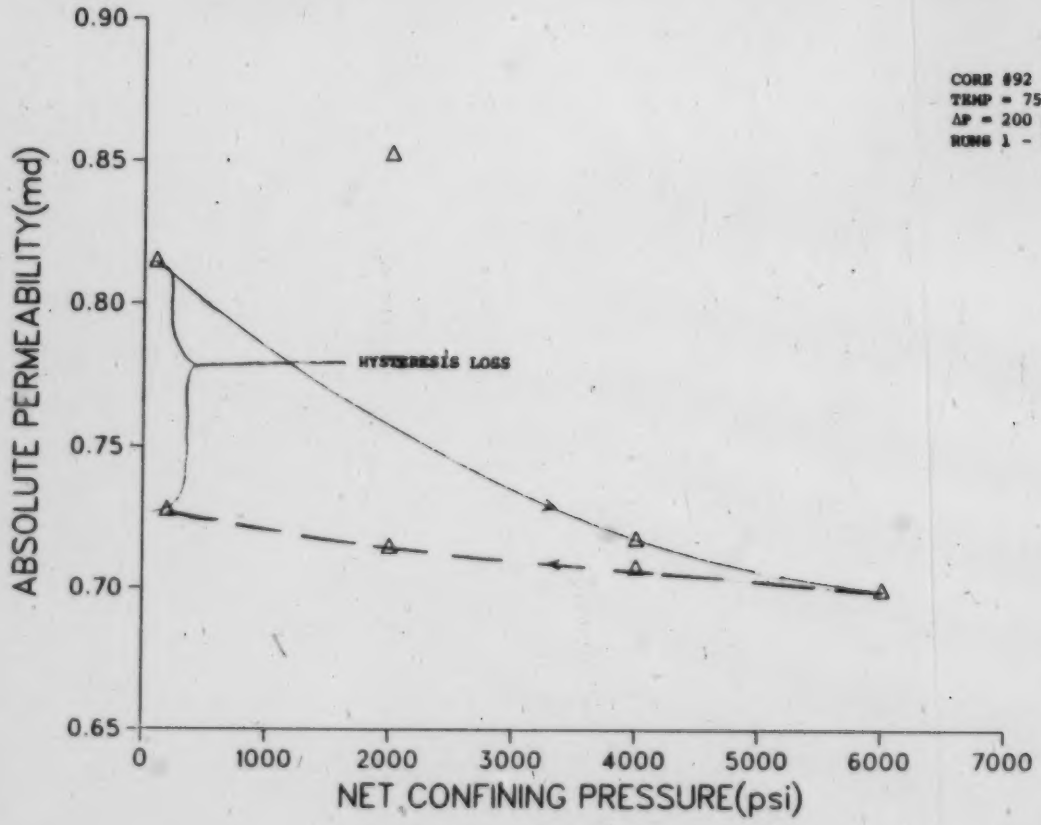

ABSOLUTE PERMEABILITY vs. TEMPERATURE

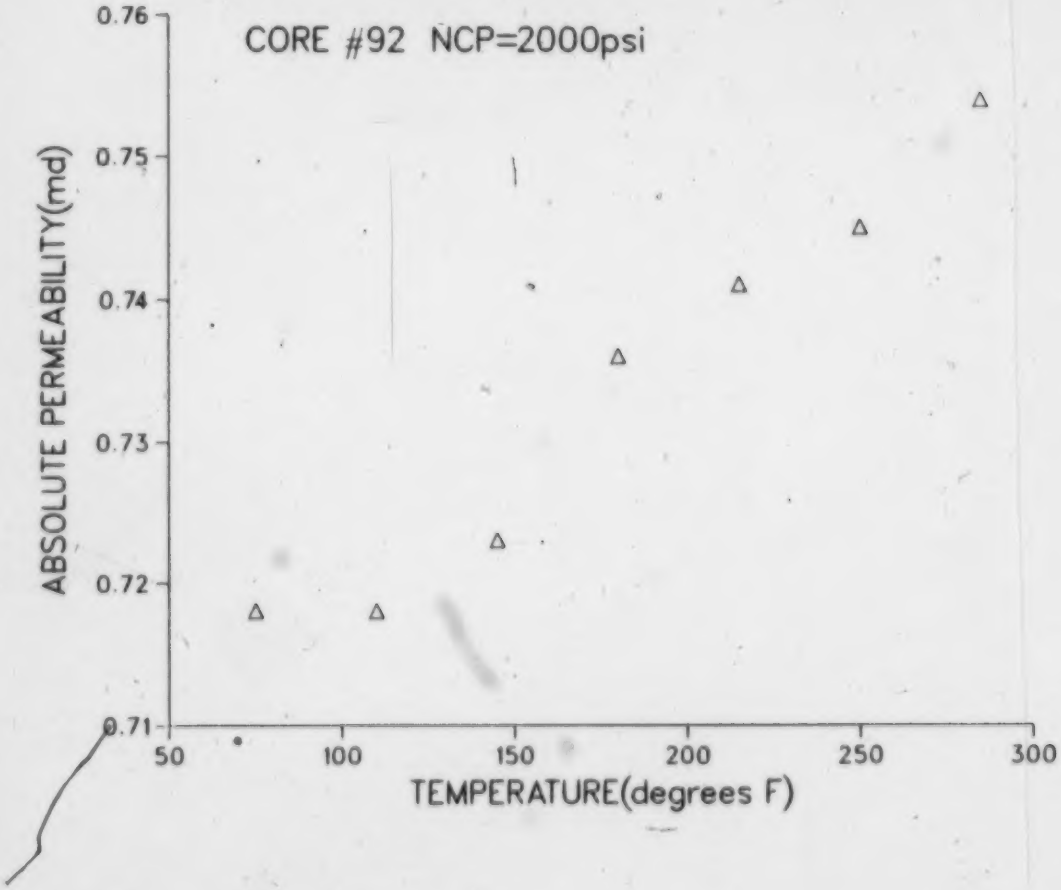

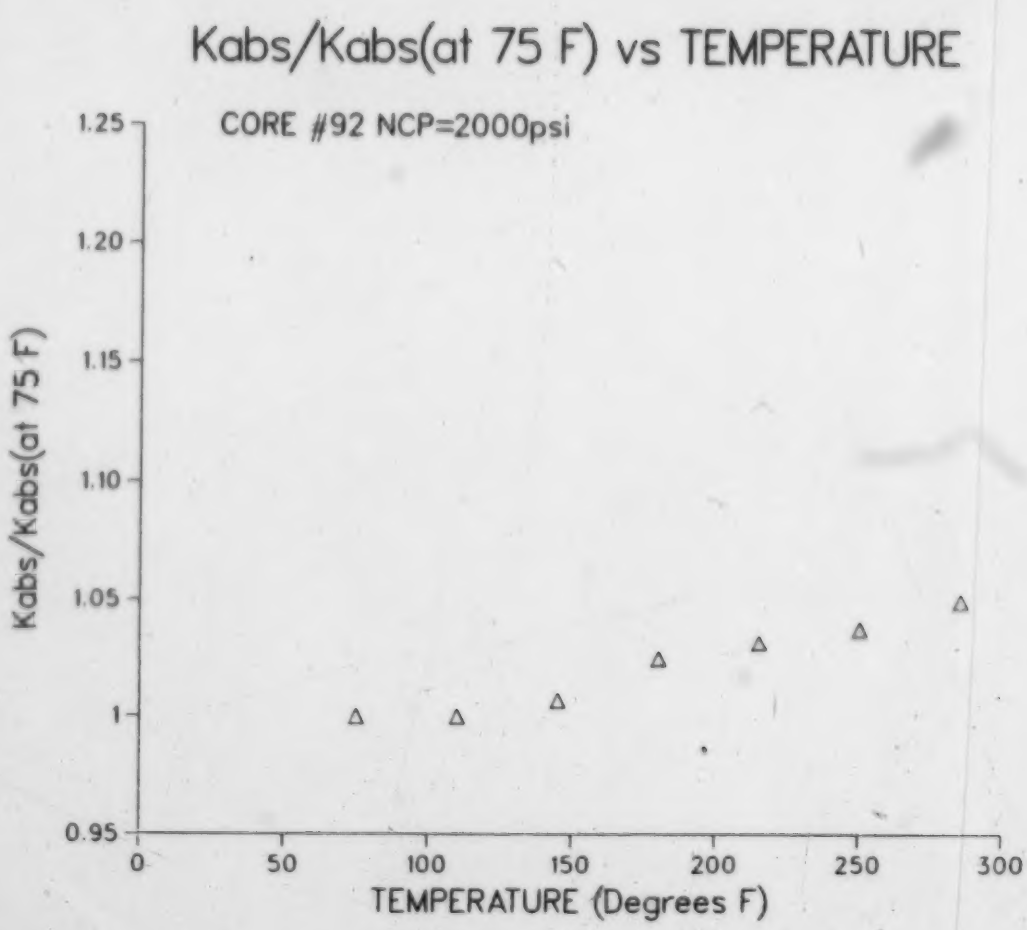
Kabs/Kabs(at 75 F) vs TEMPERATURE
CORE #92 NCP=2000psi
Kabs/Kabs(at 75 F)
1.25
1.20
1.15
1.10
1.05
1
0.95
0
50
100
150
200
250
300
TEMPERATURE (Degrees F)

SLIP FACTOR vs. TEMPERATURE

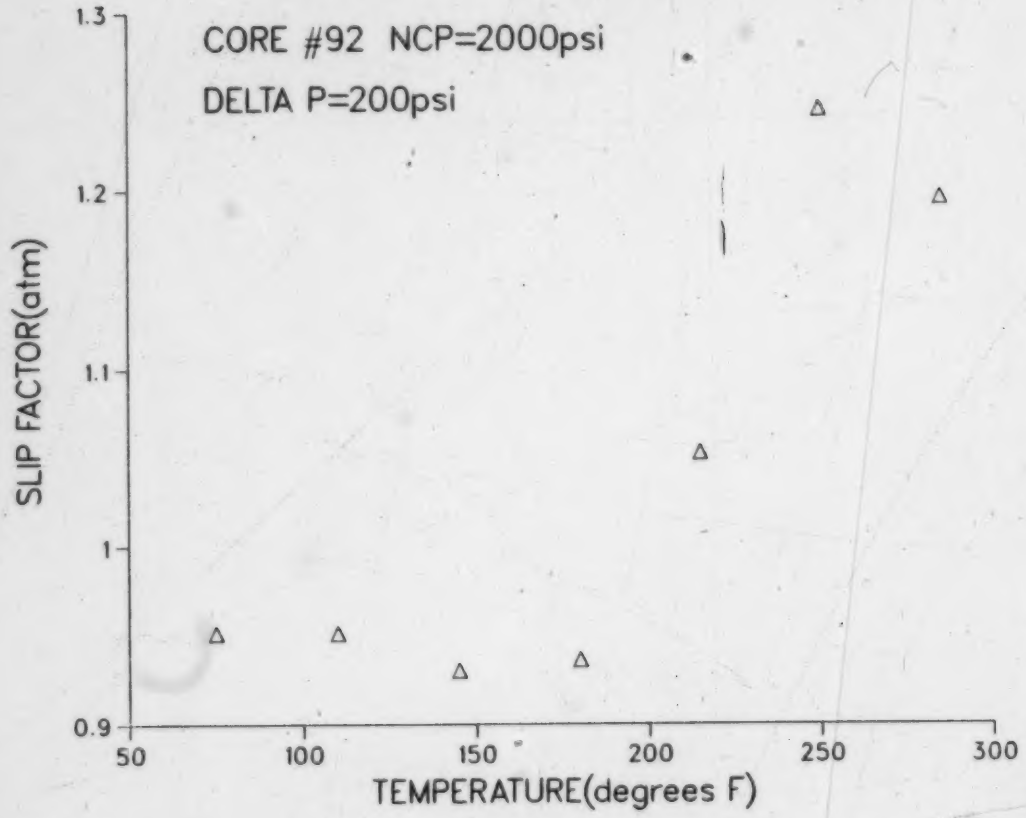

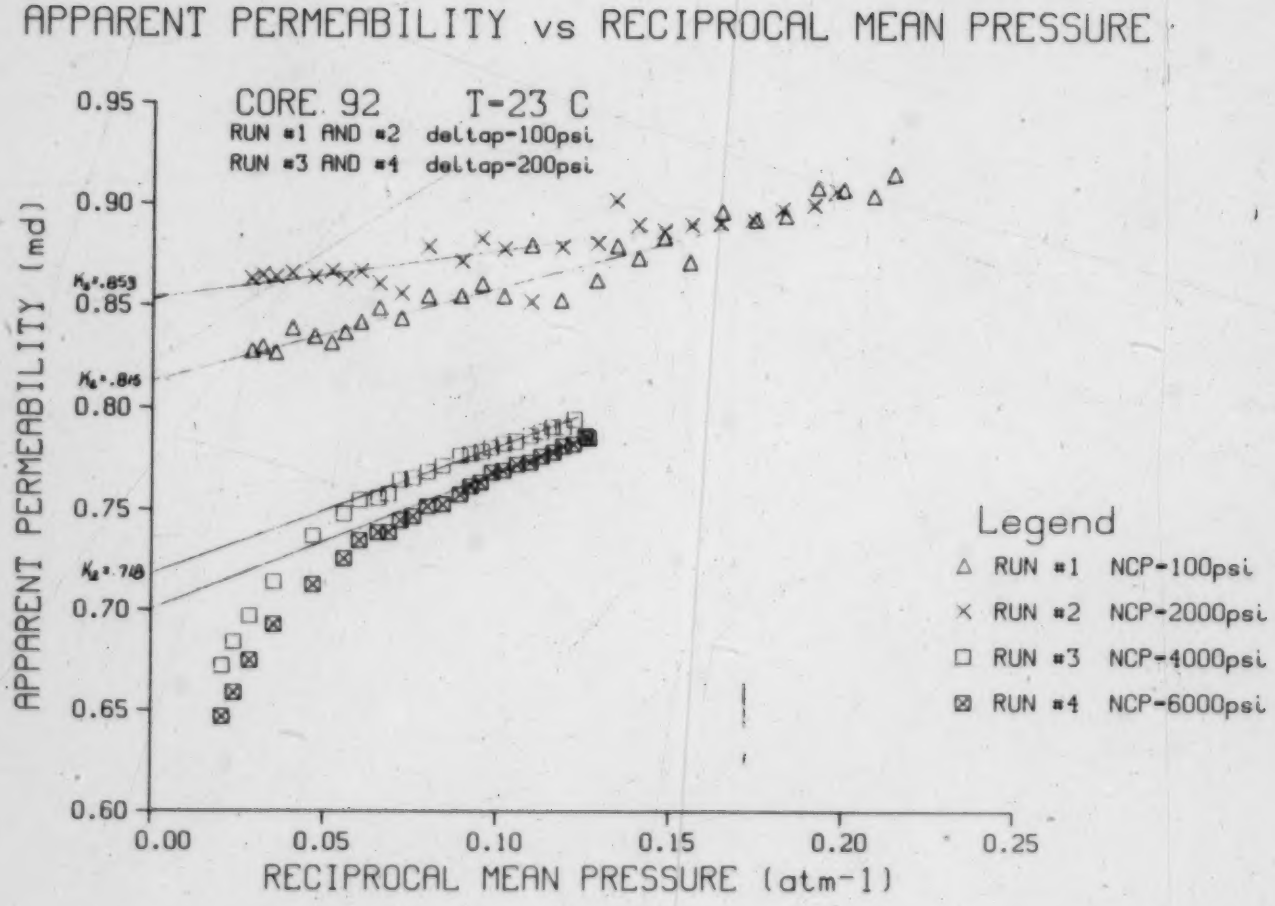
APPARENT PERMEABILITY vs RECIPROCAL MEAN PRESSURE
CORE 92 T-23 C
RUN #1 AND #2 deltap-100psi
RUN #3 AND #4 deltap-200psi
APPARENT PERMEABILITY (md)
0.95
0.90
0.85
0.80
0.75
0.70
0.65
0.60
0.00
0.05
0.10
0.15
0.20
0.25
RECIPROCAL MEAN PRESSURE (atm-1)
Legend
RUN #1 NCP-100psi
RUN #2 NCP-2000psi
RUN #3 NCP-4000psi
RUN #4 NCP-6000psi

APPARENT PERMEABILITY vs RECIPROCAL MEAN PRESSURE

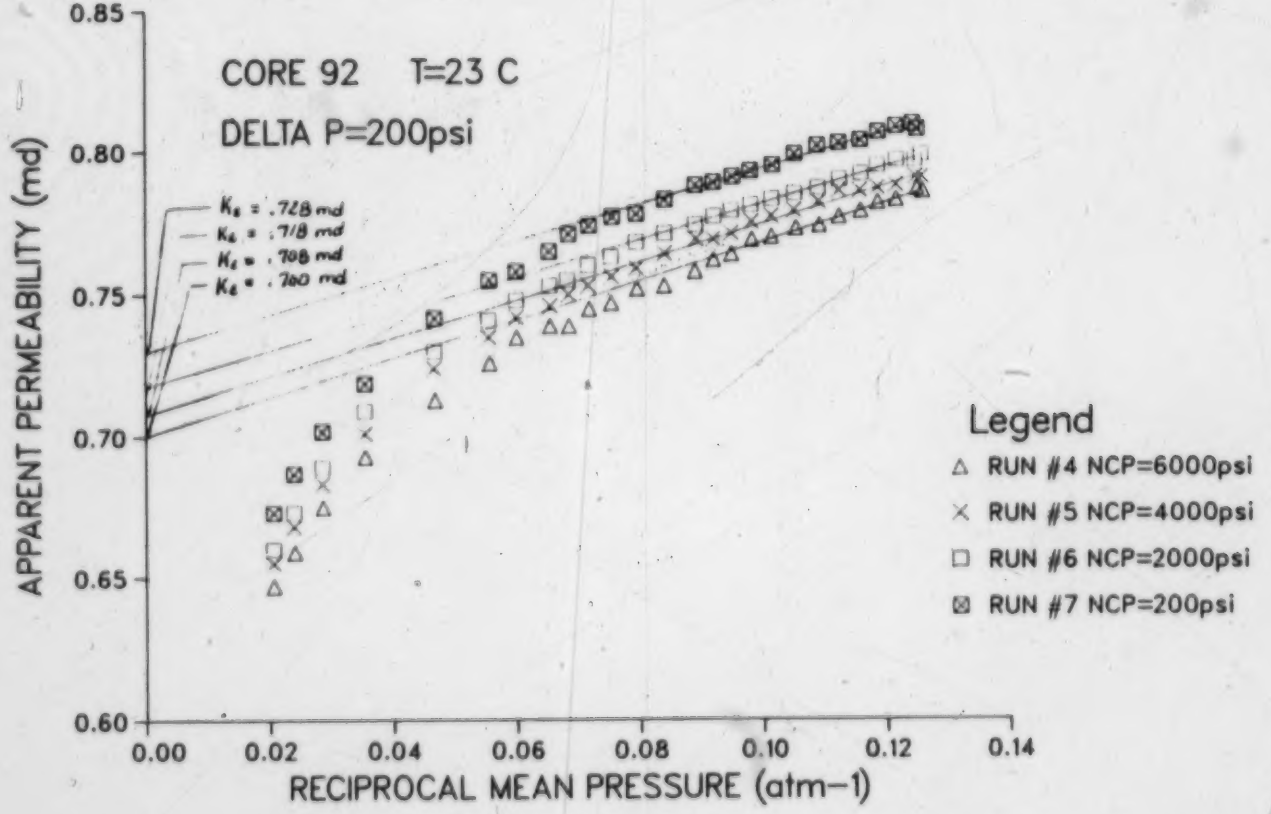

APPARENT PERMEABILITY vs RECIPROCAL MEAN PRESSURE

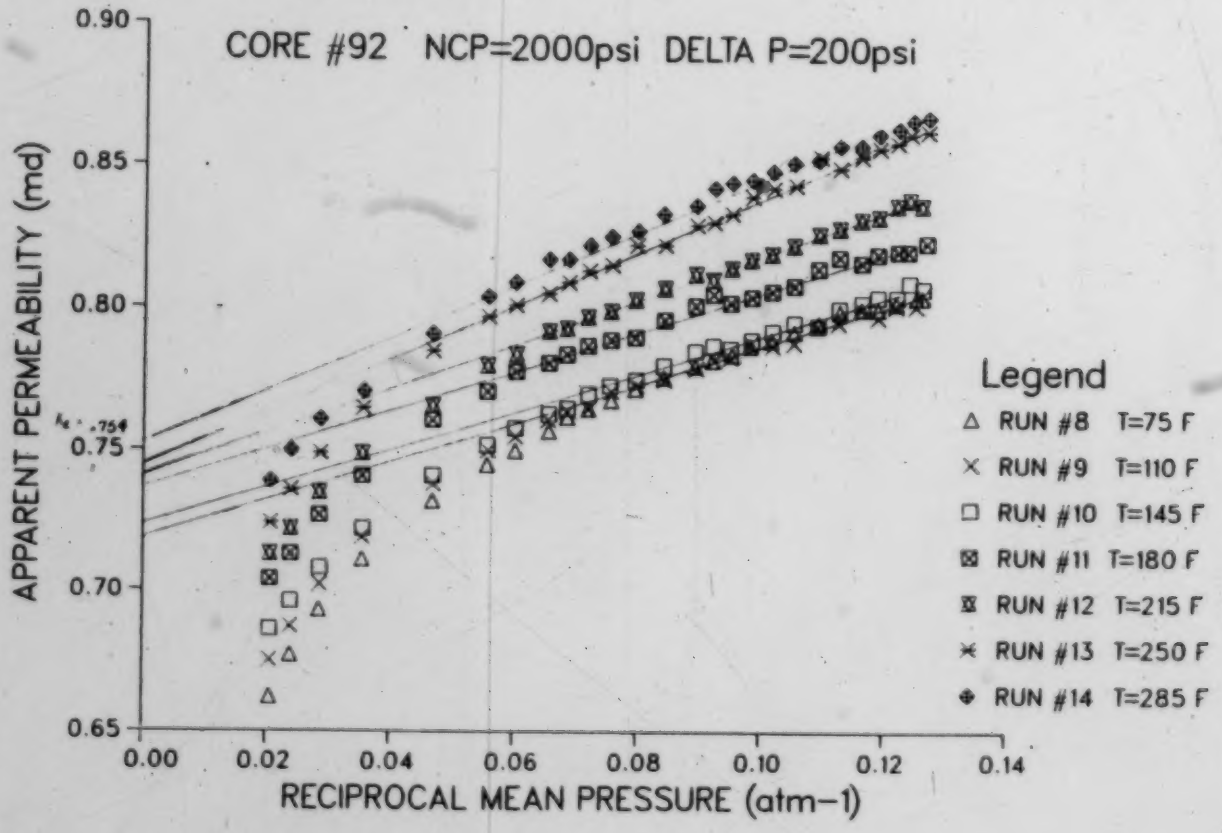

APPARENT PERMEABILITY vs RECIPROCAL MEAN PRESSURE

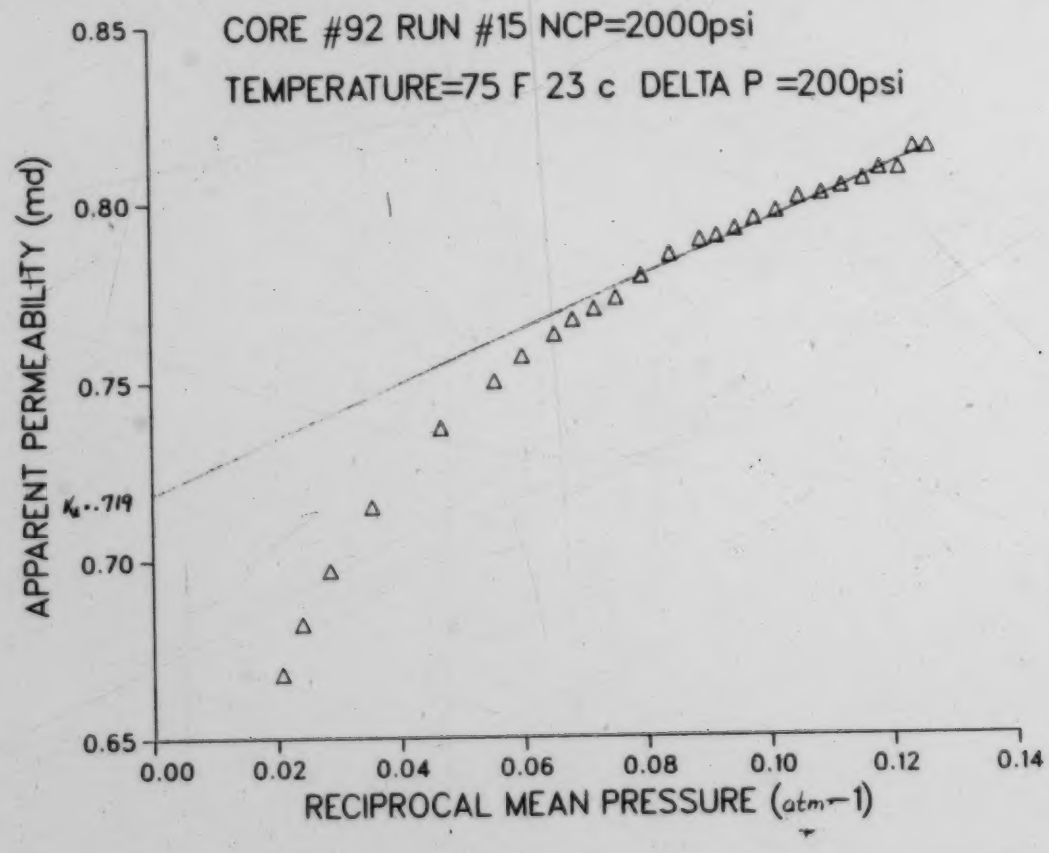

APPENDIX B4

HORIZONTAL PLUG 93B: Dolomite

K/K100 versus NET CONFINING PRESSURE

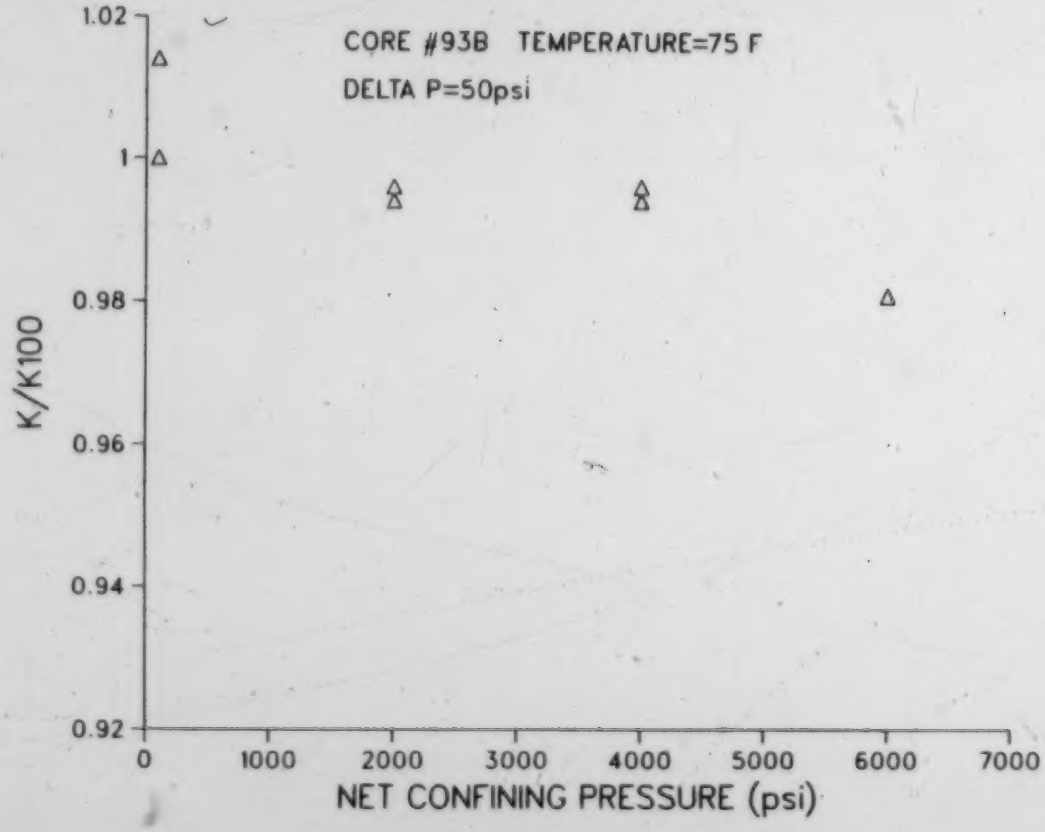

K/K75 versus TEMPERATURE

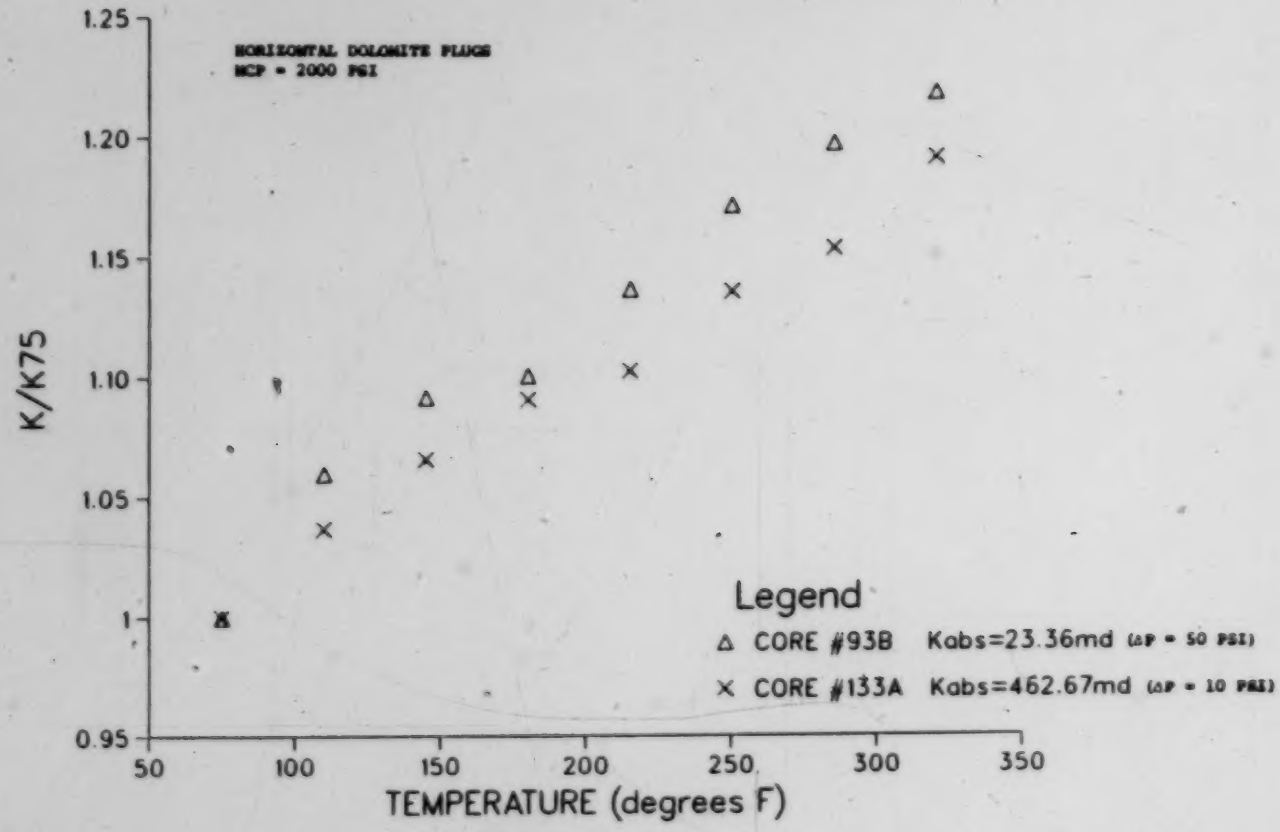

SLIP FACTOR versus TEMPERATURE

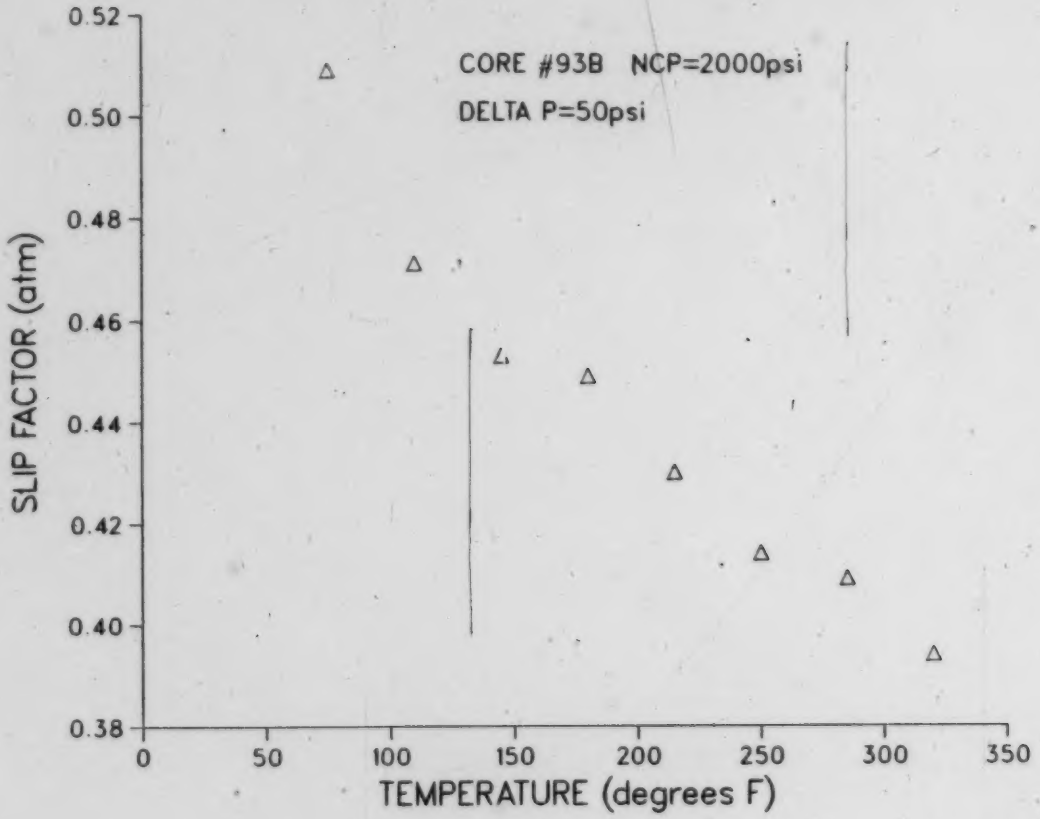

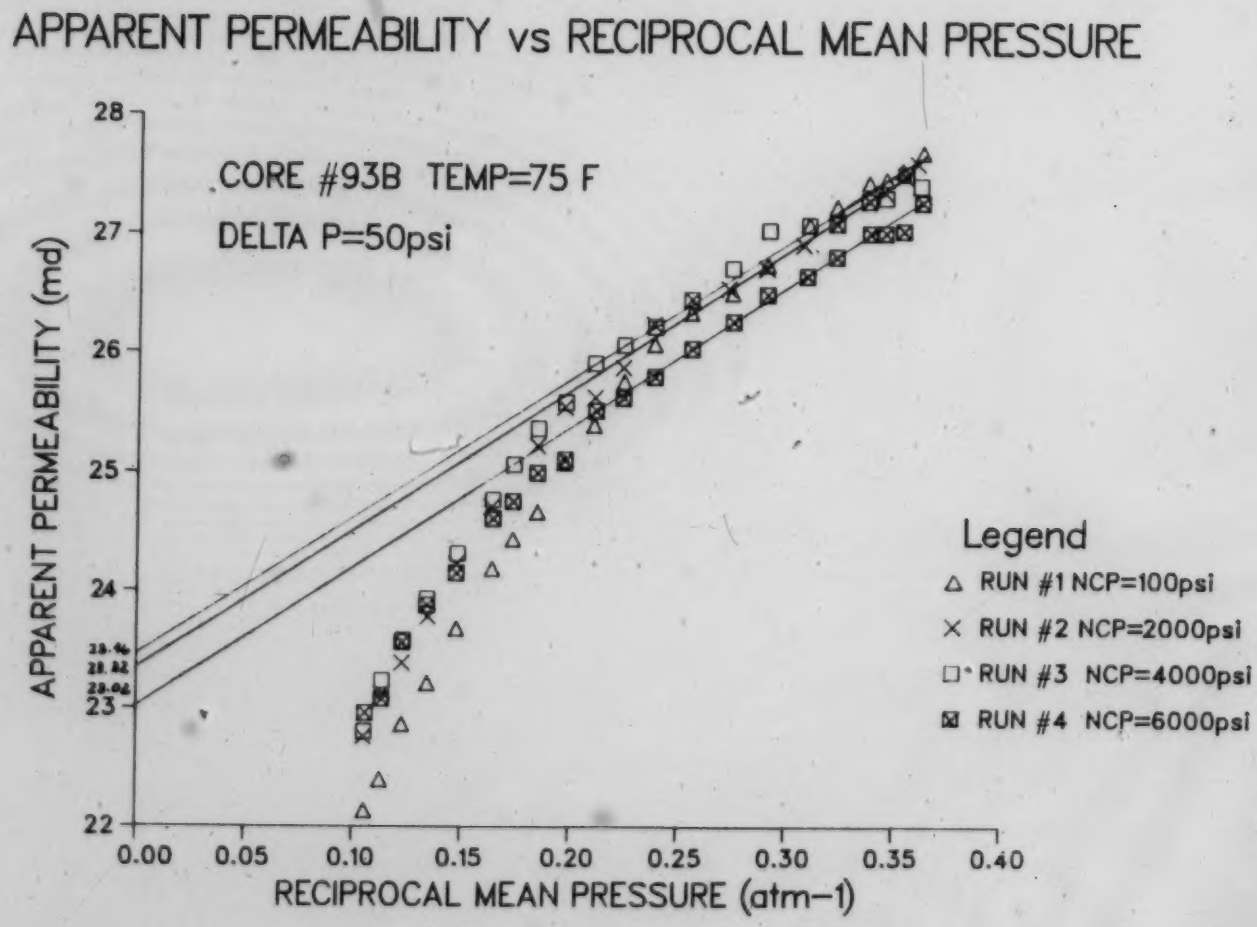
APPARENT PERMEABILITY vs RECIPROCAL MEAN PRESSURE
CORE #93B TEMP=75 F
DELTA P=50psi
APPARENT PERMEABILITY (md)
28
27
26
25
24
23
22
0.00
0.05
0.10
0.15
0.20
0.25
0.30
0.35
0.40
RECIPROCAL MEAN PRESSURE (atm-1)
Legend
RUN #1 NCP=100psi
RUN #2 NCP=2000psi
RUN #3 NCP=4000psi
RUN #4 NCP=6000psi

APPARENT PERMEABILITY vs RECIPROCAL MEAN PRESSURE

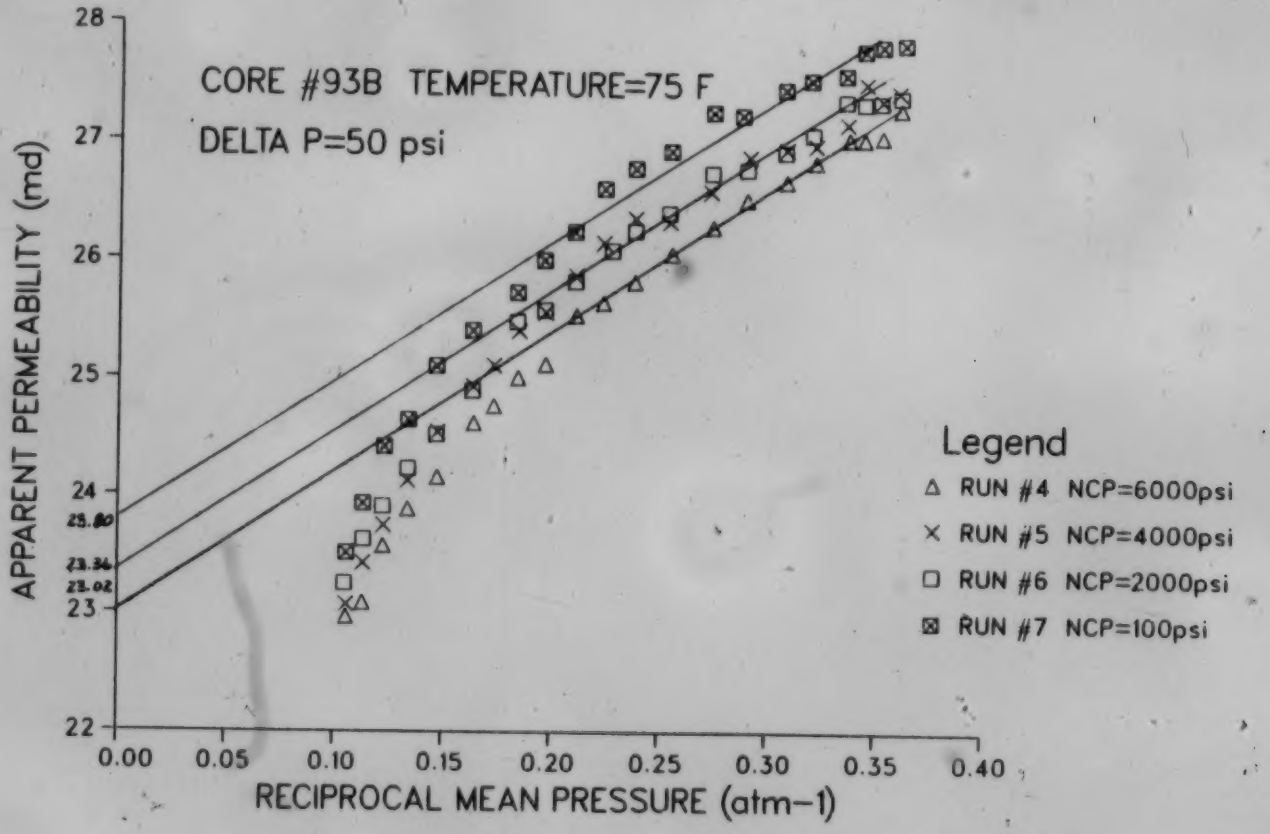

APPARENT PERMEABILITY vs RECIPROCAL MEAN PRESSURE

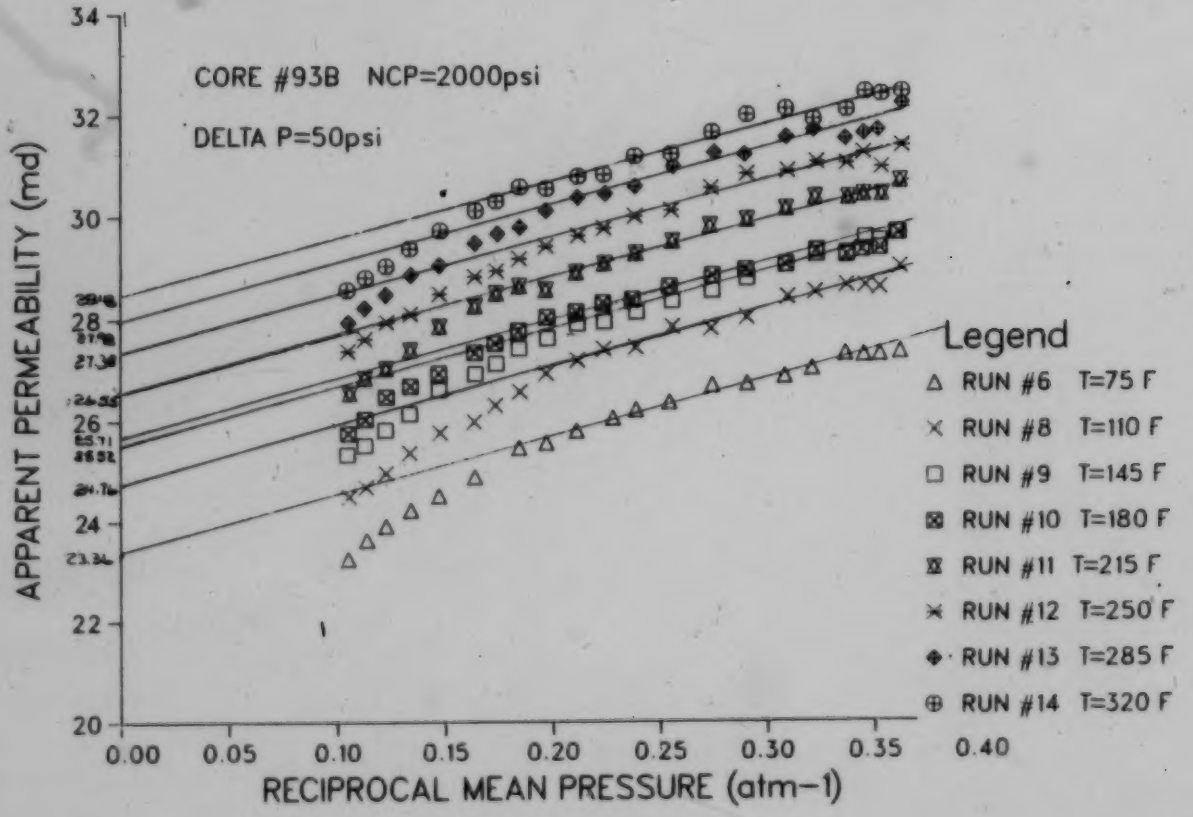

APPENDIX B5

HORIZONTAL PLUG 133A: Dolomite

K/K100 versus NET CONFINING PRESSURE

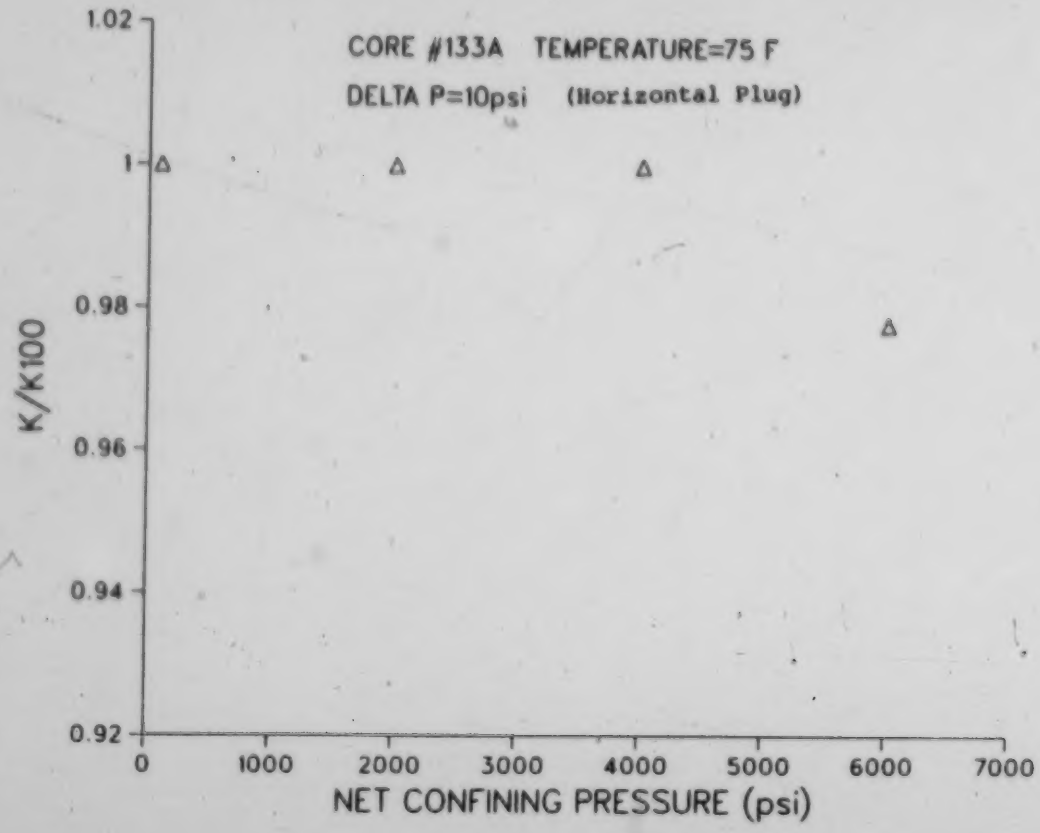

K/K75 versus TEMPERATURE

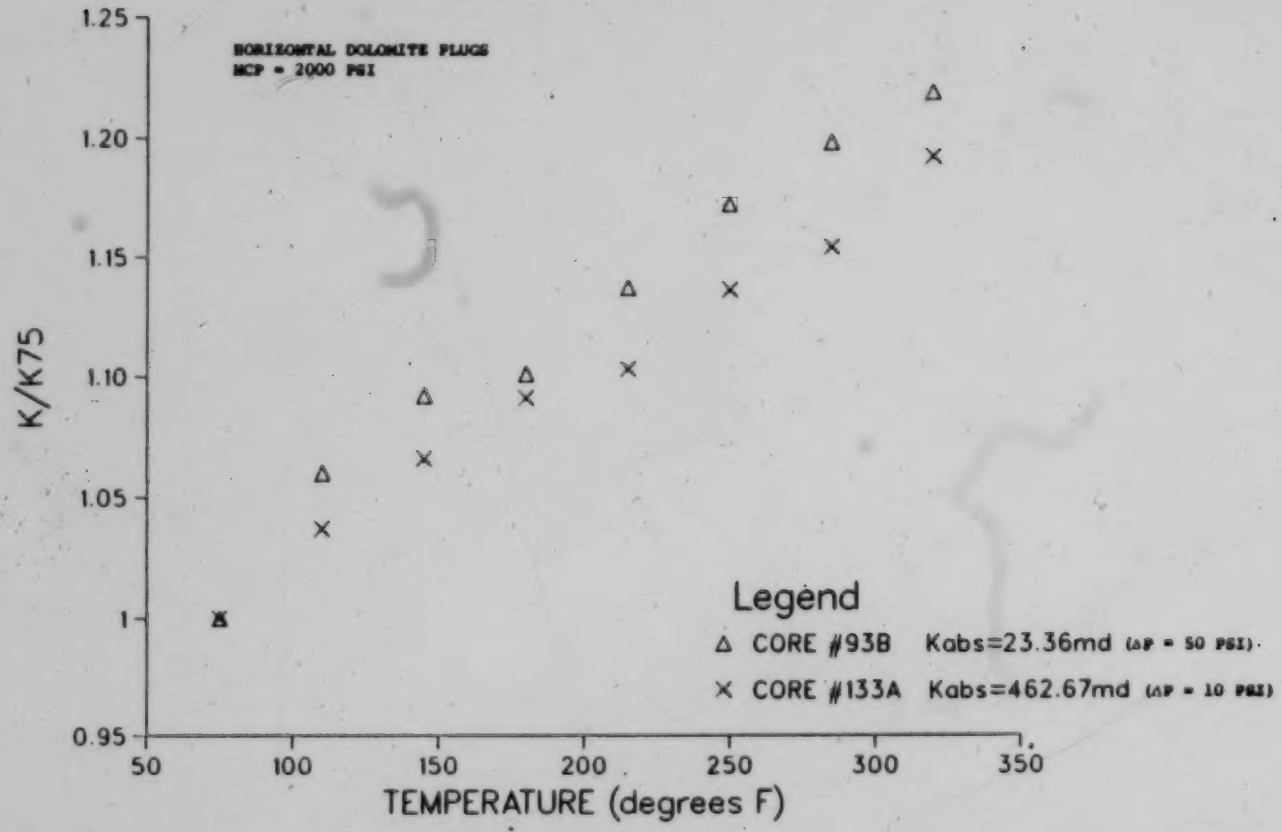

SLIP FACTOR versus TEMPERATURE

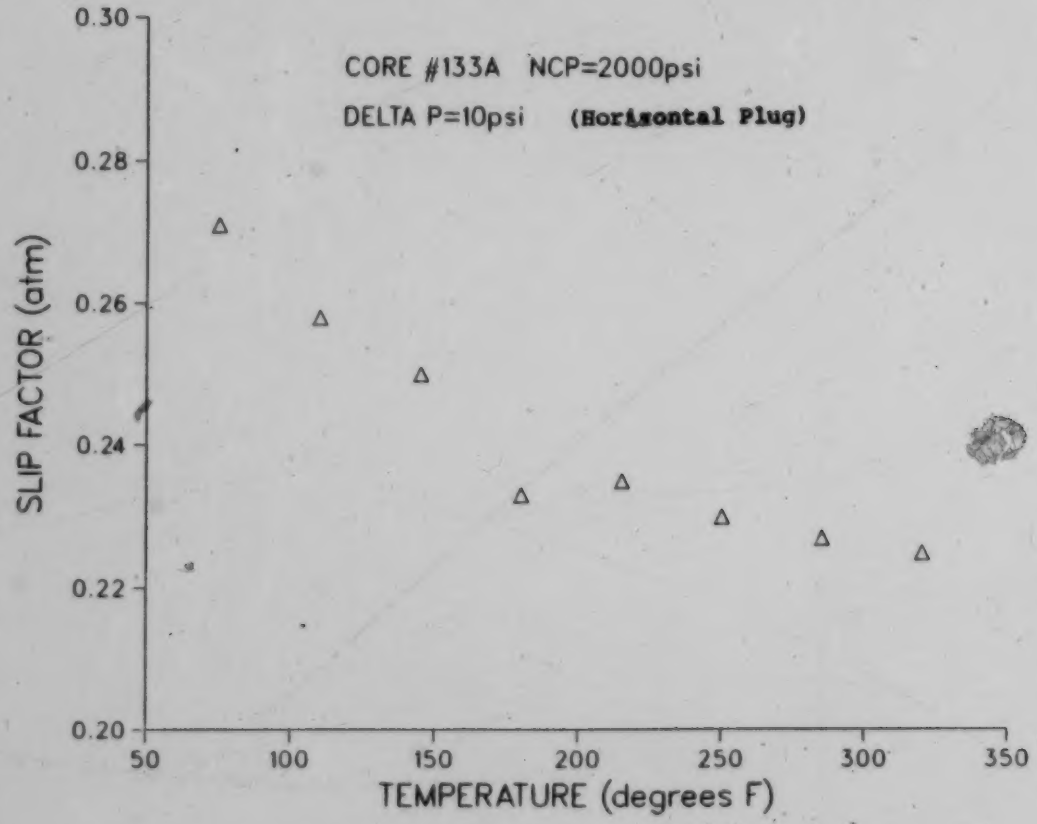

APPARENT PERMEABILITY vs RECIPROCAL MEAN PRESSURE

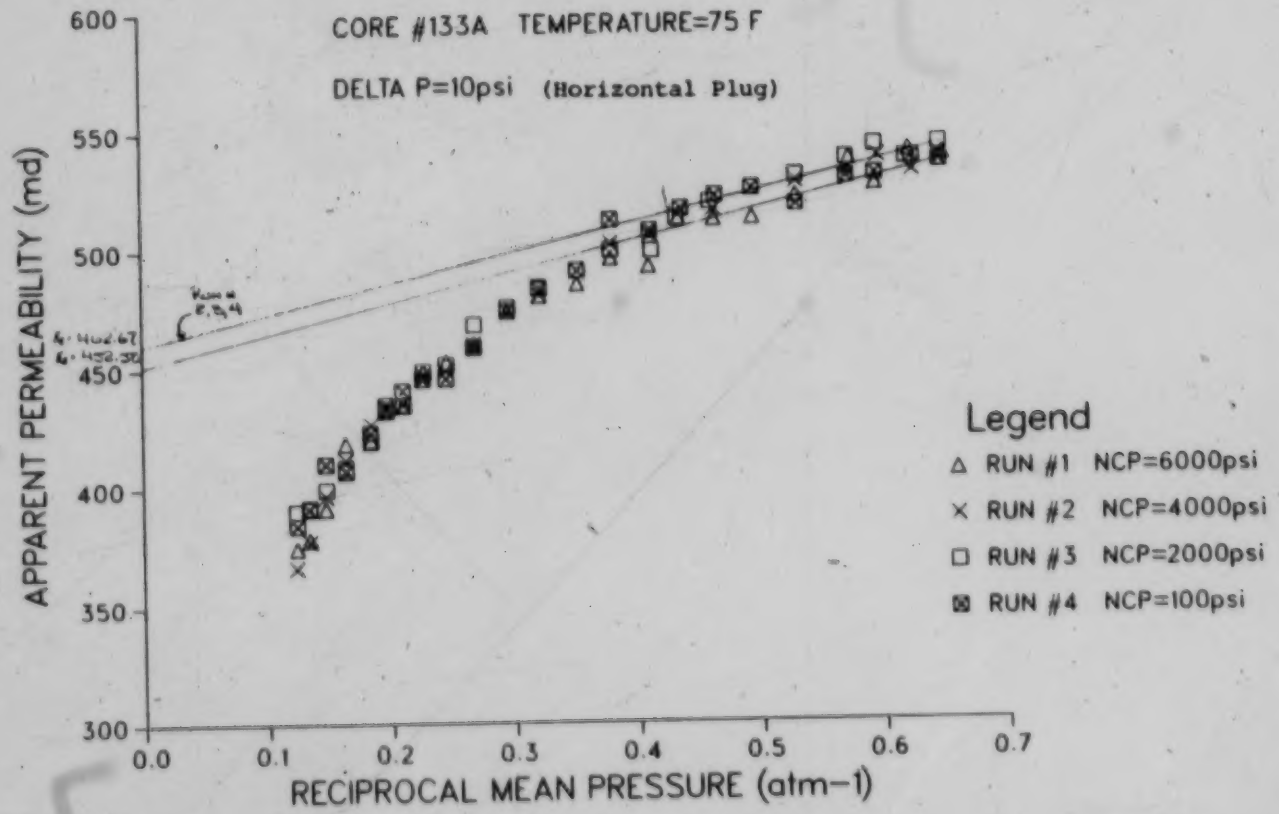

APPARENT PERMEABILITY vs RECIPROCAL MEAN PRESSURE

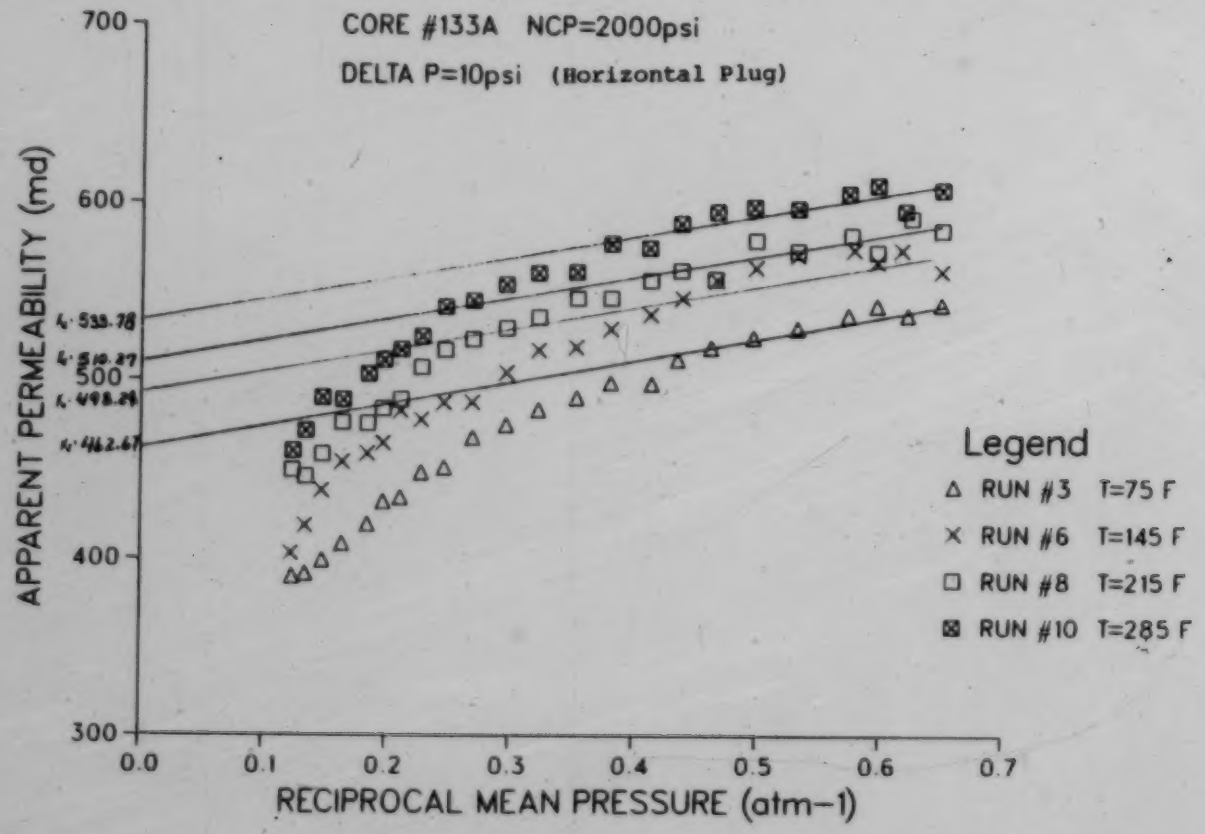

APPARENT PERMEABILITY vs RECIPROCAL MEAN PRESSURE

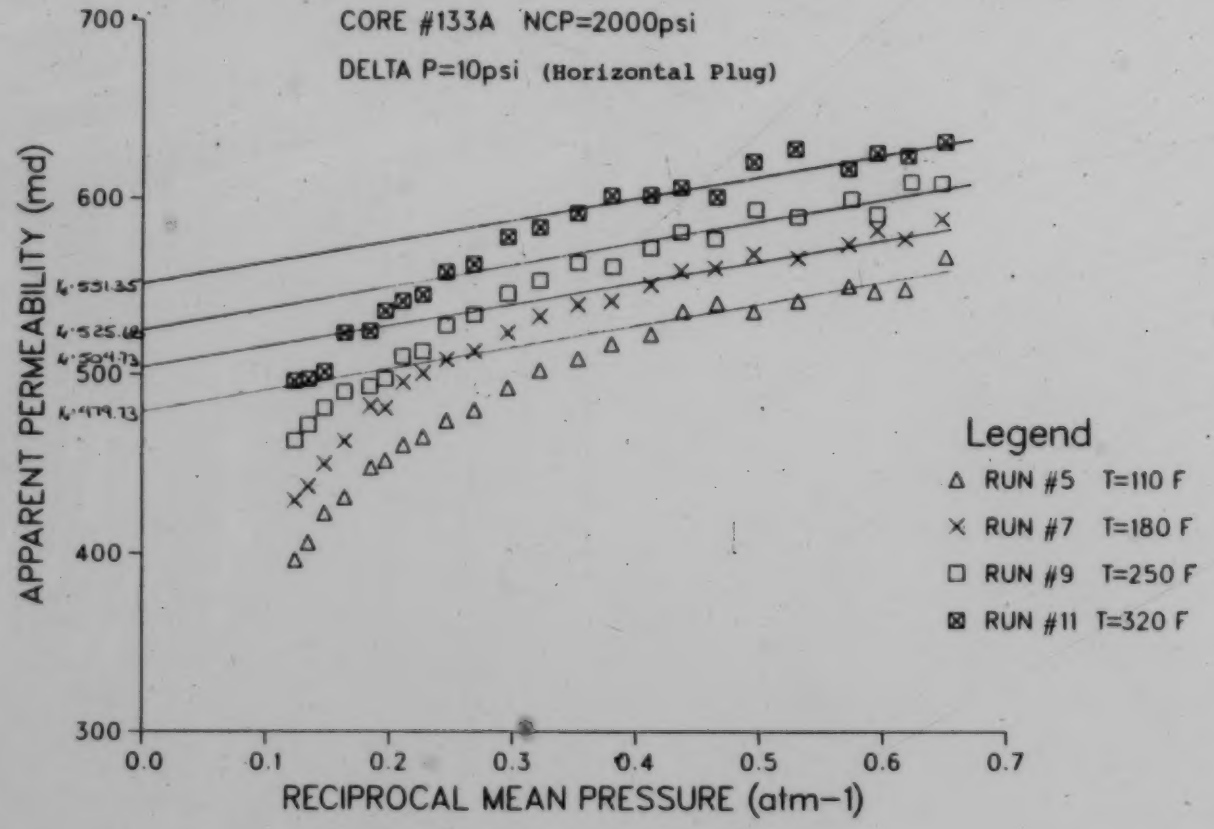

APPARENT PERMEABILITY vs RECIPROCAL MEAN PRESSURE

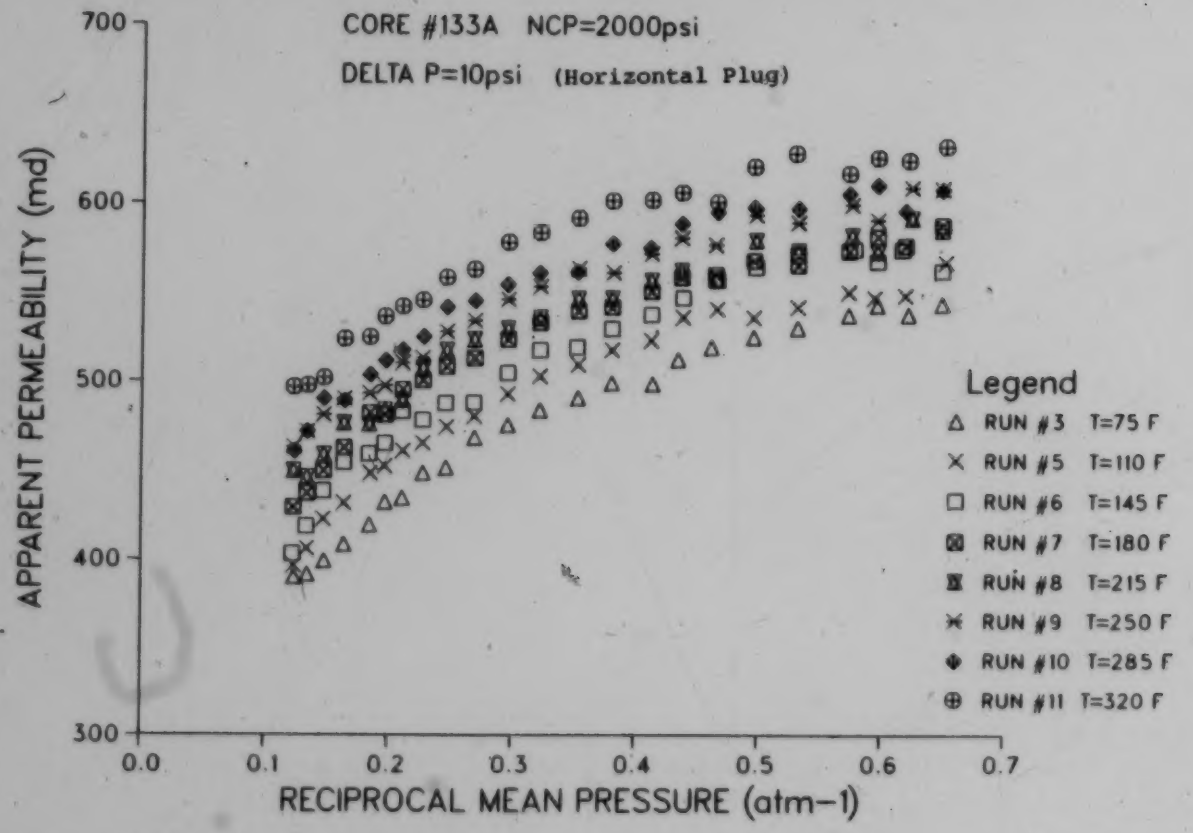

APPENDIX B6

VERTICAL PLUG 133A: Dolomite

Kabs vs Net Confining Pressure

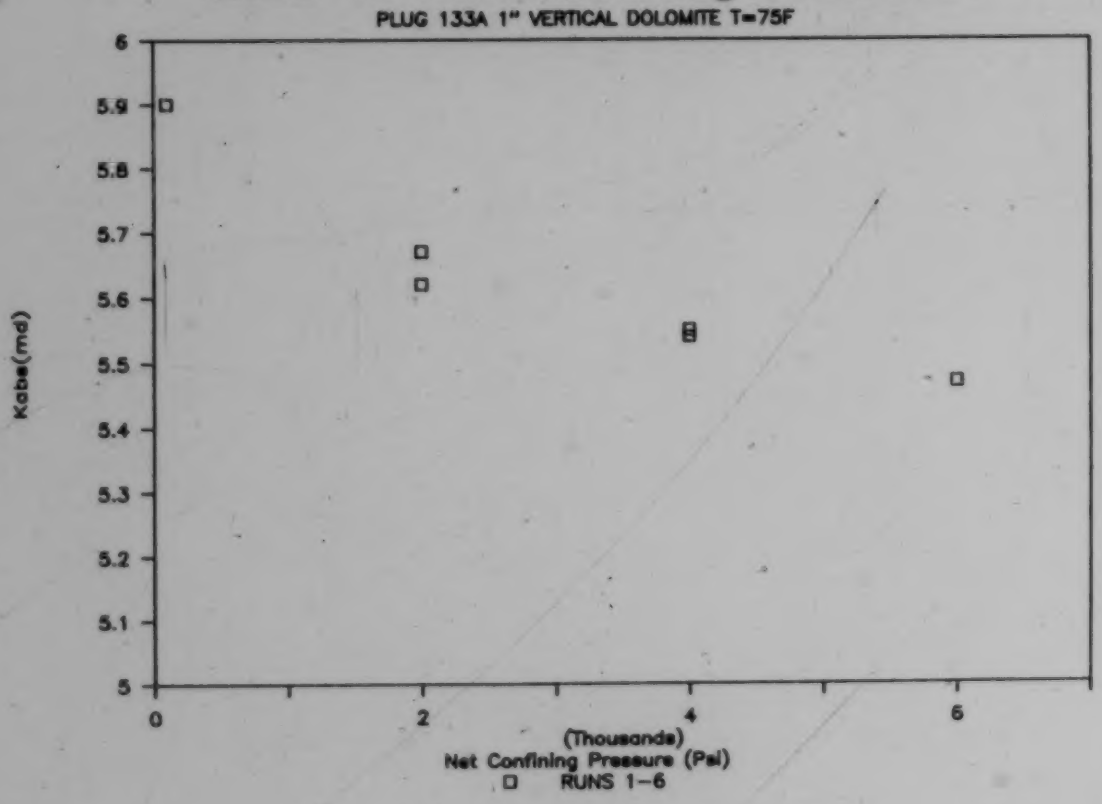

K/K75 versus TEMPERATURE

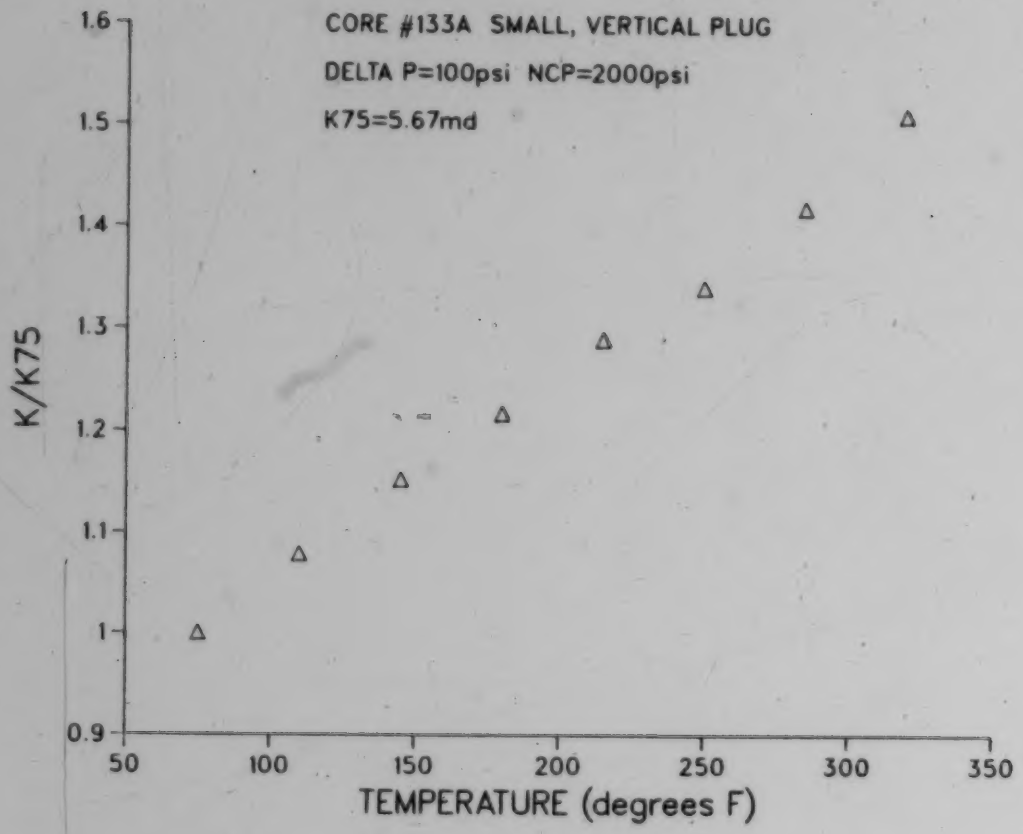

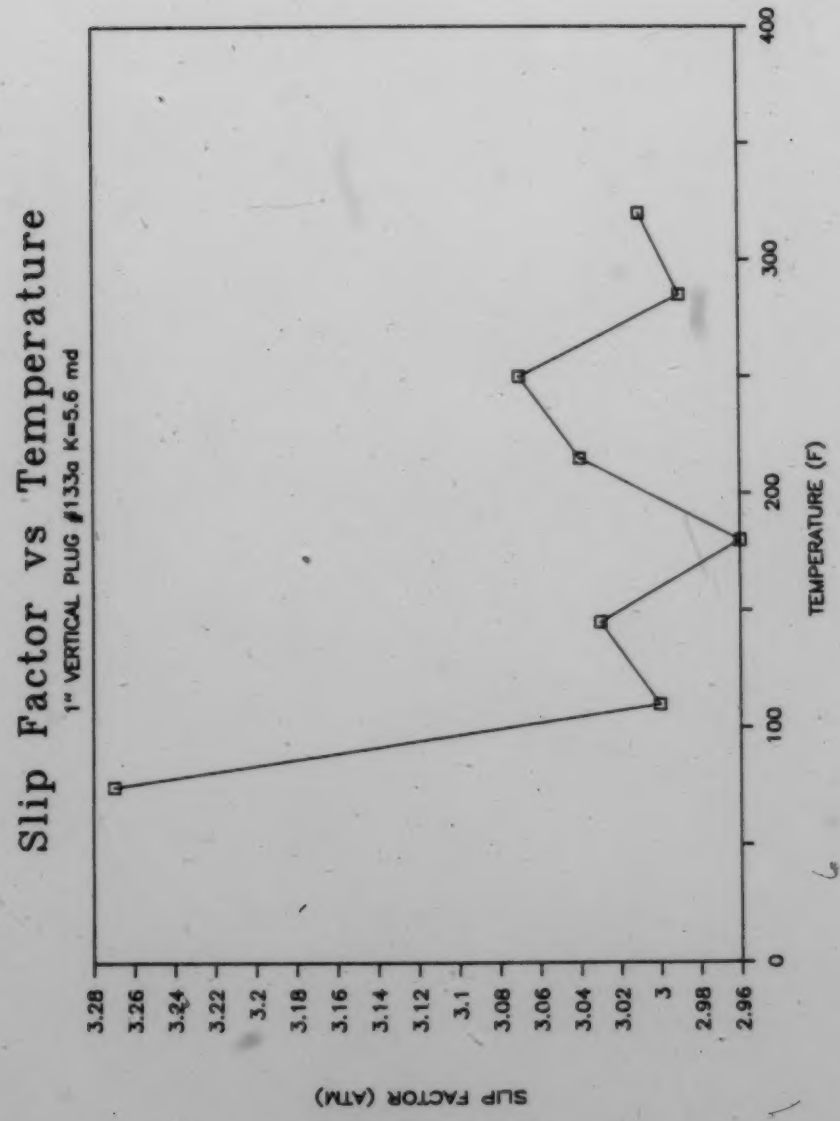
Slip Factor vs Temperature
1" VERTICAL PLUG #133a K=5.6 md
SLIP FACTOR (ATM)
TEMPERATURE (F)
3.28
3.26
3.24
3.22
3.2
3.18
3.16
3.14
3.12
3.1
3.08
3.06
3.04
3.02
3
2.98
2.96
0
100
200
300
400

APPARENT PERMEABILITY vs RECIPROCAL MEAN PRESSURE

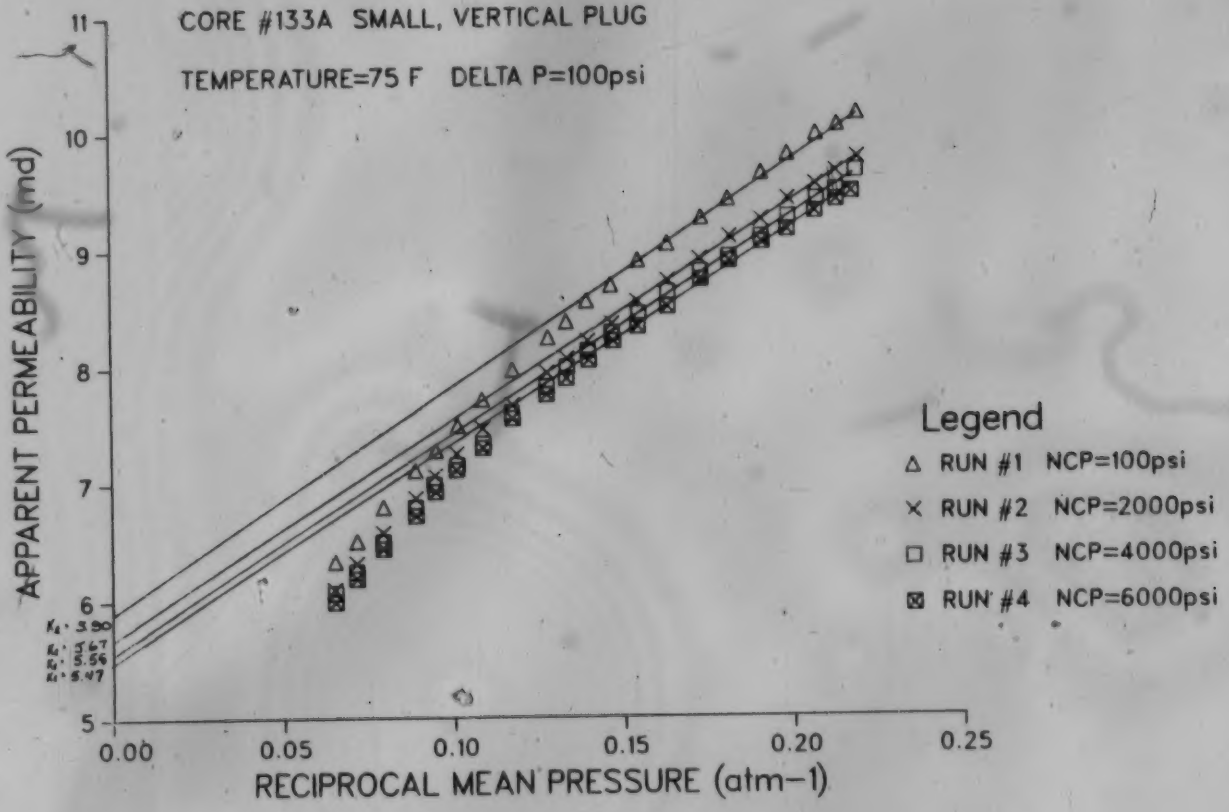

APPARENT PERMEABILITY vs RECIPROCAL MEAN PRESSURE

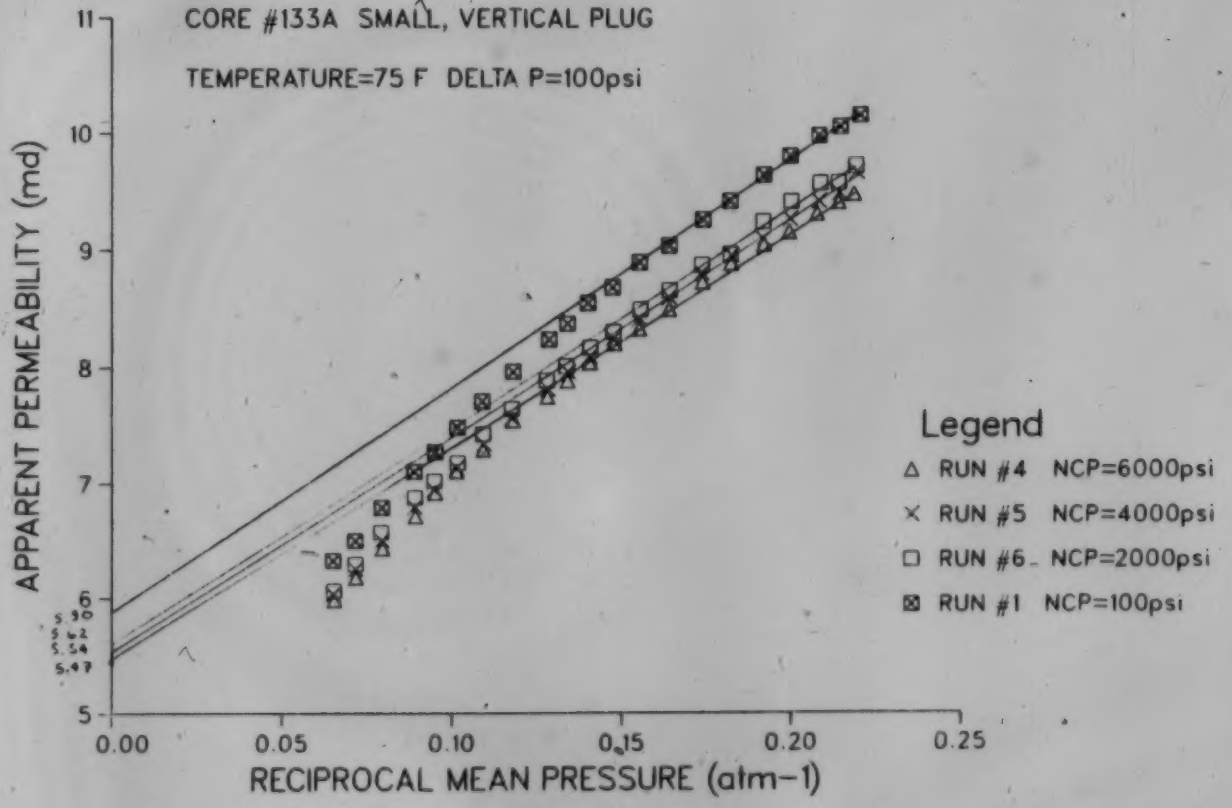

APPARENT PERMEABILITY vs RECIPROCAL MEAN PRESSURE

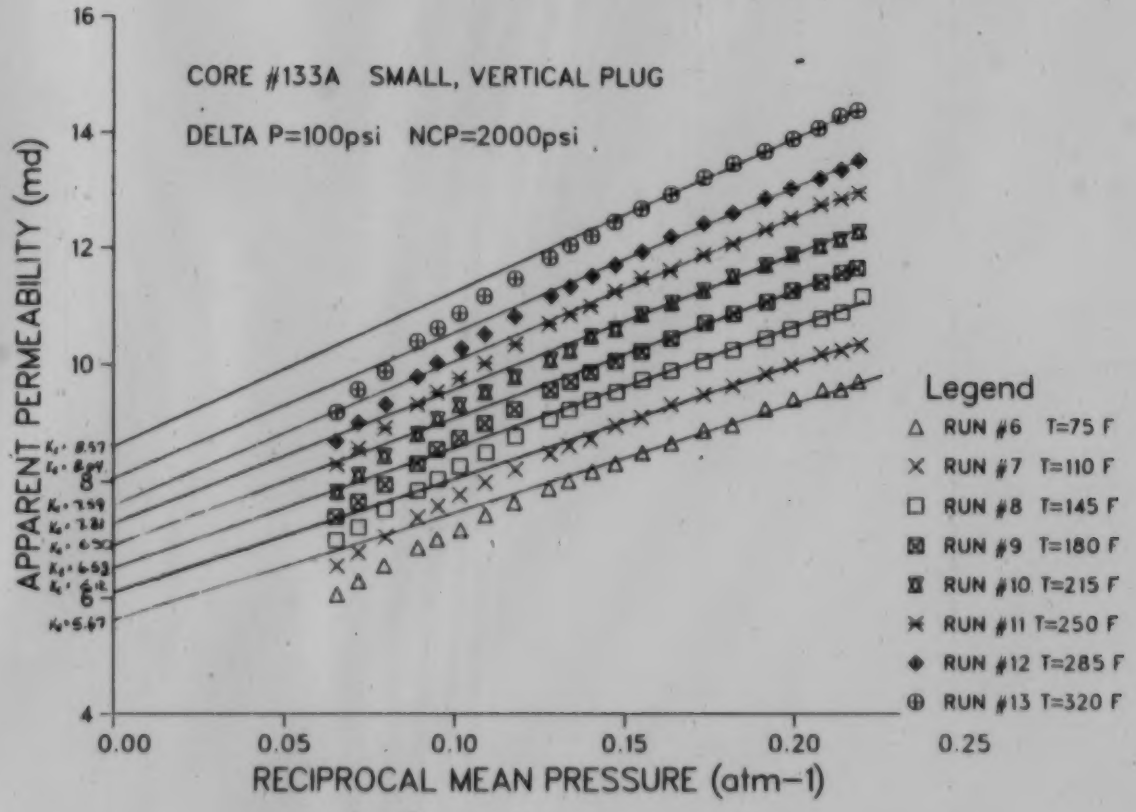

APPENDIX B7

CORE 1L: 3" Limestone

K APPARENT vs RECIPROCAL MEAN PRESSURE

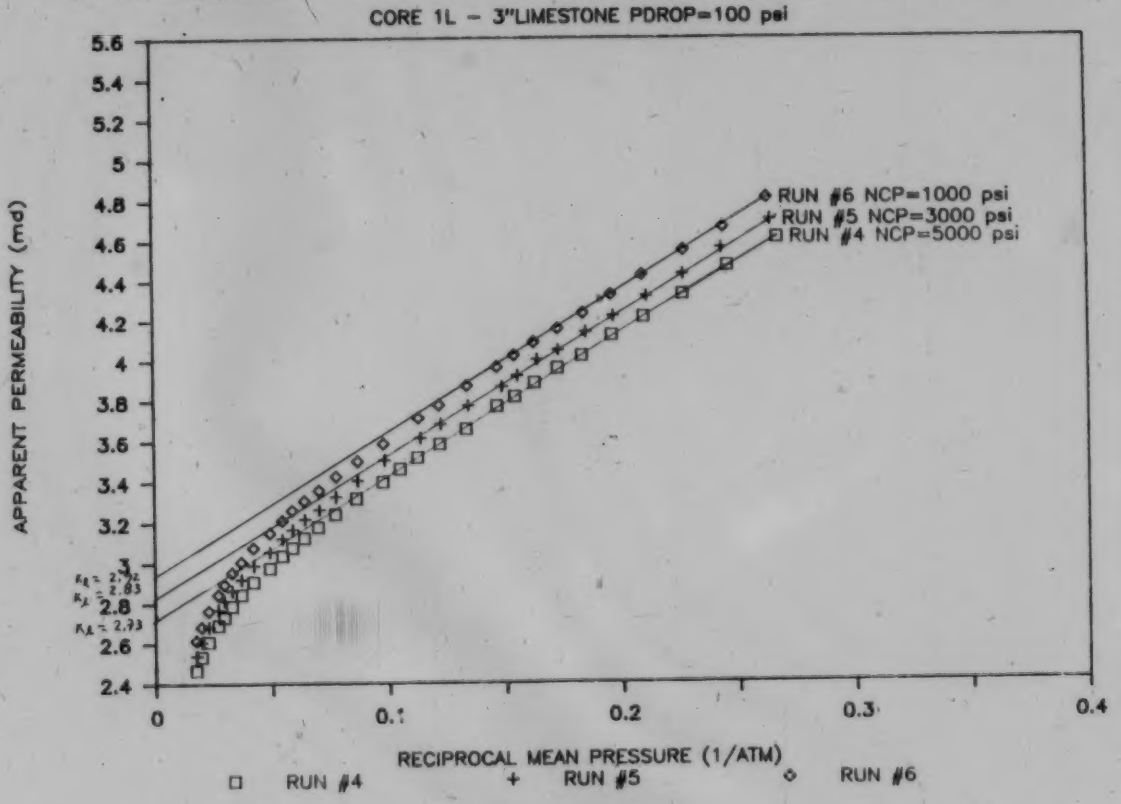

K APPARENT vs RECIPROCAL MEAN PRESSURE

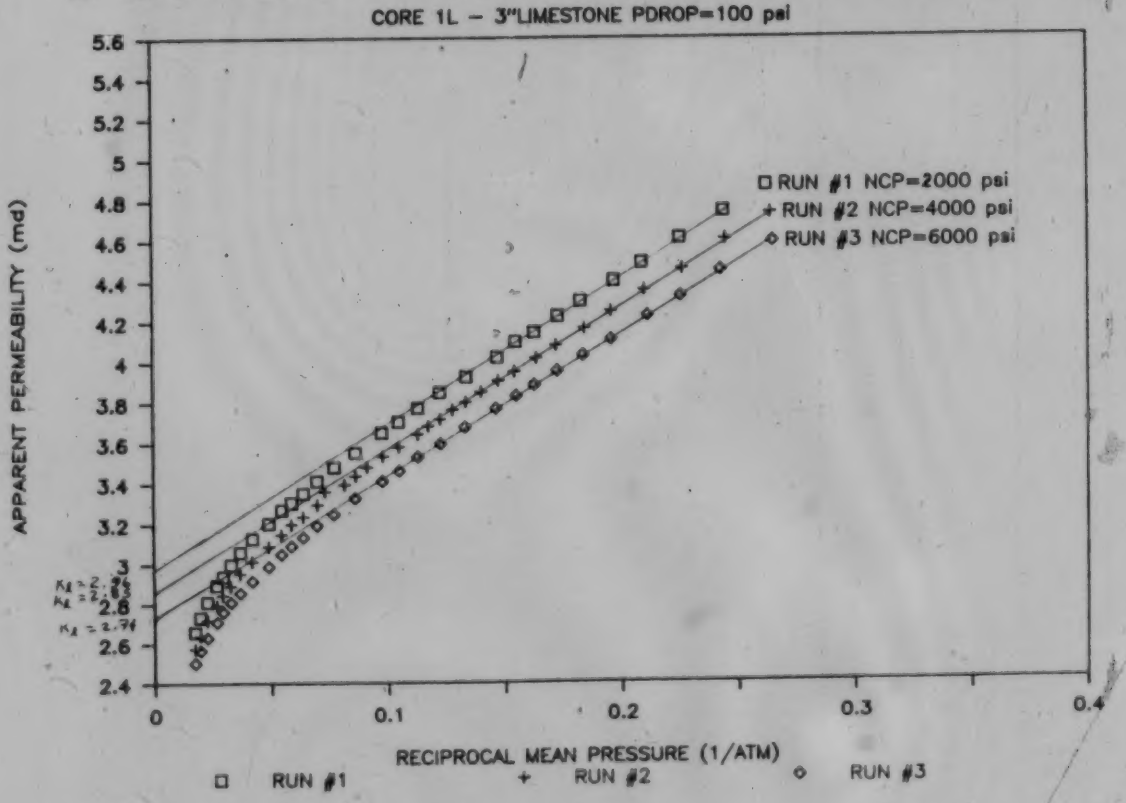

Kabs vs Net Confining Pressure

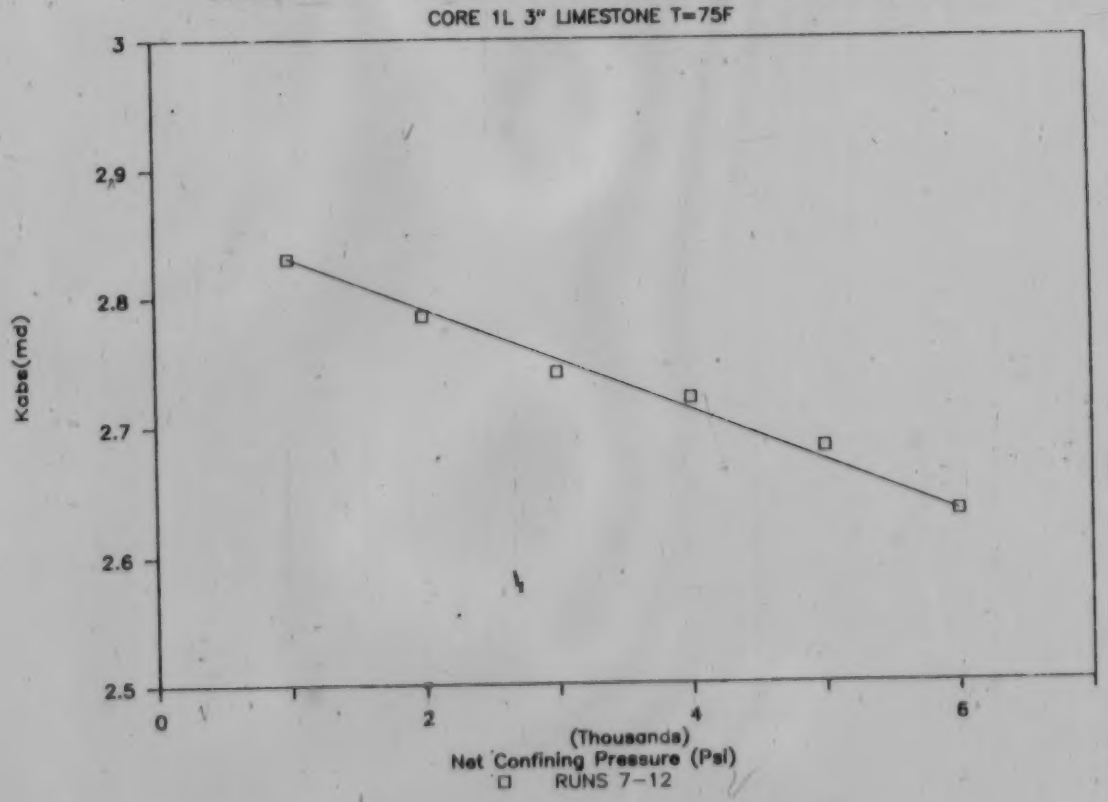

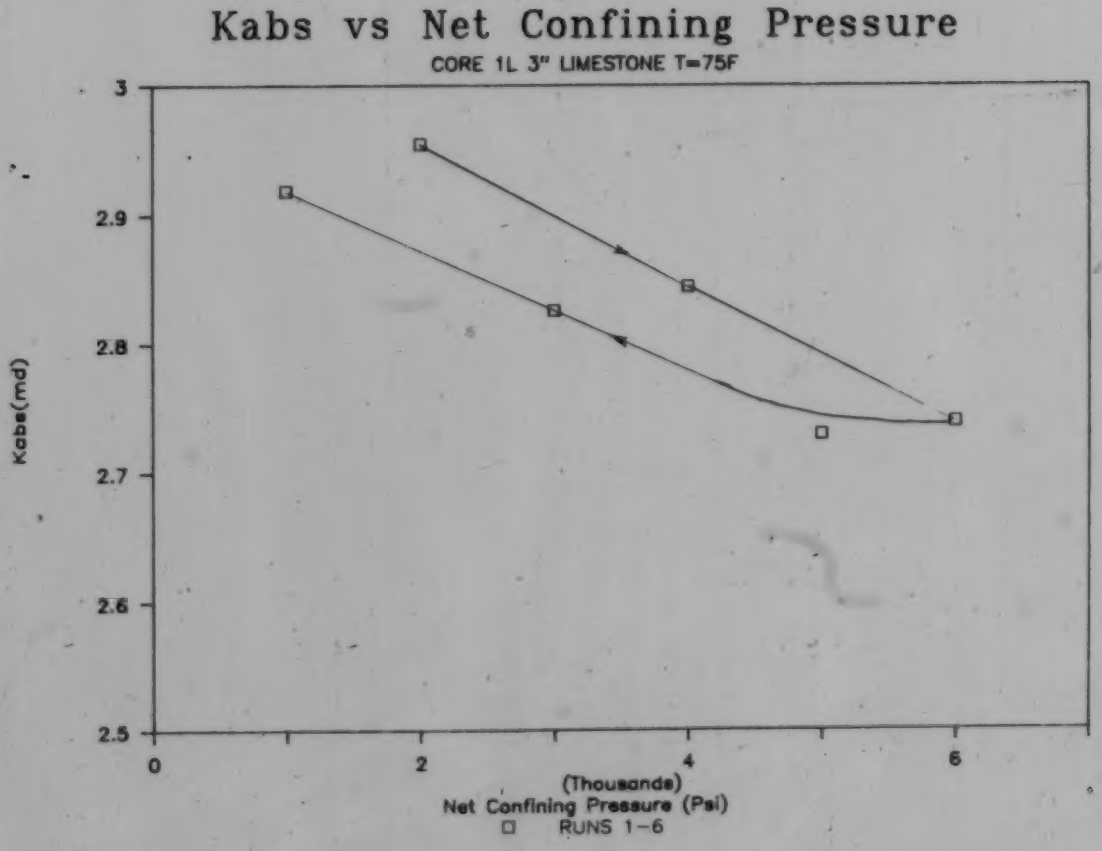
Kabs vs Net Confining Pressure
CORE 1L 3" LIMESTONE T=75F
Kabs(md)
3
2.9
2.8
2.7
2.6
2.5
0
2
4
6
(Thousands)
Net Confining Pressure (Psi)
RUNS 1-6

K APPARENT vs RECIPROCAL MEAN PRESSURE

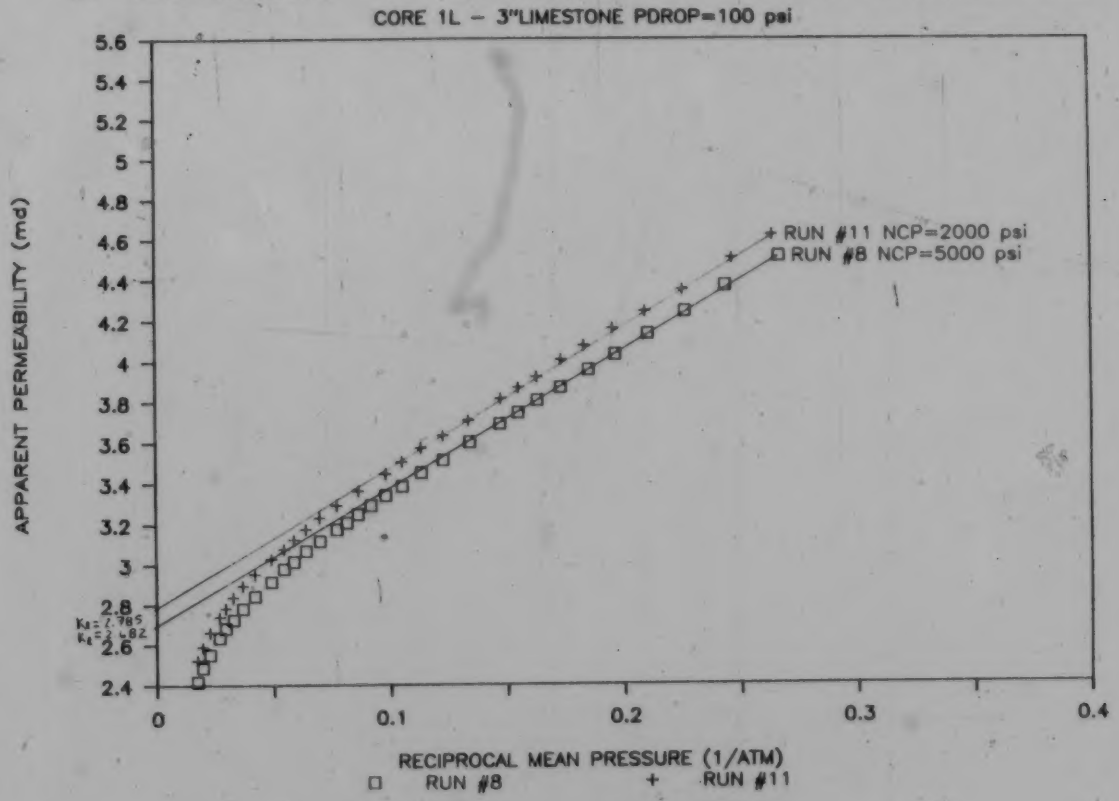

K APPARENT vs RECIPROCAL MEAN PRESSURE

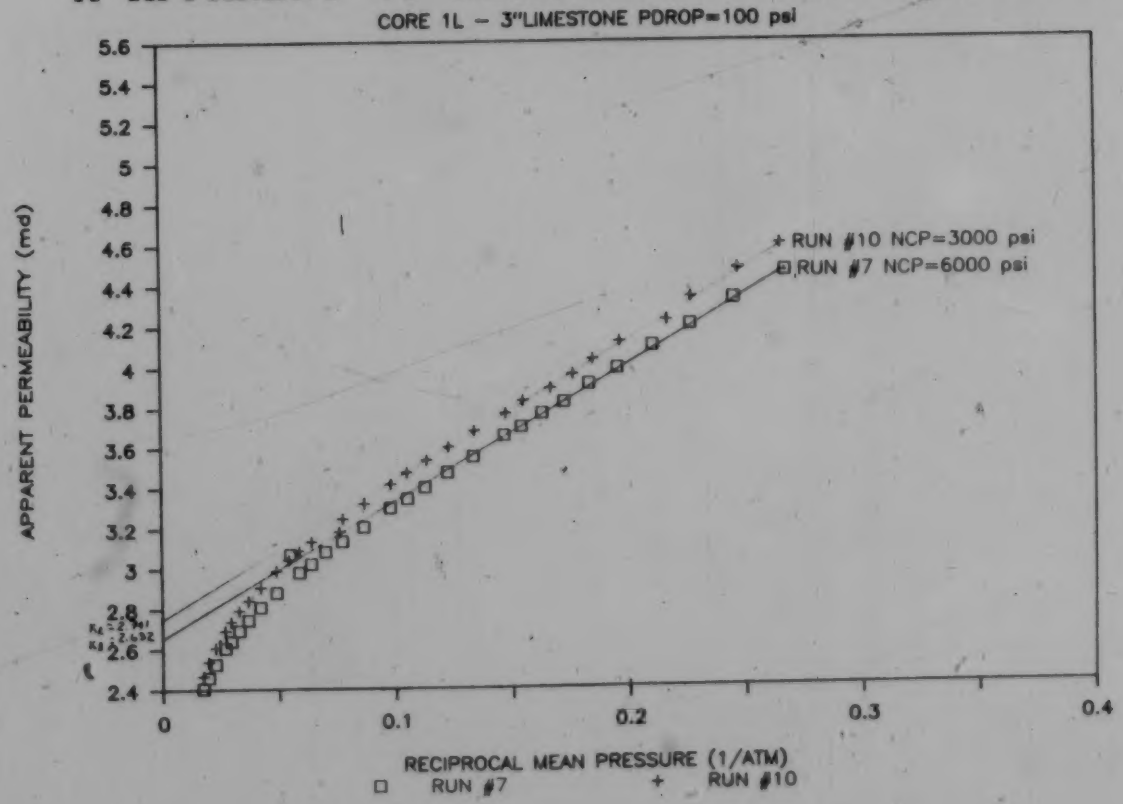

K APPARENT vs RECIPROCAL MEAN PRESSURE

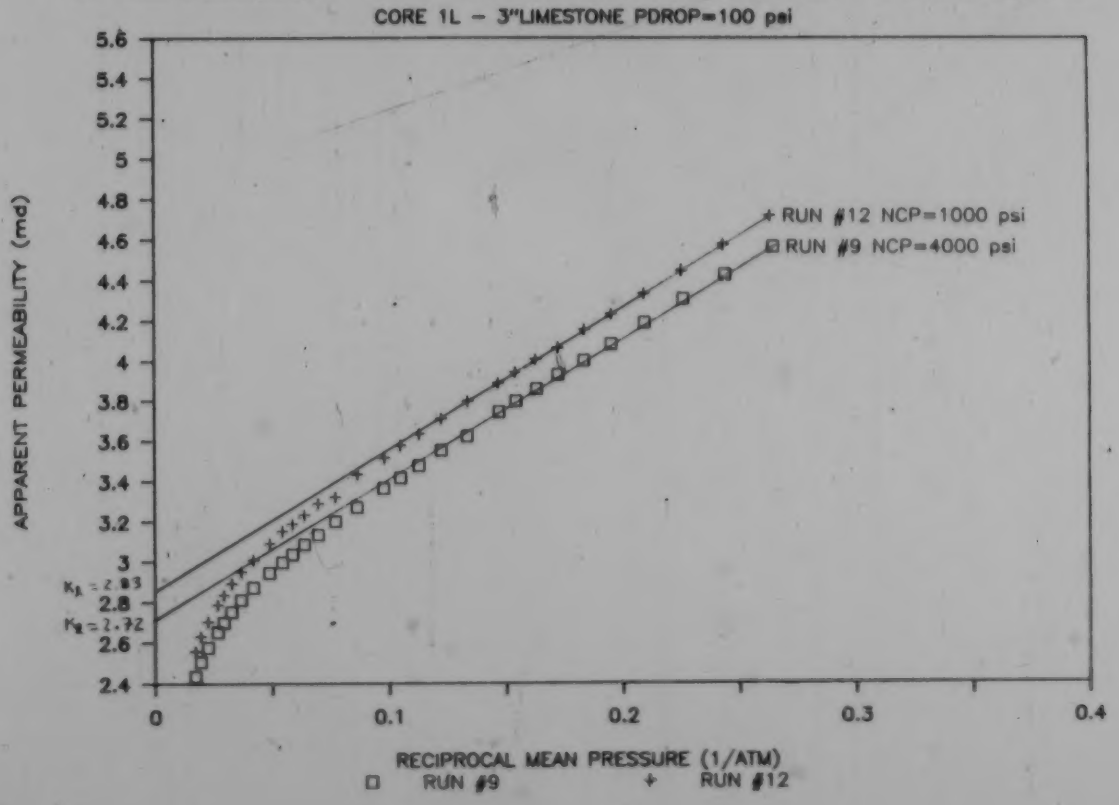

APPENDIX B8

CORE 3L: 3" Limestone

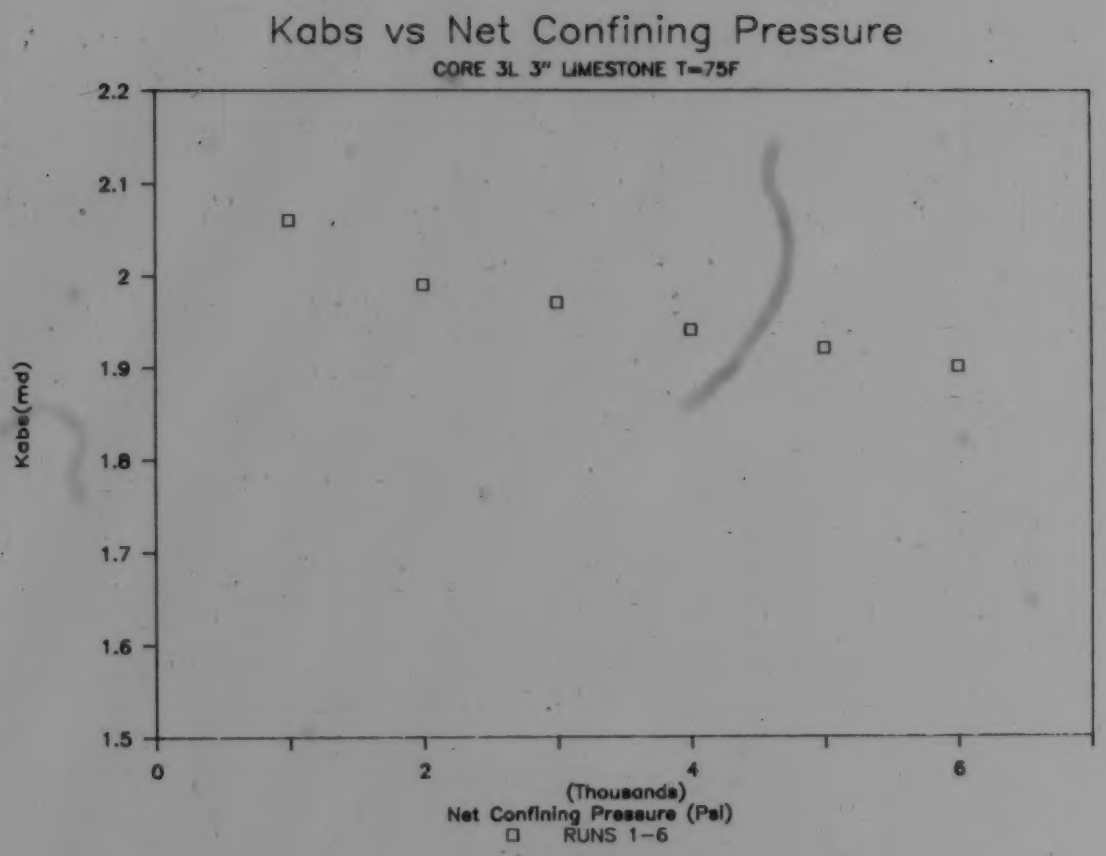
Kabs vs Net Confining Pressure
CORE 3L 3" LIMESTONE T=75F
2.2
2.1
2
1.9
1.8
1.7
1.6
1.5
Kabs(md)
0
2
4
6
(Thousands)
Net Confining Pressure (Psi)
RUNS 1-6

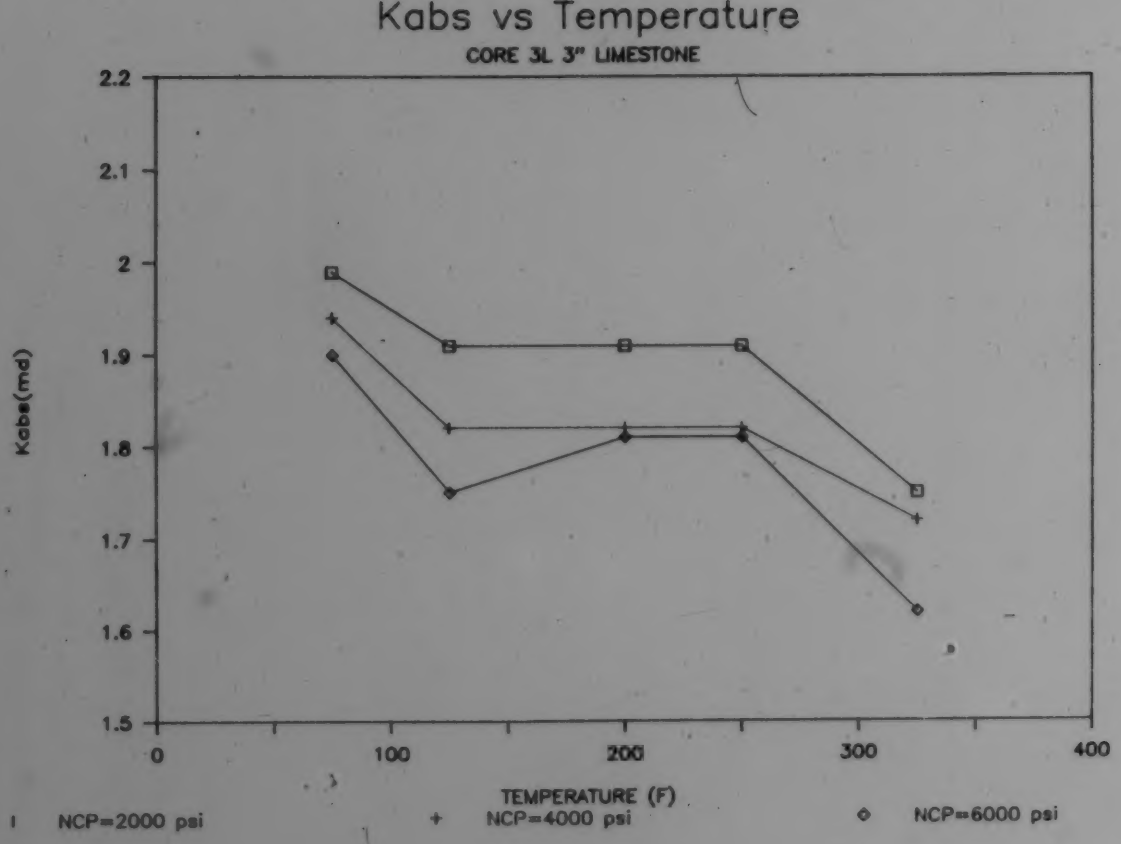
Kabs vs Temperature
CORE 3L 3" LIMESTONE
Kabs(md)
2.2
2.1
2
1.9
1.8
1.7
1.6
1.5
0
100
200
300
400
TEMPERATURE (F)
NCP=2000 psi
NCP=4000 psi
NCP=6000 psi

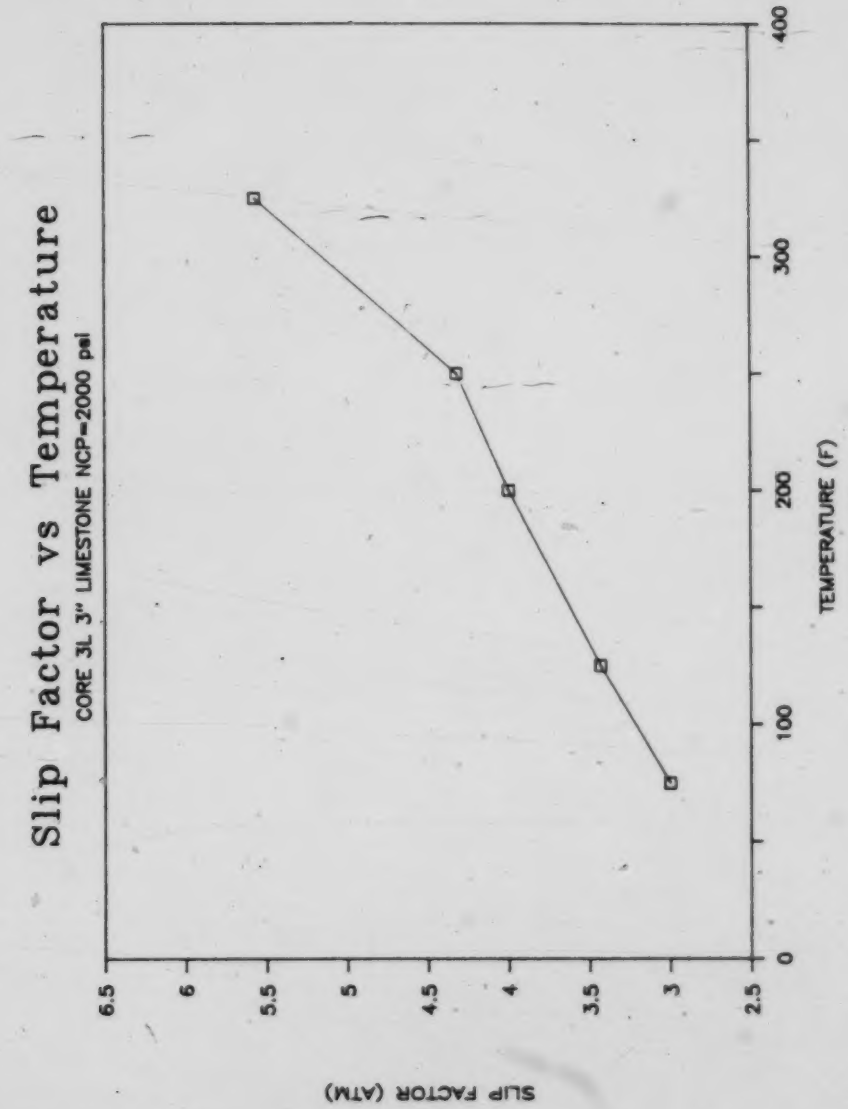
Slip Factor vs Temperature
CORE 3L 3" LIMESTONE NCP-2000 psi
SLIP FACTOR (ATM)
6.5
6
5.5
5
4.5
4
3.5
3
2.5
0
100
200
300
400
TEMPERATURE (F)

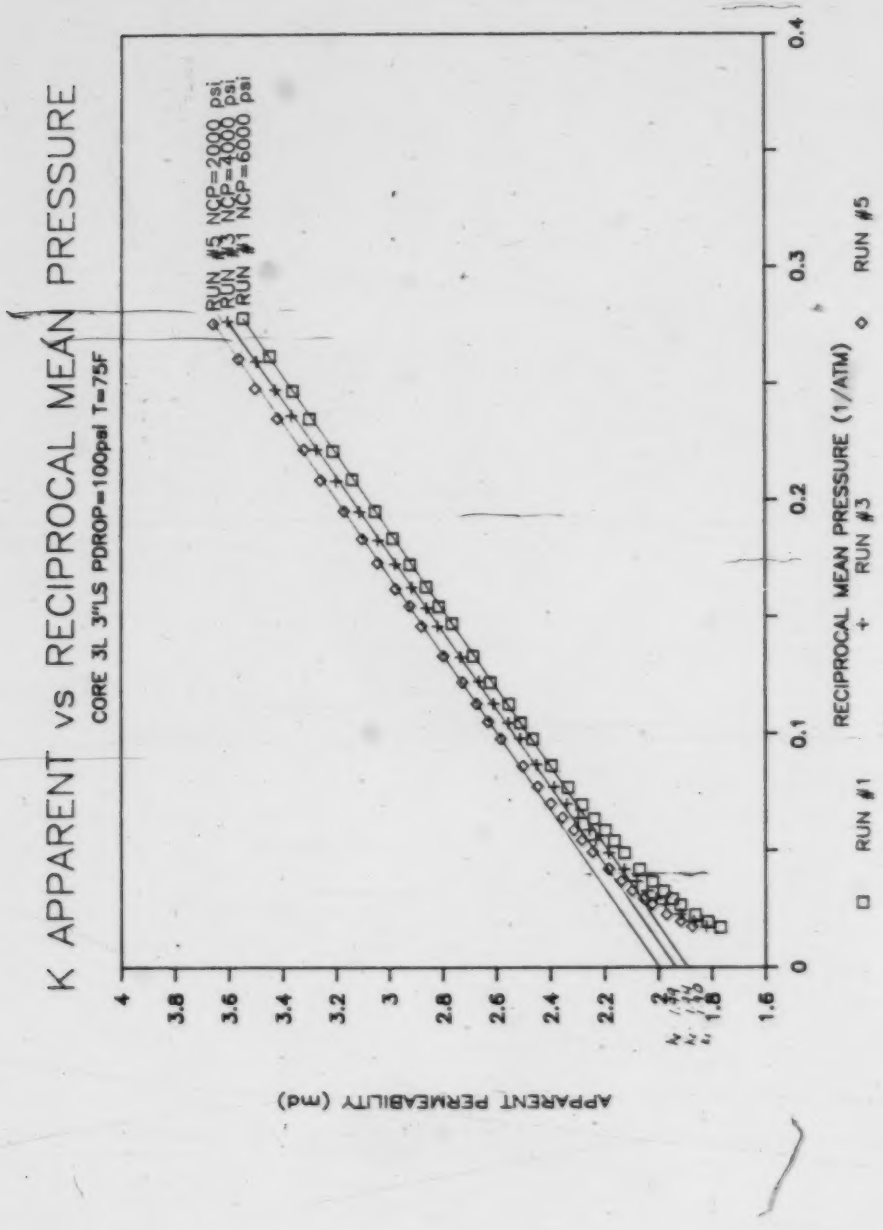
K APPARENT vs RECIPROCAL MEAN PRESSURE
CORE 3L 3"LS PDROP=100psi T=75F
RUN #5 NCP=2000 psi
RUN #3 NCP=4000 psi
RUN #1 NCP=6000 psi
APPARENT PERMEABILITY (md)
RECIPROCAL MEAN PRESSURE (1/ATM)
RUN #1
RUN #3
RUN #5
4
3.8
3.6
3.4
3.2
3
2.8
2.6
2.4
2.2
2
1.8
1.6
0
0.1
0.2
0.3
0.4

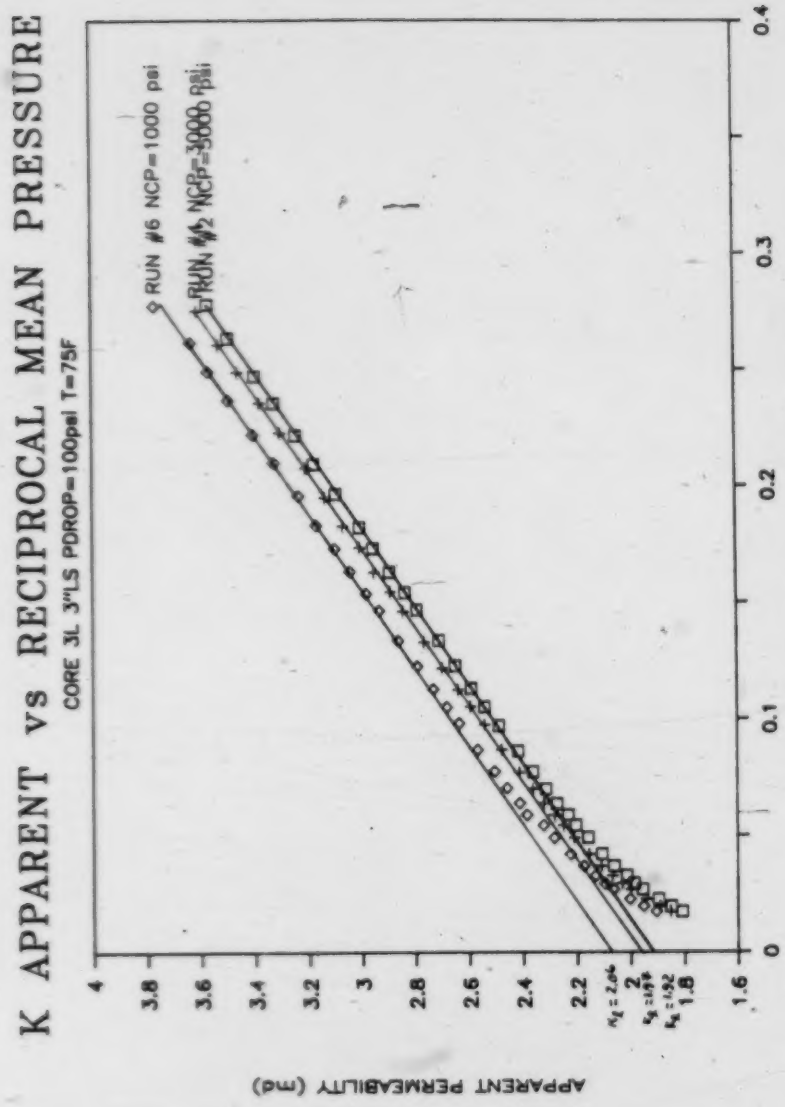
K APPARENT vs RECIPROCAL MEAN PRESSURE
CORE 3L 3"LS PDROP=100psi T=75F
◇ RUN #6 NCP=1000 psi
△ RUN #4 NCP=3000 psi
APPARENT PERMEABILITY (md)
RECIPROCAL MEAN PRESSURE (1/ATM)
□ RUN #2
+ RUN #4
◇ RUN #6
4
3.8
3.6
3.4
3.2
3
2.8
2.6
2.4
2.2
2
1.8
1.6
0
0.1
0.2
0.3
0.4

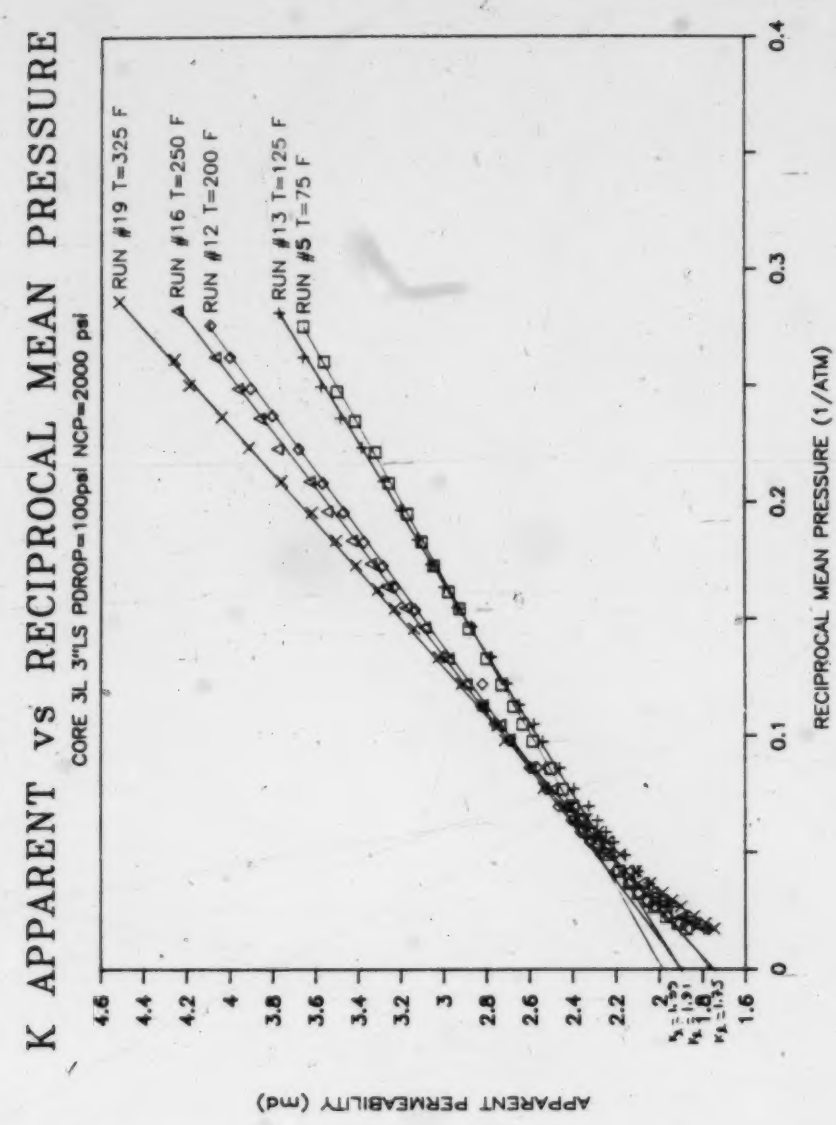
K APPARENT vs RECIPROCAL MEAN PRESSURE
CORE 3L 3"LS PDROP=100psi NCP=2000 psi
RUN #19 T=325 F
RUN #16 T=250 F
RUN #12 T=200 F
RUN #13 T=125 F
RUN #5 T=75 F
APPARENT PERMEABILITY (md)
RECIPROCAL MEAN PRESSURE (1/ATM)
4.6
4.4
4.2
4
3.8
3.6
3.4
3.2
3
2.8
2.6
2.4
2.2
2
1.8
1.6
0
0.1
0.2
0.3
0.4

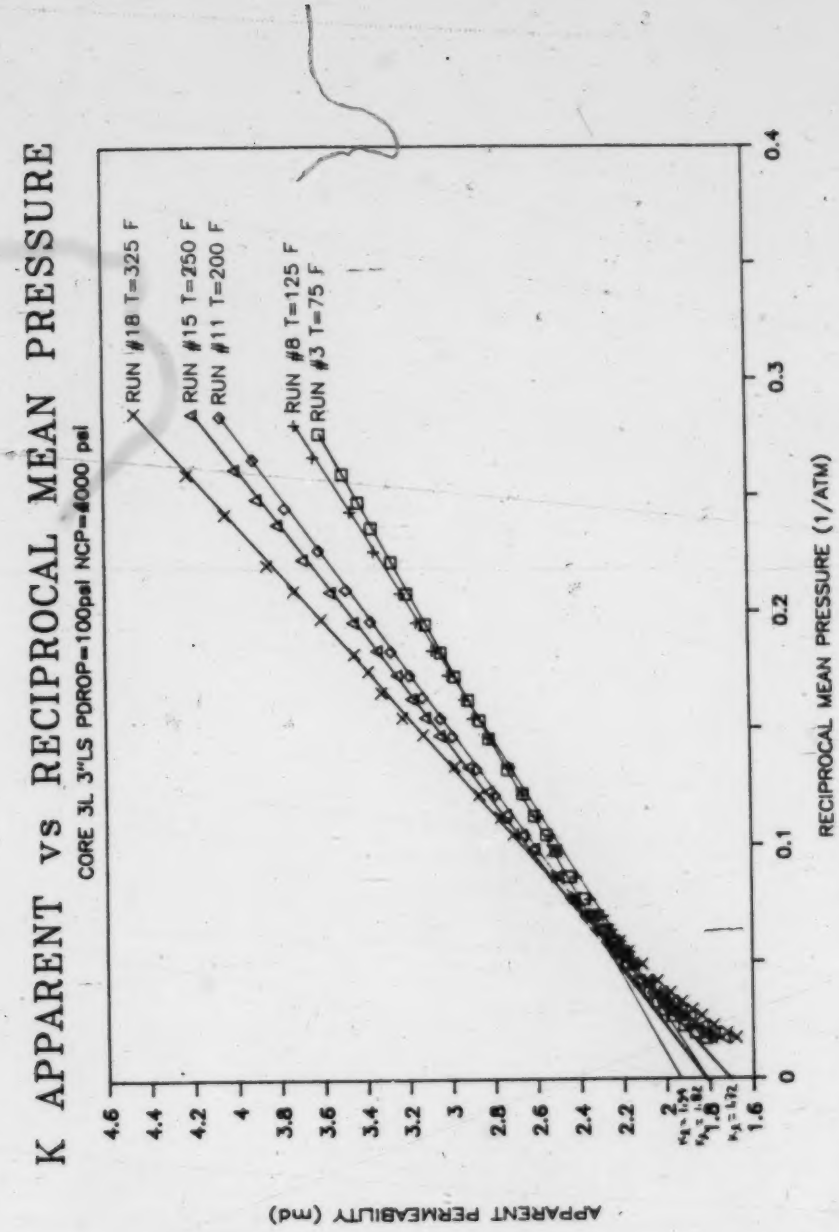
K APPARENT vs RECIPROCAL MEAN PRESSURE
CORE 3L 3"LS PDROP=100psi NCP=4000 psi
RUN #18 T=325 F
RUN #15 T=250 F
RUN #11 T=200 F
RUN #8 T=125 F
RUN #3 T=75 F
APPARENT PERMEABILITY (md)
RECIPROCAL MEAN PRESSURE (1/ATM)
4.6
4.4
4.2
4
3.8
3.6
3.4
3.2
3
2.8
2.6
2.4
2.2
2
1.8
1.6
0
0.1
0.2
0.3
0.4

K APPARENT vs RECIPROCAL MEAN PRESSURE

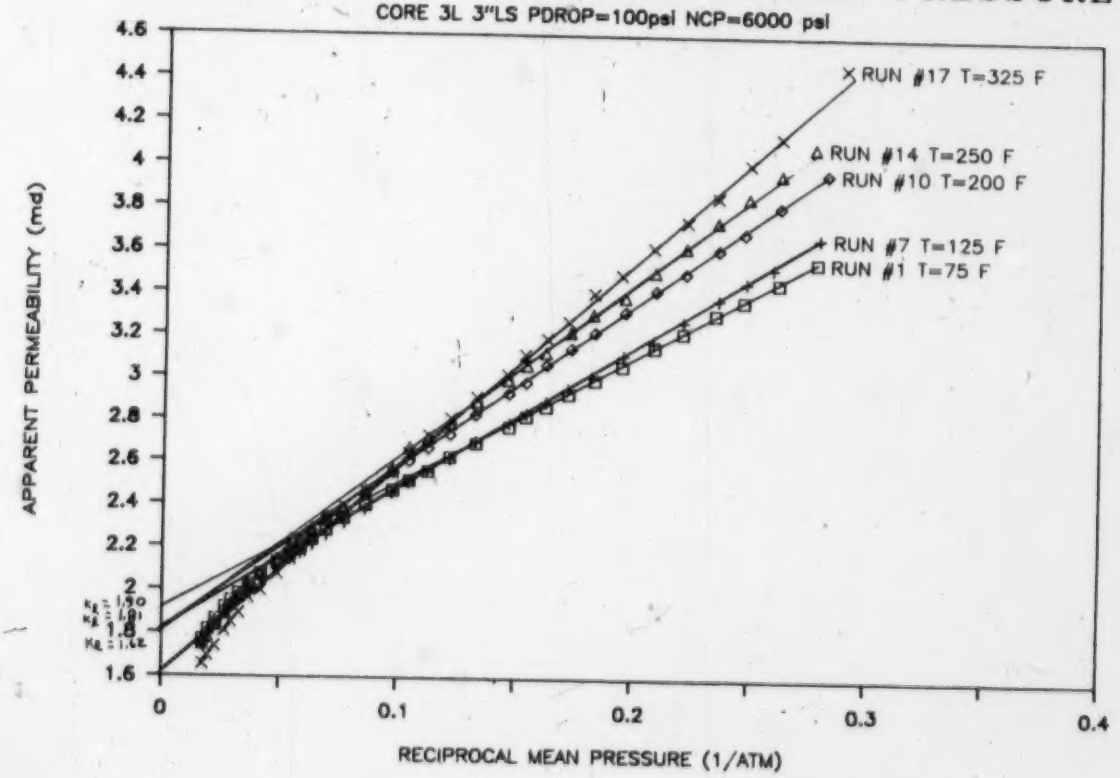

APPENDIX B9

CORE 4L: 3" Limestone

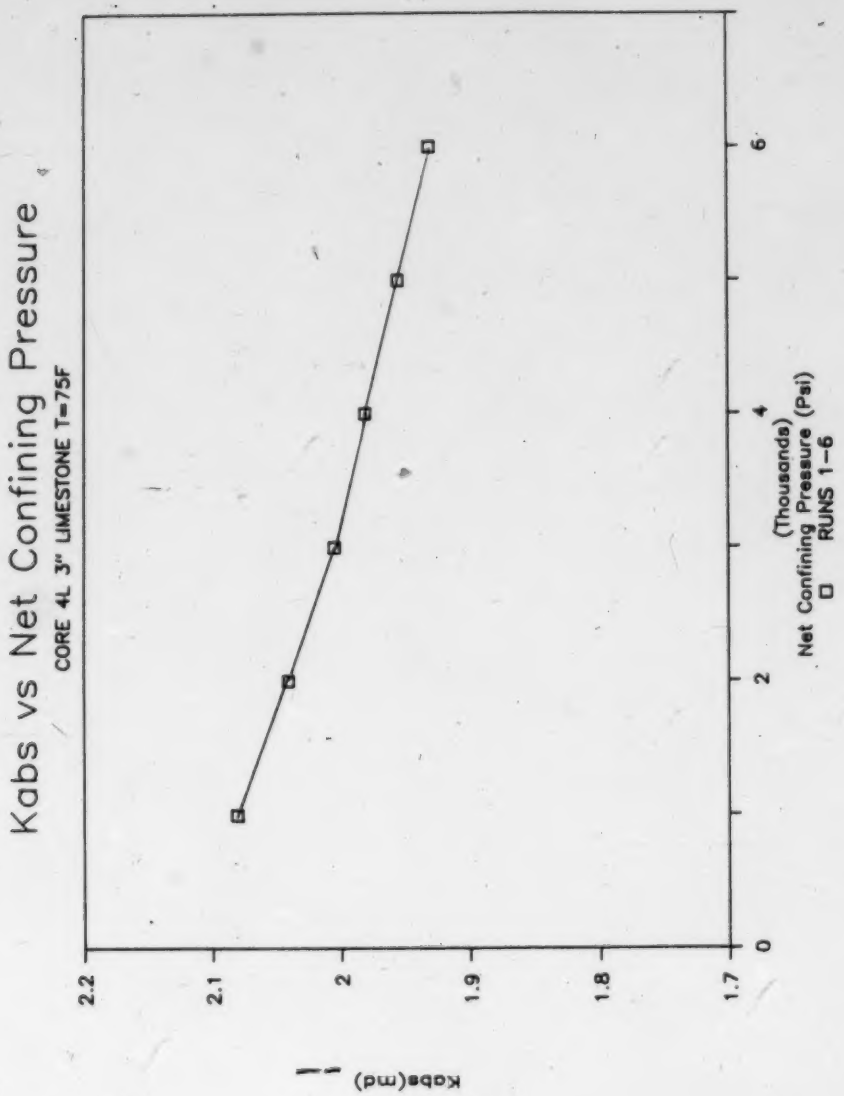
Kabs vs Net Confining Pressure
CORE 4L 3" LIMESTONE T=75F
Kabs(md)
2.2
2.1
2
1.9
1.8
1.7
0
2
4
6
(Thousands)
Net Confining Pressure (Psi)
RUNS 1-6

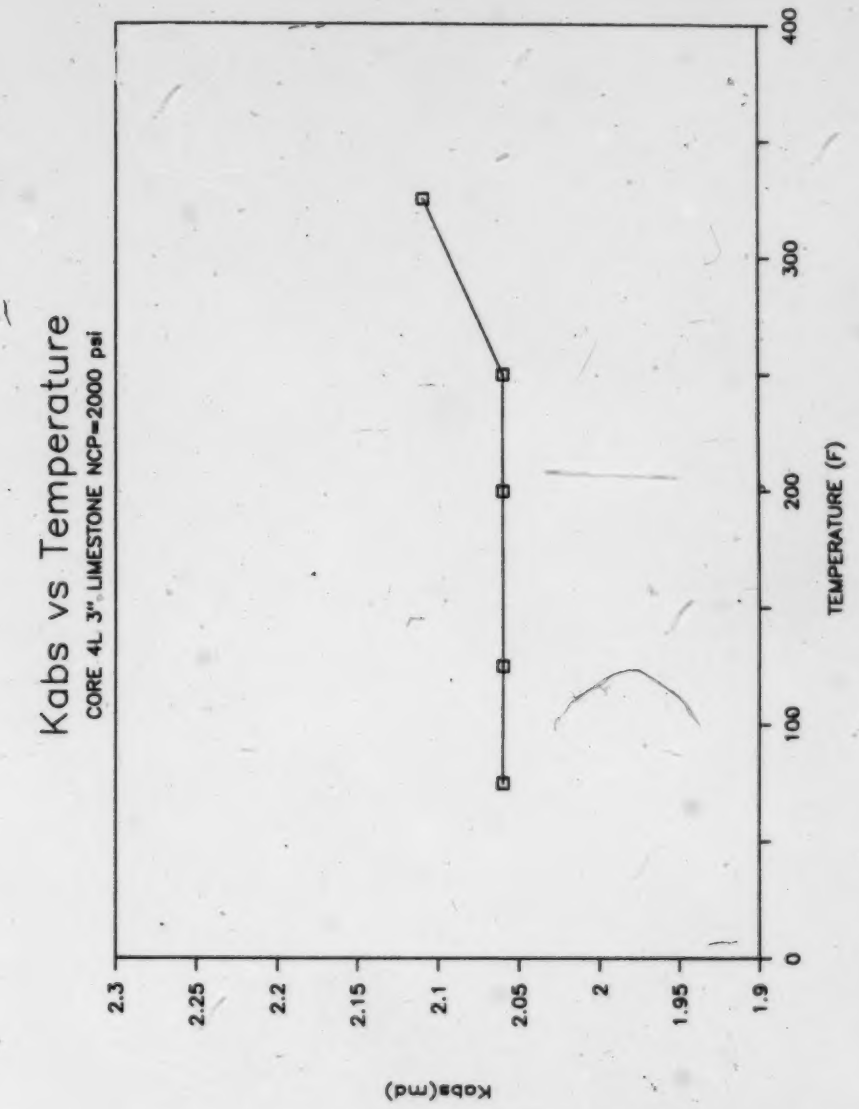
Kabs vs Temperature
CORE 4L 3" LIMESTONE NCP=2000 psi
Kobs(md)
2.3
2.25
2.2
2.15
2.1
2.05
2
1.95
1.9
0
100
200
300
400
TEMPERATURE (F)

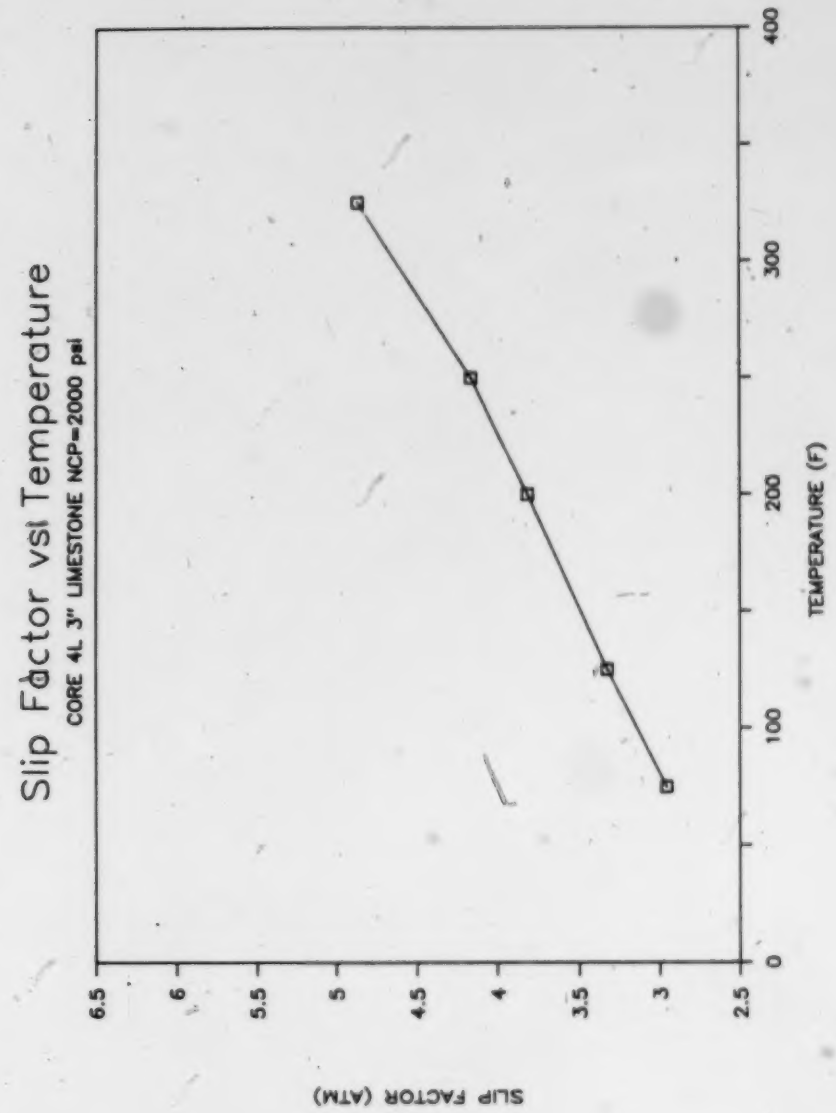
Slip Factor vsi Temperature
CORE 4L 3" LIMESTONE NCP=2000 psi
SLIP FACTOR (ATM)
6.5
6
5.5
5
4.5
4
3.5
3
2.5
0
100
200
300
400
TEMPERATURE (F)

K APPARENT vs RECIPROCAL MEAN PRESSURE

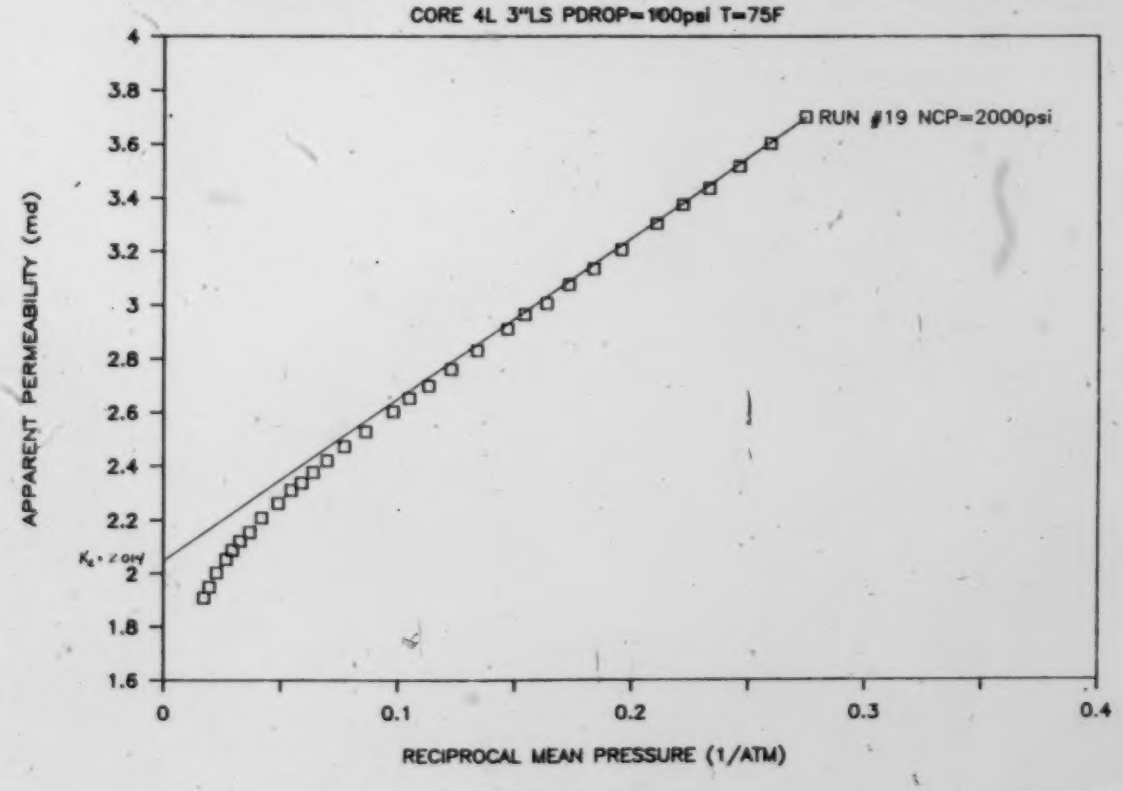

K APPARENT vs RECIPROCAL MEAN PRESSURE

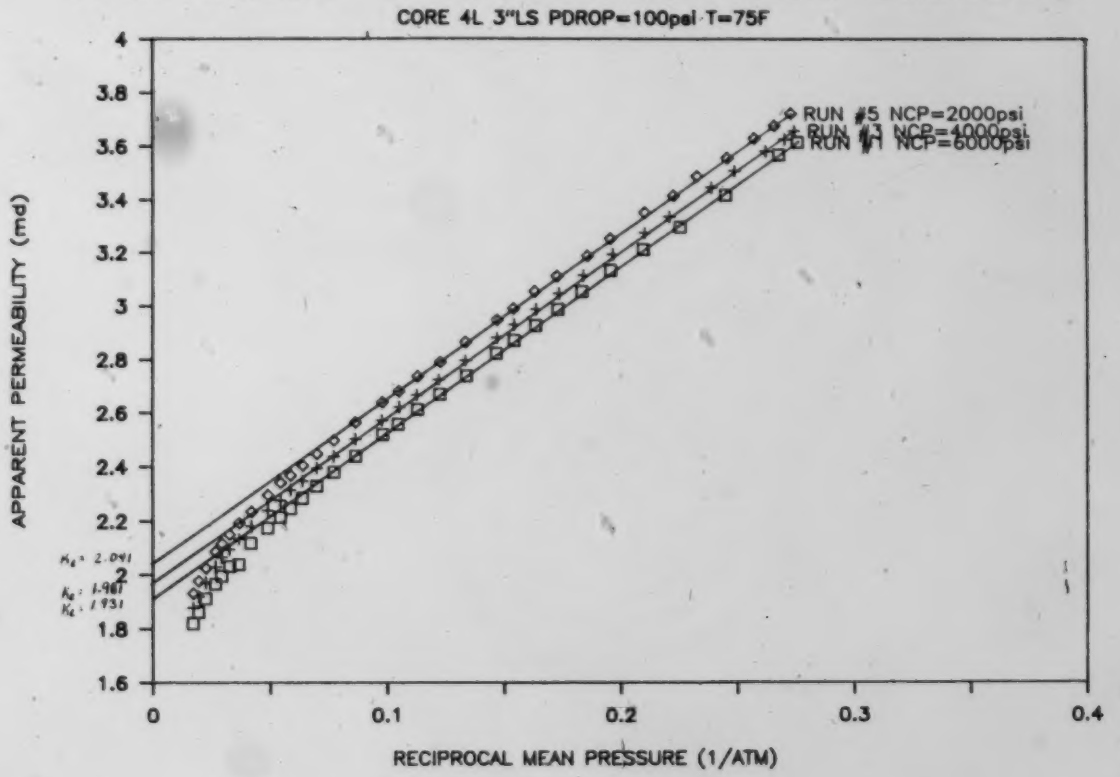

K APPARENT vs RECIPROCAL MEAN PRESSURE

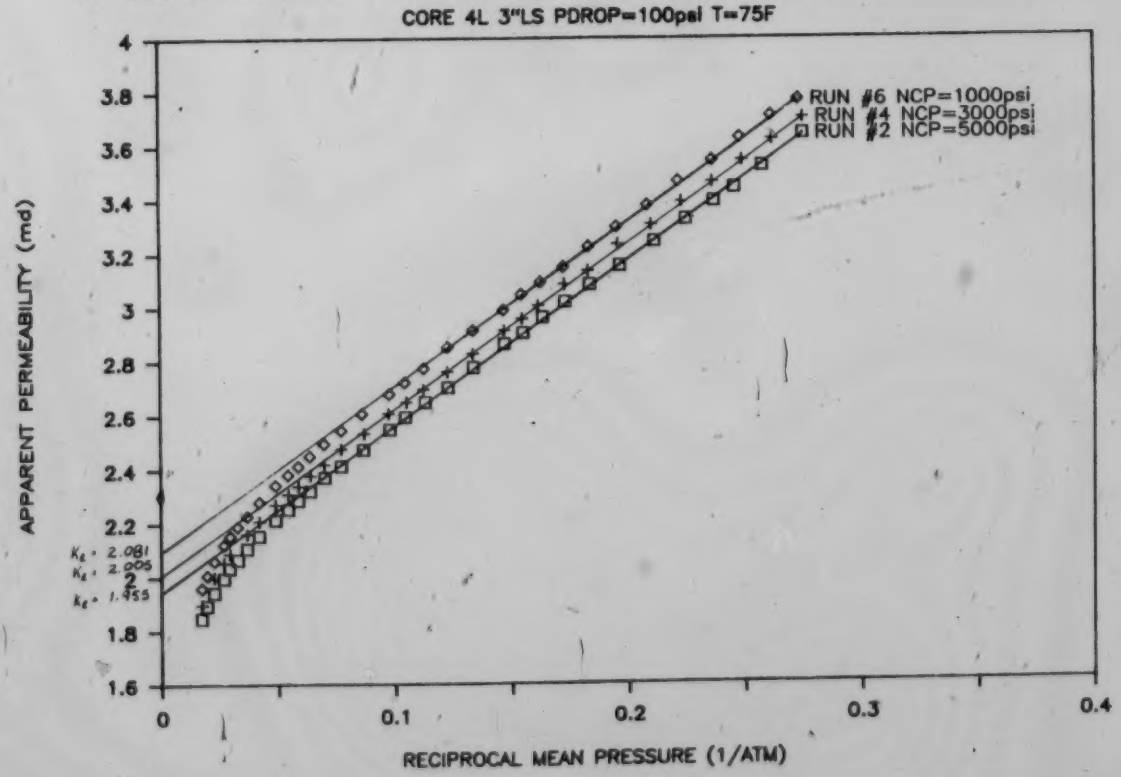

APPARENT PERMEABILITY vs INVERSE MEAN PRESSURE

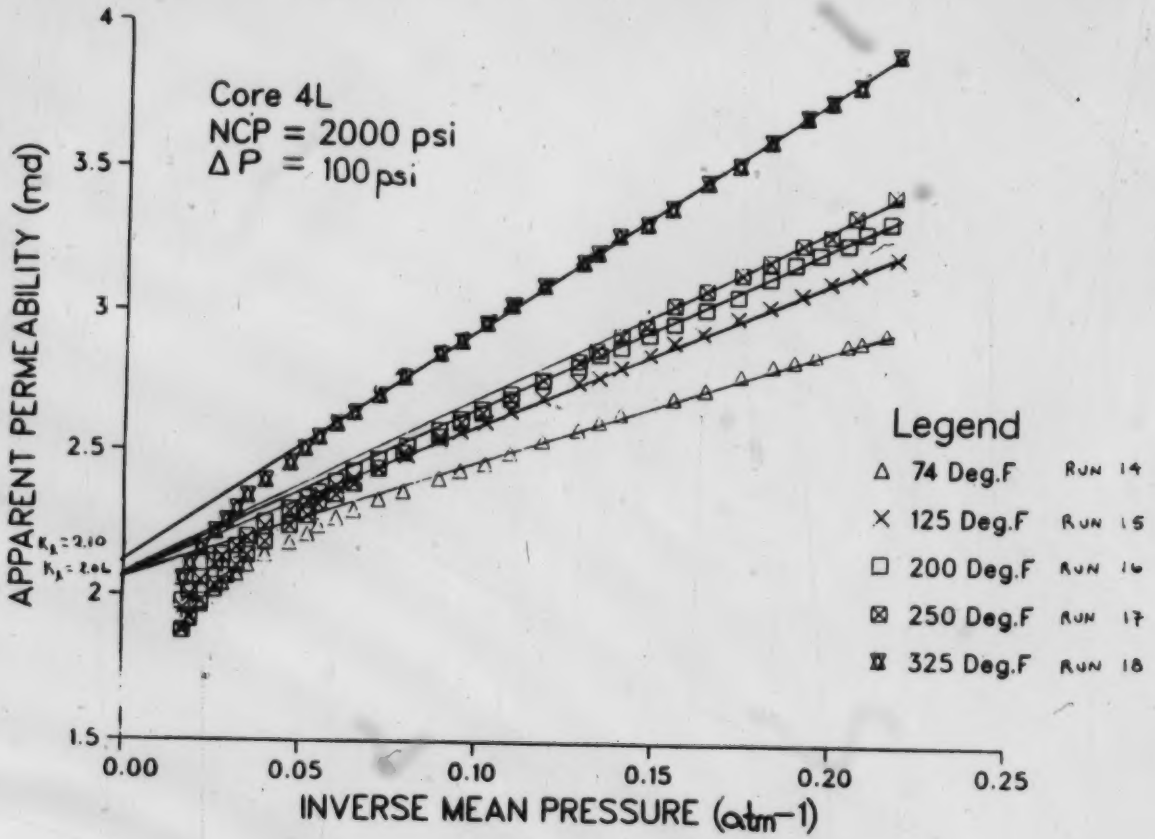

APPENDIX B10

CORE 6L: 3" Limestone

K/K100 versus NET CONFINING PRESSURE

*** AFTER HYSTERESIS LOSSES**

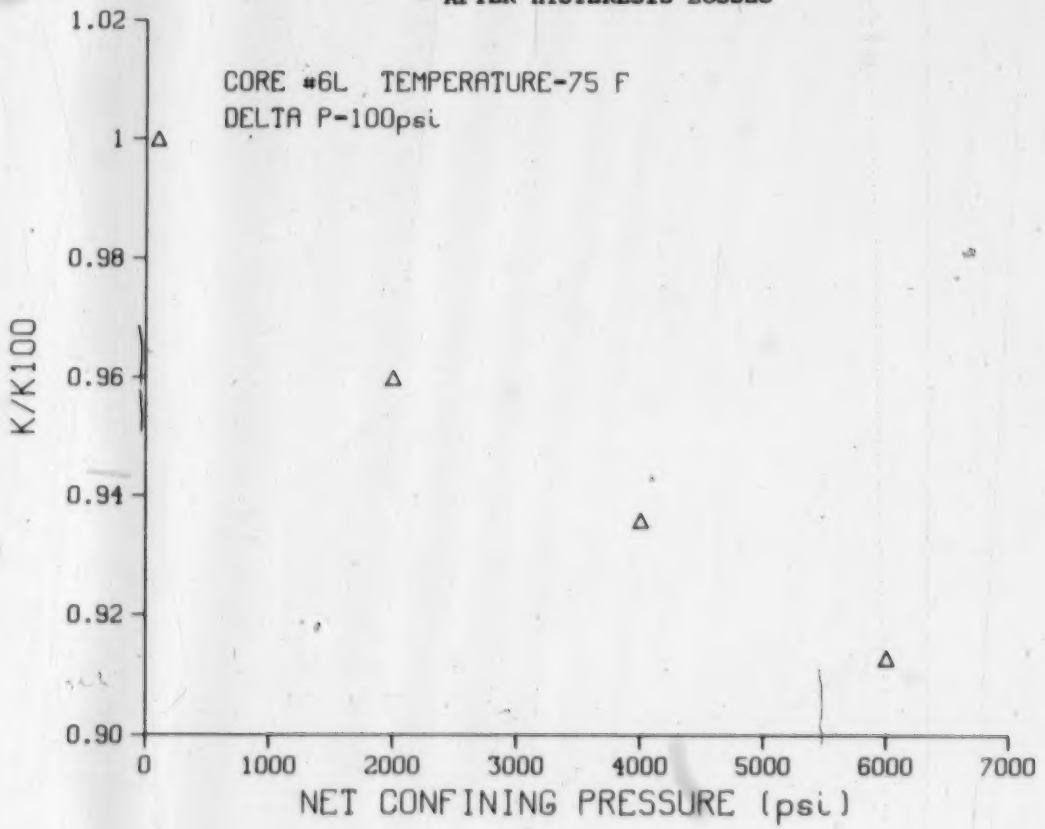

K/Katm vs NET CONFINING PRESSURE

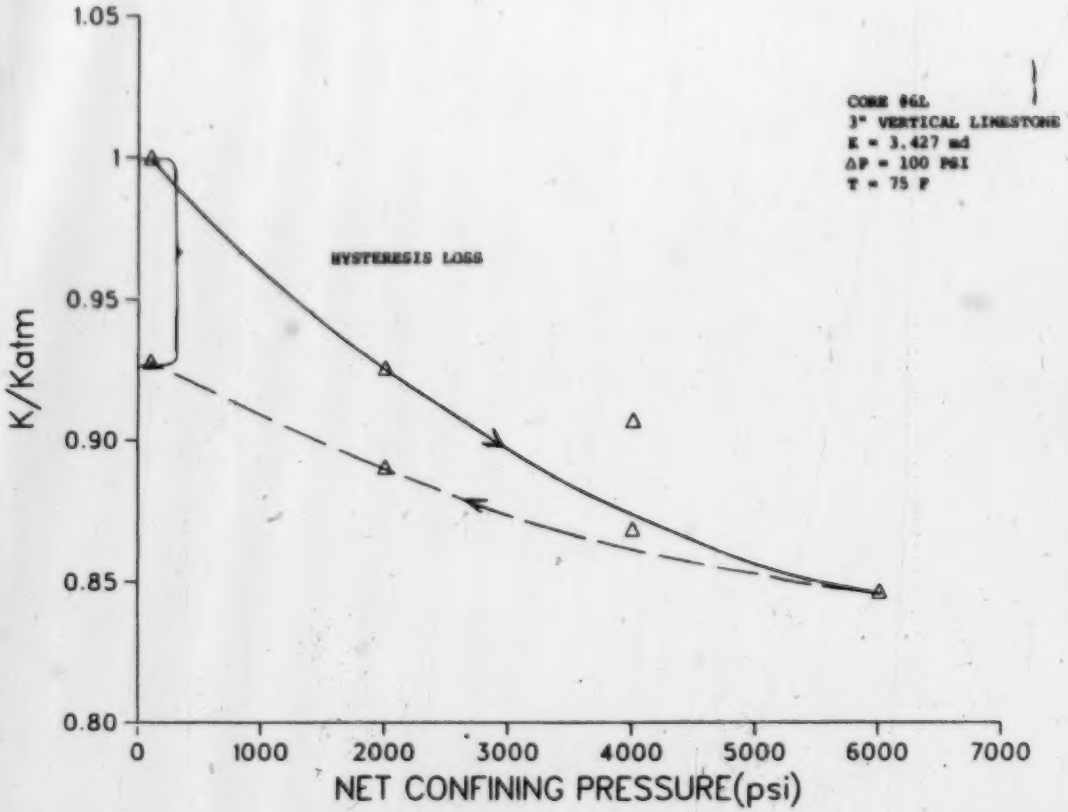

K/K75 versus TEMPERATURE

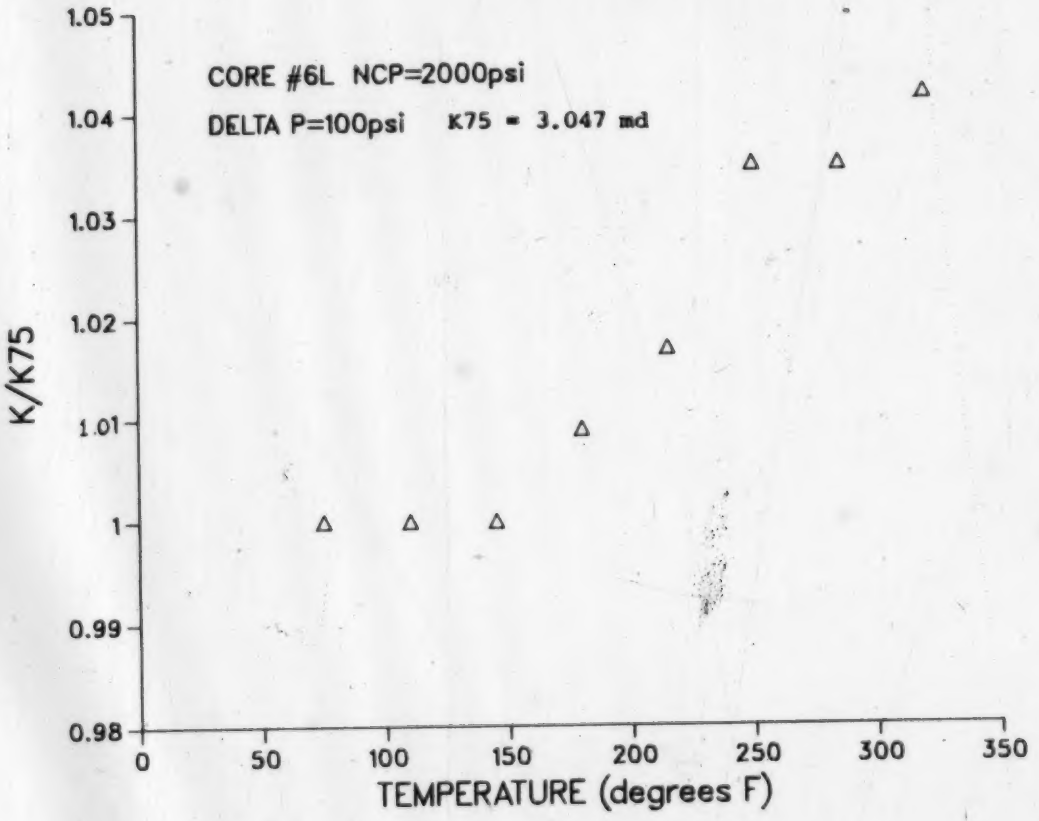

SLIP FACTOR versus TEMPERATURE

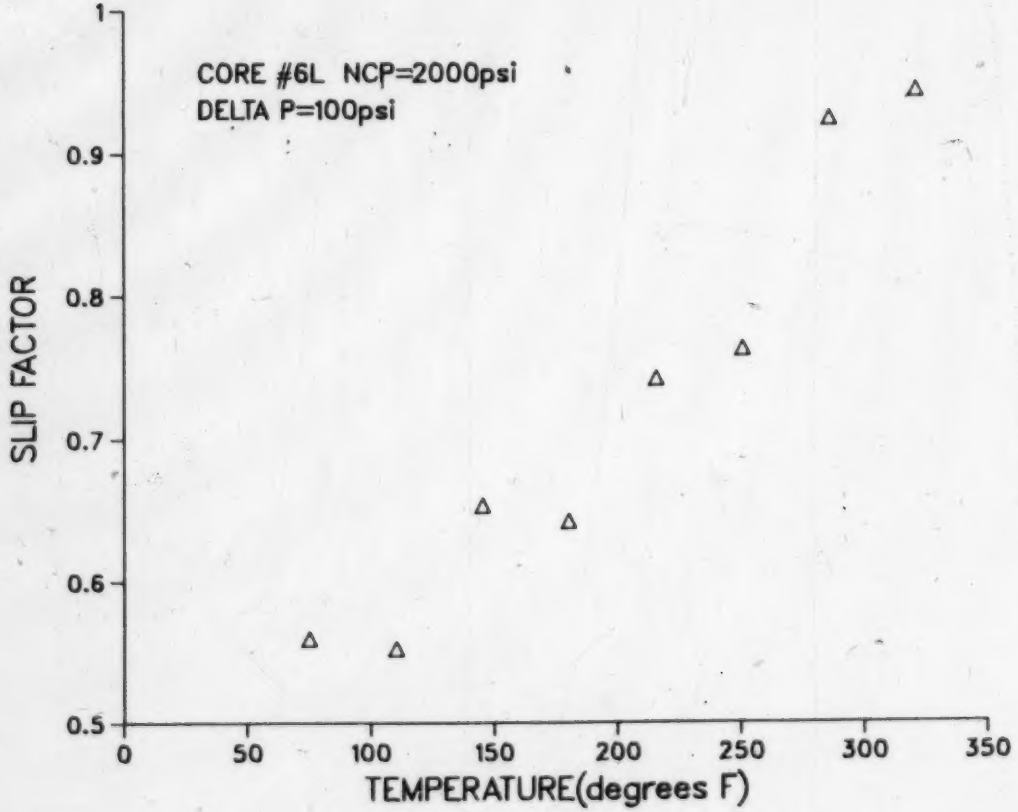

APPARENT PERMEABILITY vs RECIPROCAL MEAN PRESSURE

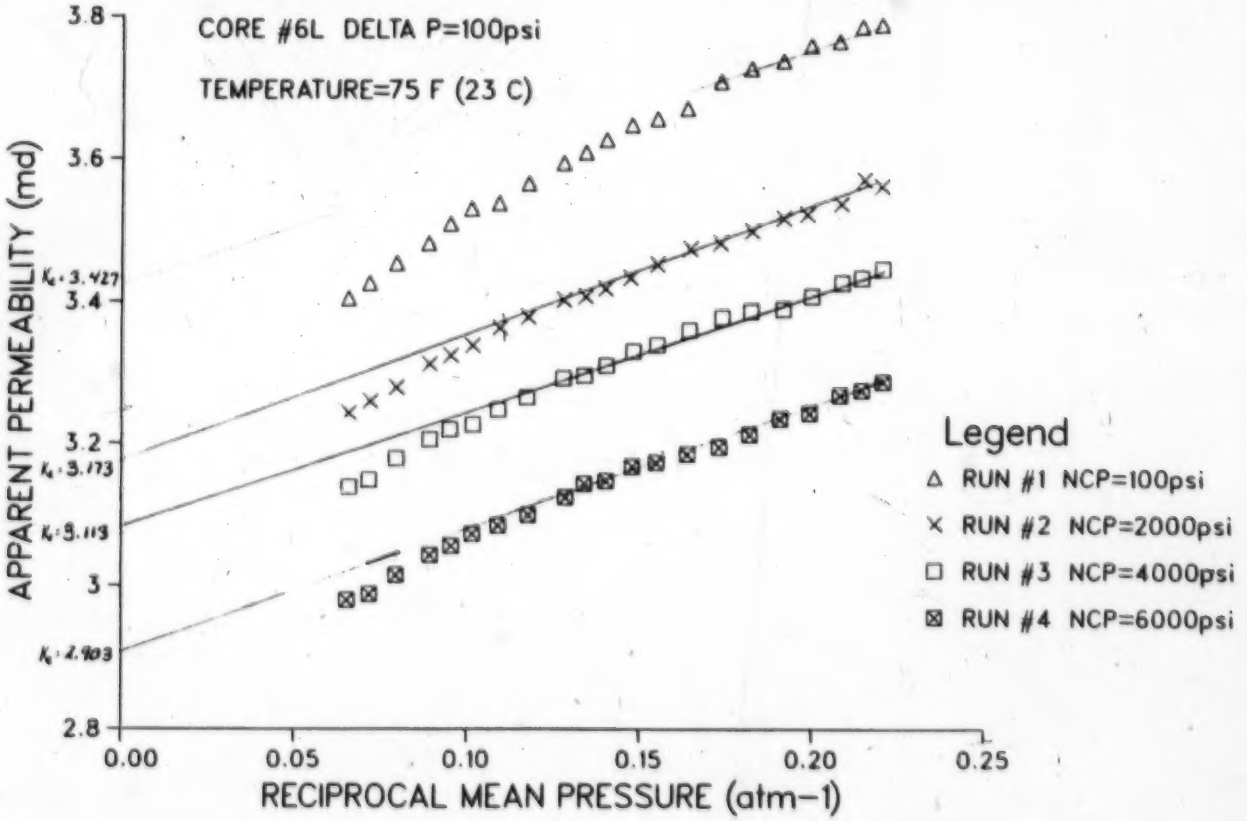

APPARENT PERMEABILITY vs RECIPROCAL MEAN PRESSURE

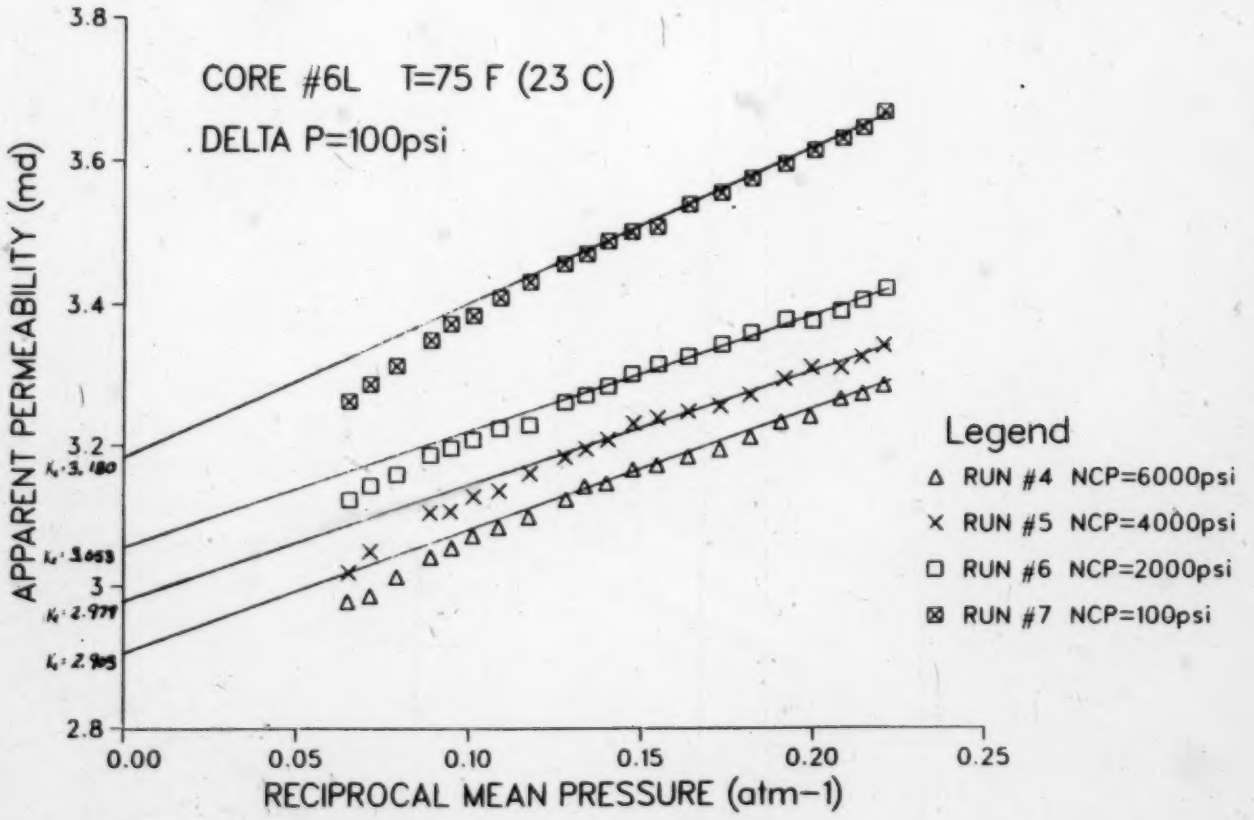

APPARENT PERMEABILITY vs RECIPROCAL MEAN PRESSURE

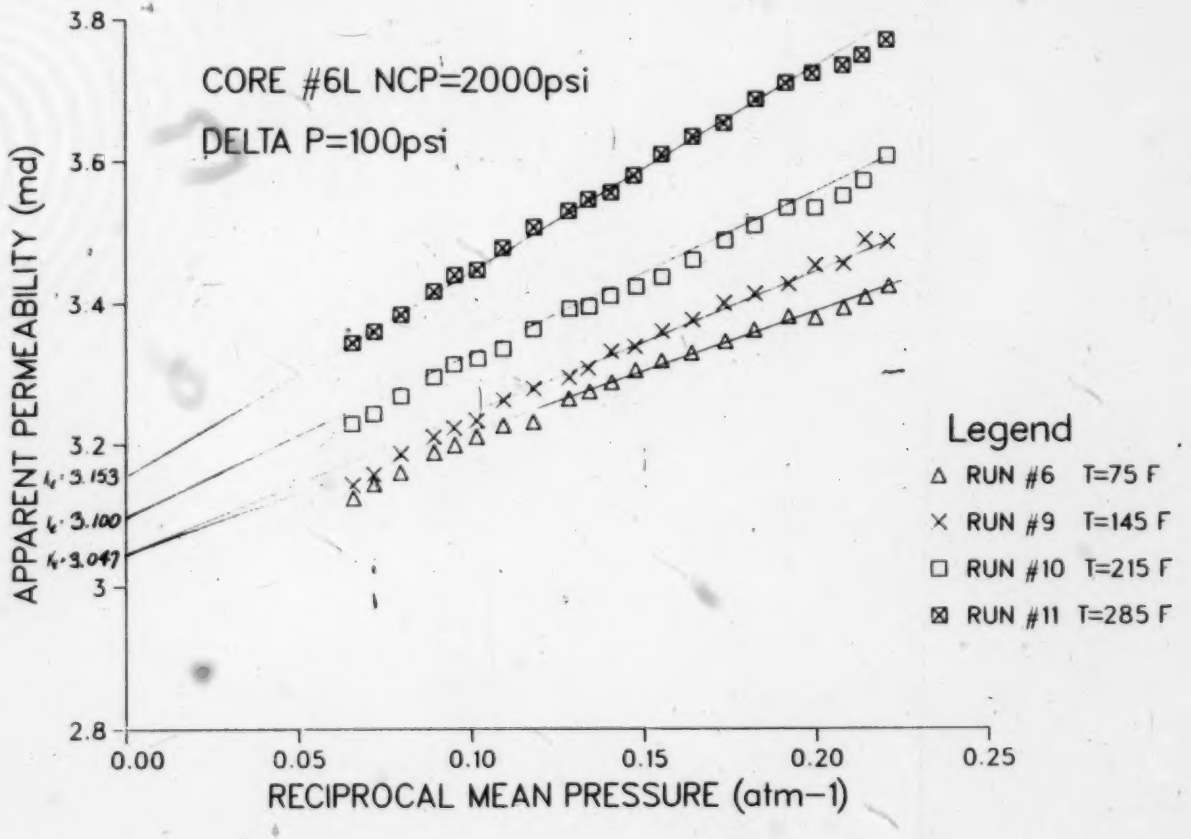

APPARENT PERMEABILITY vs RECIPROCAL MEAN PRESSURE

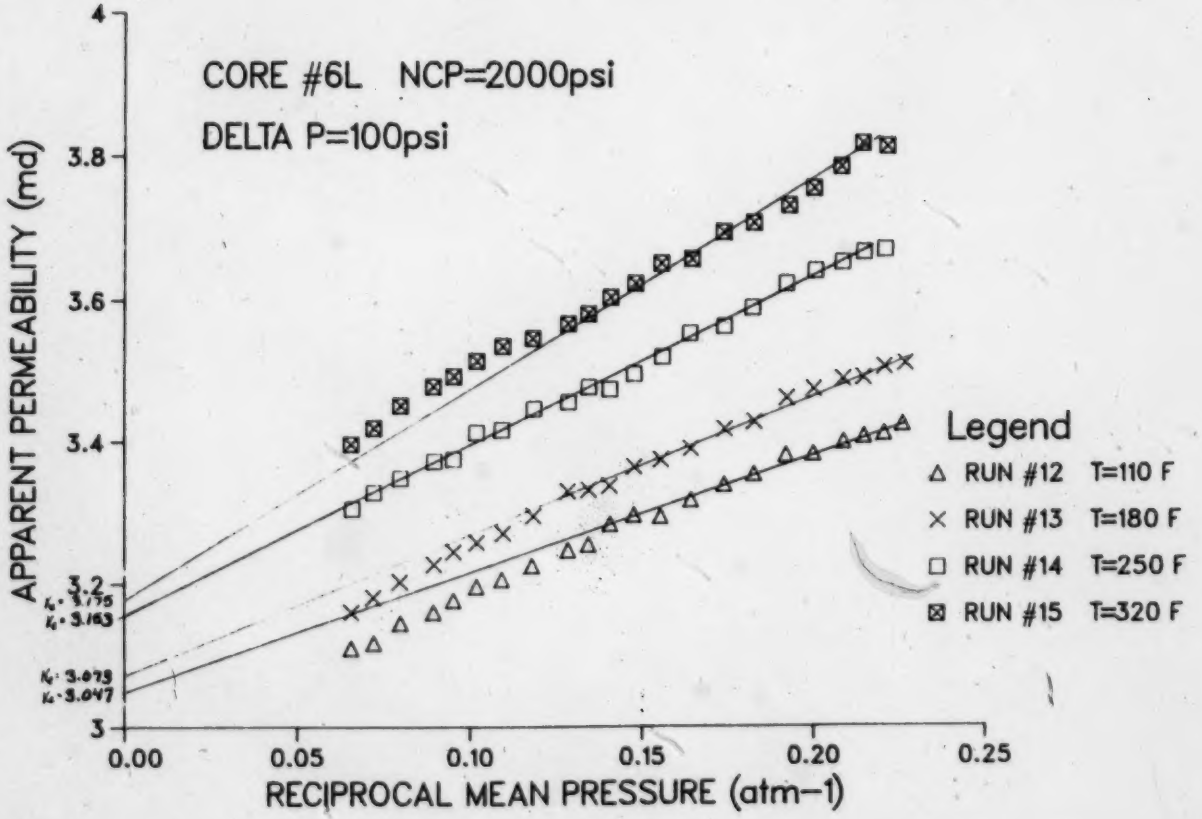

APPENDIX B11

CORE 2S: 3" Sandstone

K/K(75 F) vs TEMPERATURE

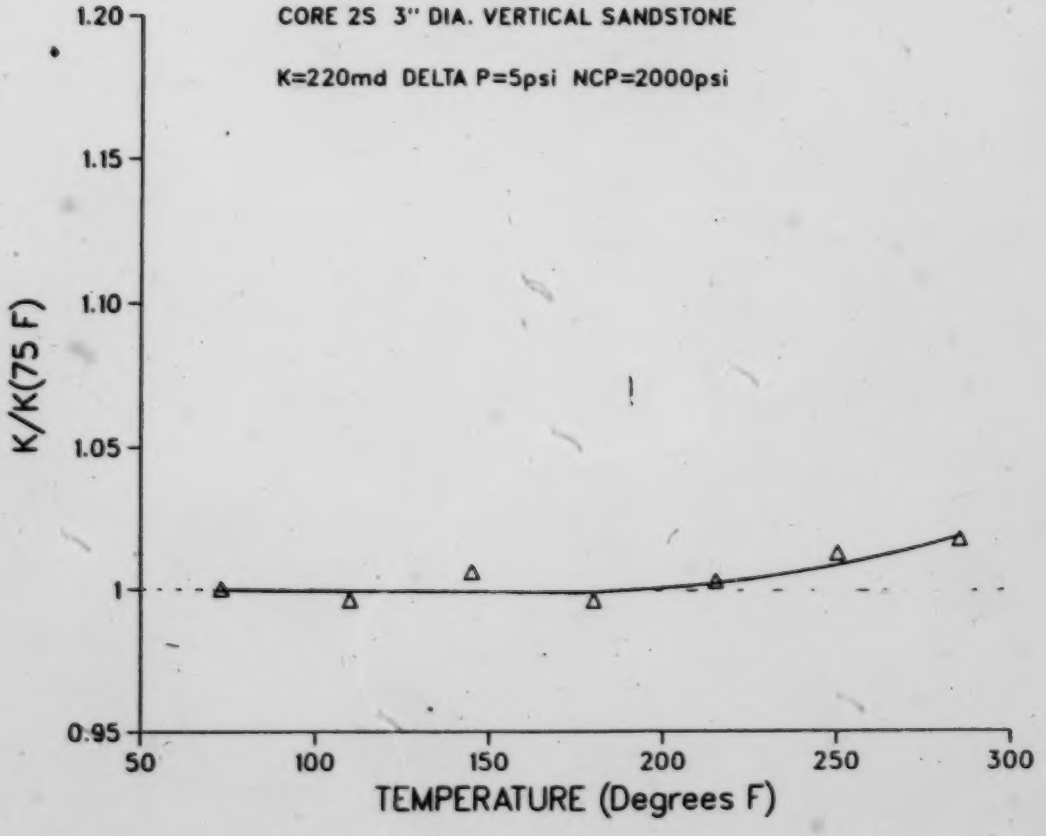

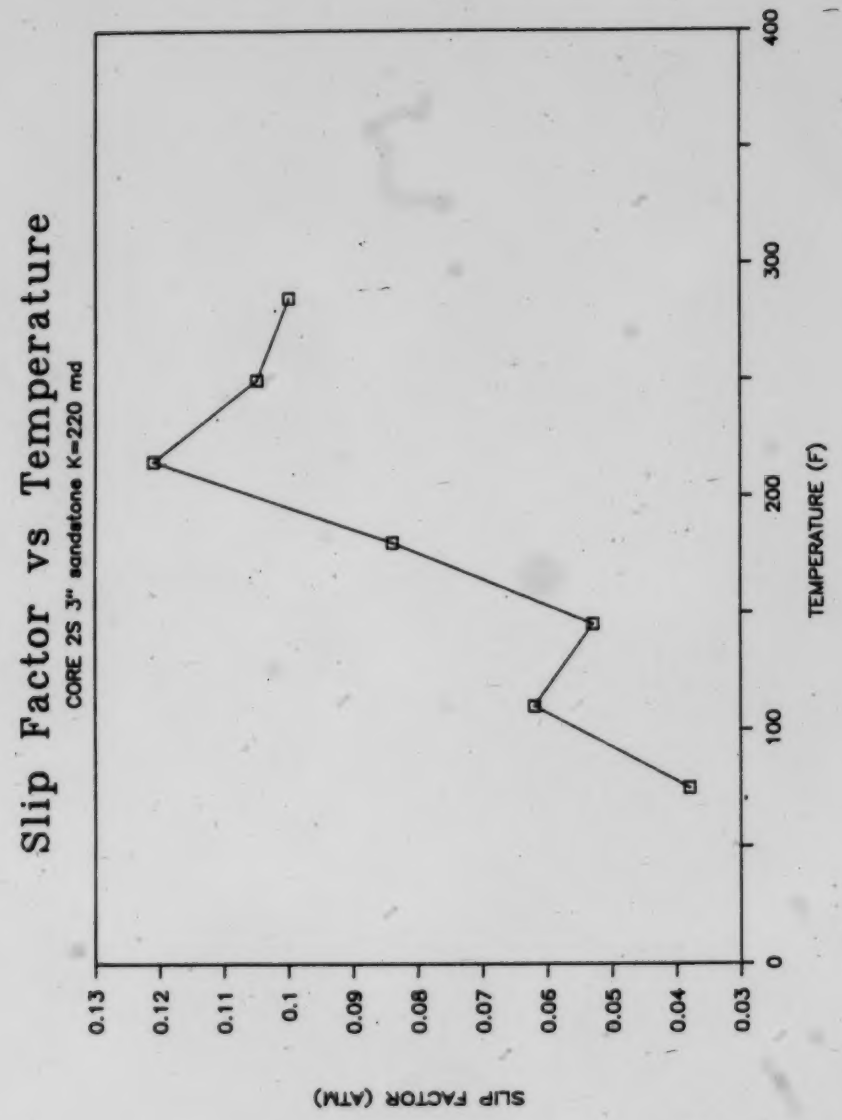
Slip Factor vs Temperature
CORE 2S 3" sandstone K=220 md
SLIP FACTOR (ATM)
0.13
0.12
0.11
0.1
0.09
0.08
0.07
0.06
0.05
0.04
0.03
0
100
200
300
400
TEMPERATURE (F)

APPARENT PERMEABILITY vs RECIPROCAL MEAN PRESSURE